4-4-2001

A Search for Previously Unrecognized Metal-Poor Subdwarfs in the Hipparcos Astrometric Catalogue

I. N. Reid
University of Pennsylvania

F. van Wyk
South African Astronomical Observatory

F. Marang
South African Astronomical Observatory

G. Roberts
South African Astronomical Observatory

D. Kilkenny
South African Astronomical Observatory

See next page for additional authors

Authors
I. N. Reid, F. van Wyk, F. Marang, G. Roberts, D. Kilkenny, and S. Mahoney

Mon. Not. R. Astron. Soc. **325,** 931–962 (2001)

A search for previously unrecognized metal-poor subdwarfs in the *Hipparcos* astrometric catalogue

I. Neill Reid,[1]★ F. van Wyk,[2] F. Marang,[2] G. Roberts,[2] D. Kilkenny[2] and S. Mahoney[3]
[1]*Department of Physics and Astronomy, University of Pennsylvania, 209 S. 33rd Street, Philadelphia, PA 19104-6396, USA*
[2]*South African Astronomical Observatory, PO Box 9, Observatory 7935, South Africa*
[3]*Hinman Box 1709, Dartmouth College, Hanover, NH 03755, USA*

Accepted 2001 January 15. Received 2000 December 19; in original form 2000 September 29

ABSTRACT

We have identified 317 stars included in the *Hipparcos* astrometric catalogue that have parallaxes measured to a precision of better than 15 per cent, and the location of which in the $(M_V, (B-V)_T)$ diagram implies a metallicity comparable to or less than that of the intermediate-abundance globular cluster M5. We have undertaken an extensive literature search to locate Strömgren, Johnson/Cousins and Walraven photometry for over 120 stars. In addition, we present new $UBV(RI)_C$ photometry of 201 of these candidate halo stars, together with similar data for a further 14 known metal-poor subdwarfs. These observations provide the first extensive data set of $R_C I_C$ photometry of metal-poor, main-sequence stars with well-determined trigonometric parallaxes. Finally, we have obtained intermediate-resolution optical spectroscopy of 175 stars.

47 stars still lack sufficient supplementary observations for population classification; however, we are able to estimate abundances for 270 stars, or over 80 per cent of the sample. The overwhelming majority have near-solar abundance, with their inclusion in the present sample stemming from errors in the colours listed in the *Hipparcos* catalogue. Only 44 stars show consistent evidence of abundances below [Fe/H] $= -1.0$. Nine are additions to the small sample of metal-poor subdwarfs with accurate photometry. We consider briefly the implication of these results for cluster main-sequence fitting.

Key words: stars: abundances – subdwarfs – Galaxy: halo.

1 INTRODUCTION

Main-sequence fitting remains one of the principal methods of determining distances, and hence turn-off luminosities and age estimates, for Galactic globular clusters. While recent investigations suggest that cluster ages may no longer set stringent constraints on cosmological models (Perlmutter et al. 1998; Schmidt et al. 1998; Riess et al. 2000), these measurements remain an important probe of the formation and evolution of the Milky Way. Empirical main sequence fitting demands calibrators with chemical abundances well matched to the target cluster, and spanning a sufficient range in colour on the unevolved main sequence to provide a reliable distance modulus estimate. Unfortunately, those conditions are met for scarcely any Galactic globulars, even with the addition of milliarcsecond-accuracy astrometric data from the *Hipparcos* satellite (ESA 1997). The local space density of the halo is sufficiently low that distance analyses (Gratton et al. 1997; Reid 1997, 1998; Pont et al. 1998; Carretta et al. 2000a) rest on data for barely two dozen subdwarfs which have both accurate parallax and abundance determinations, and, to the best of present knowledge, are single stars.

The situation is particularly acute for metal-poor globular clusters, with abundances [m/H] < -1.6. While several halo stars with extreme abundances have reliable *Hipparcos* parallax measurements, most of those stars have $M_V < 5$, placing them near the main-sequence turn-off. Evolutionary effects lead to a steepening of the main sequence at those luminosities in globular clusters, and a small mismatch in age, colour or abundance between calibrator and cluster can lead to substantial systematic errors in inferred distance moduli in main-sequence fitting. Of the few lower main-sequence subdwarfs with [m/H] < -1.5, the only star widely used as a distance calibrator is BD $+ 66°268$. Unfortunately, that star is a binary of uncertain mass ratio, and hence uncertain true luminosity.

The scarcity of G and K subdwarfs with accurate parallaxes is not surprising. Unevolved subdwarfs have $M_V > 5.5$; the *Hipparcos* sample is complete to a magnitude limit of $V = 7.9 + 1.1 \sin b$. Adopting $\langle V_{\rm lim} \rangle = 8.5$, this gives a sampling

★E-mail: inr@stsci.edu

volume of $\sim 1.3\times10^5\,\mathrm{pc}^3$ at $M_V = 6$. The space density of subdwarfs at that absolute magnitude is only $\sim 0.002\times\rho_{\rm disc}$, or $\sim 6\times10^{-6}\,\mathrm{star\,pc^{-1}\,mag^{-1}}$, so we expect only one such halo star (spanning the full abundance range) in the *Hipparcos* catalogue. HD 103095 meets these criteria, with $M_V = 6.61$, [m/H] $= -1.22$ and $V = 6.42$.

Clementini et al. (1999) have addressed this issue, the scarcity of reliable subdwarfs calibrators, by undertaking improved abundance determinations of known subdwarfs; we adopt an alternative strategy, searching for previously unrecognized subdwarfs. More distant subdwarfs have lower precision parallax measurements, which can lead to systematic biases, such as the Lutz–Kelker effect, if the relative uncertainties, σ_π/π, exceed ~15 per cent. Since *Hipparcos* parallaxes have typical uncertainties, ϵ_π, of 1 to 1.5 milliarcseconds (mas), this effectively limits the survey volume to $r < 100$ pc. None the less, given the local subdwarf space density estimated above, we might expect 15 to 20 subdwarfs with $M_V > 5.5$ and $V < 12$ to lie within range of *Hipparcos* measurement.

The *Hipparcos* catalogue is far from complete at magnitudes fainter than $V = 9$, but does include a significant number of proper motion stars, mainly from the Lowell survey (Giclas et al. 1963). Proper motion surveys are biased toward high-velocity stars, and are therefore good hunting grounds for halo subdwarfs. Despite extensive work by Carney and collaborators (Carney et al. 1994, and references therein), only a subset of the Lowell stars have accurate photometry and/or spectroscopy. Thus it remains possible that subdwarfs lie unrecognized amongst the fainter stars observed by *Hipparcos*.

Besides proper motions and parallaxes, the *Hipparcos* catalogue provides photometric data. We can therefore place each star on the HR diagram. Since metal-poor stars are known to be subluminous with respect to the disc main sequence at a given colour (or, more correctly, hotter at a given mass), those photometric data offer the possibility of identifying additional subdwarfs. This paper marks the first phase in such an analysis. We identify 317 stars with colours consistent with abundances [m/H] ≤ -1.1. Using both previously published data and our own observations, we have collected accurate photometry and spectroscopy for 80 per cent of the sample. Almost all are eliminated as likely subdwarfs, and most of the survivors are well-known halo stars. None the less, our observations identify several of new calibrators, and provide the first extensive catalogue of *RI* photometry of confirmed metal-poor subdwarfs.

2 THE SAMPLE

2.1 Selection criteria

The primary source of photometry for *Hipparcos* stars is the Tycho experiment, which used grids of star mappers to measure stellar fluxes in two passbands approximating the Johnson *BV* system. As discussed in Vol. 3 of the *Hipparcos* catalogue, there are systematic differences between Tycho photometry and the standard system (see also Bessell 2000). The *Hipparcos* catalogue lists *BV* photometry culled from the literature for many sources, and Figs 1(a) and (b) use the latter measurements to illustrate the colour

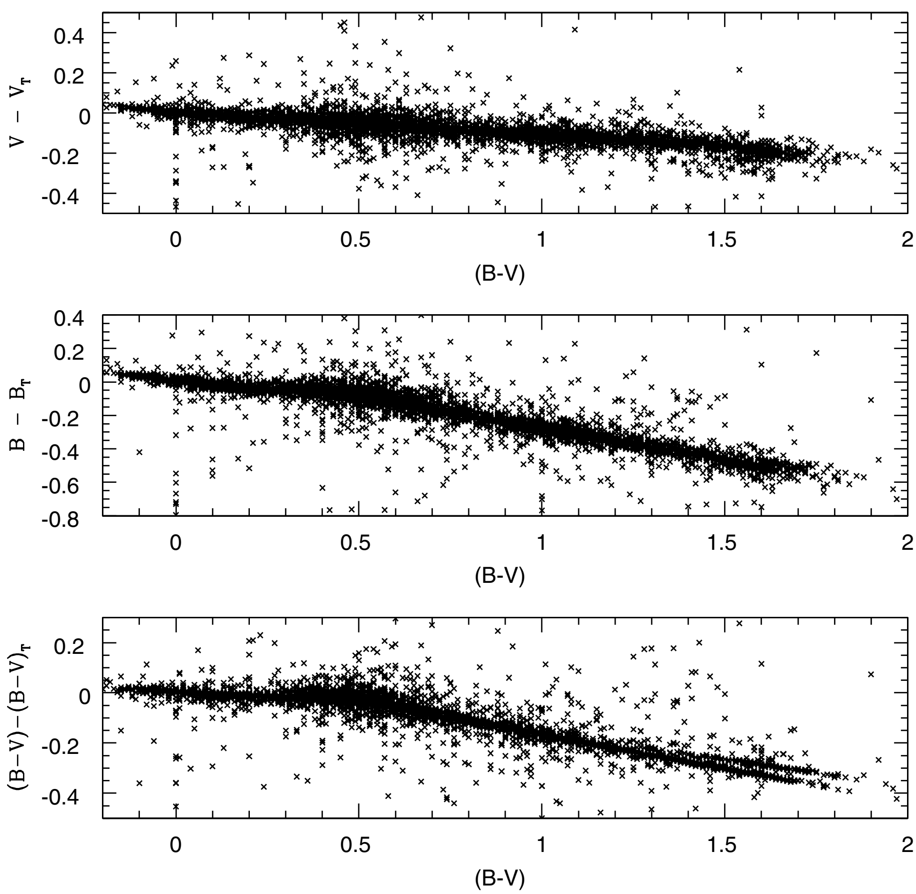

Figure 1. Colour terms in the Tycho B_T, V_T system. The comparison is based on data for 7000 stars from the *Hipparcos* catalogue, comparing the Tycho photometry against the literature *BV* data listed.

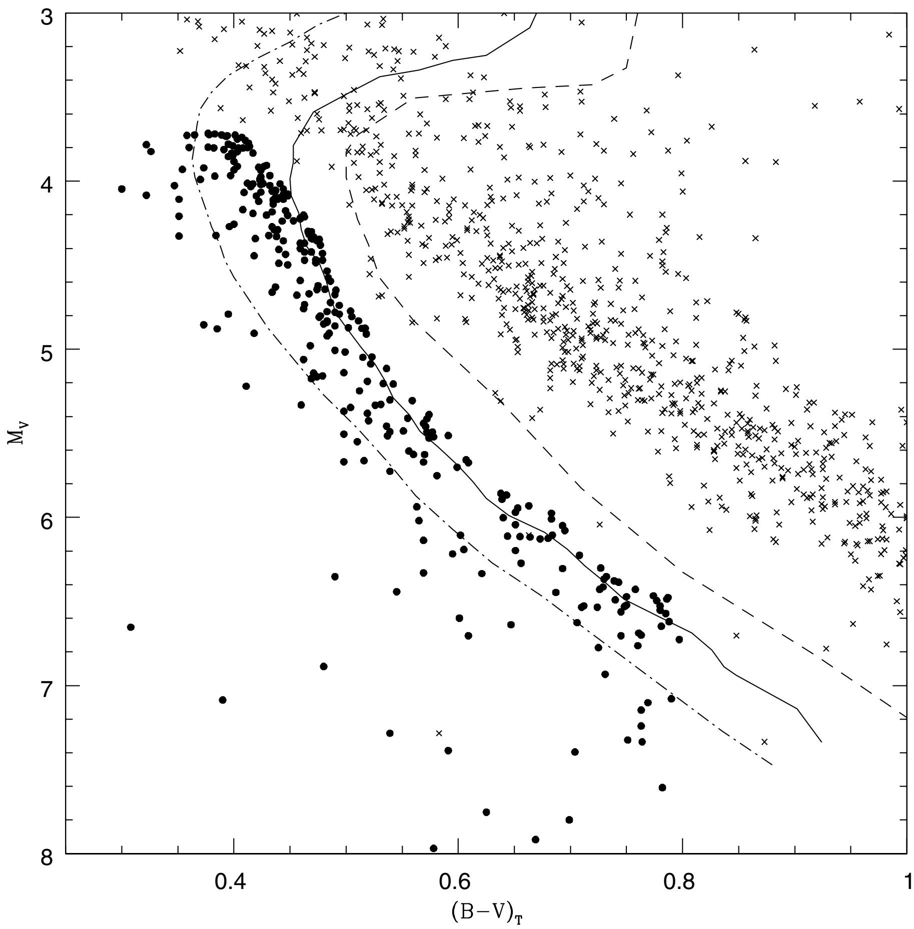

Figure 2. The $[M_V, (B-V)_T]$ colour–magnitude diagram; crosses mark stars from the *Hipparcos* catalogue with $\sigma_\pi/\pi < 15$ per cent and $\pi > 32$ mas. The dashed line outlines the schematic main sequence and giant branch in the metal-rich globular 47 Tucanae [at $(m-M) = 13.55$]; the solid line marks the relation for the intermediate-abundance cluster M5 [at $(m-M) = 14.5$]; and the dashed line plots the fiducial relation for the metal-poor cluster NGC 6397 [at $(m-M) = 12.14$]. Filled circles mark candidate metal-poor subdwarfs.

terms present in both V_T and B_T. Fig. 1(c) shows that those terms cancel to a large extent for stars bluer than $(B-V)_T = 0.6$, i.e., for F and G dwarfs $(B-V)_T \approx (B-V)$.[1] At later spectral types, $(B-V)_T$ is redder than the Johnson $(B-V)$ colour. The *Hipparcos* catalogue also lists $(V-I)$ colours, but these are drawn from such a wide variety of sources that, as noted by Clementini et al. (1999), the measurements are of little practical benefit for our purposes.

Our aim is to identify candidate metal-poor subdwarfs with reliable parallax measurements. Thus, as a first step, we consider only stars in the *Hipparcos* catalogue with parallaxes measured to a formal precision, σ_π/π, better than 15 per cent. This corresponds to a systematic Lutz–Kelker correction of $\Delta M_V = 0.3$ mag for a sample with a uniform space distribution $[N(\pi) \propto \pi^{-4}]$; in reality, subdwarf samples are likely to have a flatter parallax distribution $[N(\pi) \propto \pi^{-n}, n < 4]$, with correspondingly smaller Lutz–Kelker corrections.

Candidate metal-poor stars have been selected on the basis of their location in the $[M_V, (B-V)]$ colour–magnitude diagram (CMD). Fig. 2 plots the $[M_V, (B-V)_T]$ diagram for *Hipparcos* stars with $\sigma_\pi/\pi < 0.15$ and $\pi > 32$ mas – a sample dominated by the disc population. Superimposed on that diagram are the mean colour–magnitude relations for three globular clusters: the metal-rich cluster 47 Tucanae, $[\mathrm{Fe/H}] = -0.7$, at $(m-M) = 13.55$; the intermediate-abundance cluster M5, $[\mathrm{Fe/H}] = -1.11$, at $(m-M) = 14.5$, and the metal-poor cluster NGC 6397, $[\mathrm{Fe/H}] = -1.82$, at $(m-M) = 12.14$ (abundances from Carretta & Gratton 1997; see Reid 1999 for a summary of the distance modulus determinations[2]). These clusters provide a reference grid for the identification of candidate F- and G-type subdwarfs.

For present purposes, since we are concerned with relatively blue stars, we ignore the systematic colour difference between the Tycho and Johnson systems. Interpolating between the M5 and 47 Tuc CMDs, we define an $[M_V, (B-V)]$ relation corresponding approximately to $[\mathrm{Fe/H}] = -1$. We have identified all *Hipparcos* stars with $\sigma_\pi/\pi < 0.15$ lying blueward of that relation, truncating the sample at $(B-V)_T = 0.8$. We also impose a cut-off at $M_V < 4$, where the evolved halo colour–magnitude relations approach the

[1] This accounts for the apparent agreement between ground-based and Tycho data noted by Clementini et al. in their limited photometric comparison.

[2] Anthony-Twarog & Twarog (2000) have recently derived a distance modulus of $(m-M)_0 = 12.15$ for NGC 6397 based on main-sequence fitting using Strömgren photometry.

Table 1. Candidate subdwarf sample.

HIP	V_T	$(B-V)_T$	π	σ_π/π	M_V	V_1	$(B-V)_1$	ID	Phot	Spec	sd?	Comments
435	9.36	0.46	10.3	0.129	4.42	9.30	0.54	HD 34	C s	Y	I	uvby, *UBV*
895	8.61	0.44	12.6	0.094	4.11	8.55	0.44	HD 664		Y	I	LCO
1051	8.80	0.41	11.1	0.100	4.03	8.75	0.40	HD 864	C	Y	I	*UBV*
1300	9.80	0.46	7.7	0.123	4.22	9.74	0.45	BD+71 9				
1719	9.79	0.79	23.2	0.044	6.62	9.65	0.83	CPD −67 23	C	Y	D	*UBV*, Dbl.
3022	10.01	0.78	19.9	0.094	6.49	9.96	0.79	BD+42 126				
3139	9.38	0.41	8.6	0.142	4.07	9.27	0.47	HD 3734	C s	Y	D	*UBV*
3531	11.43	0.70	18.8	0.123	7.80	10.91	1.21	G 270-59	C	Y	D	M dwarf
3855	10.94	0.59	19.5	0.102	7.39	10.57	0.60	LP 406-78	C O	Y	D	M dwarf
4450	9.67	0.49	9.9	0.120	4.65	9.65	0.50	HD 5592	C	Y	D	*UBV*
4576	9.54	0.44	9.2	0.132	4.36	9.52	0.44	HD 5770	C	Y	D	*UBV*
4750	10.20	0.57	10.9	0.148	5.39	10.08	0.57	G 269-75	C O	Y	H	*UBV*
4981	9.22	0.57	17.4	0.073	5.41	9.11	0.58	HD 6323	C s O	Y	I	*UBV*, uvby
5004	10.37	0.76	16.3	0.108	6.43	10.25	0.76	G 269-87	C s O	Y	H	RN, uvby, *UBV*
5097	9.36	0.46	10.0	0.127	4.37	9.30	0.45	HD 6507	C	Y	D	*UBV*
5896	8.44	0.48	48.9	0.011	6.89	4.25	0.48	HD 7788 B	s O	Y	D	uvby, Dbl. C A
6251	8.50	0.51	18.9^F	0.059	4.88	8.43	0.52	HD 8068	C	Y	I	*UBV*
6758	9.74	0.58	14.1	0.116	5.49	9.67	0.64		C	Y	D	*UBV*
7303	9.89	0.57	13.0	0.131	5.46	9.84	0.60	G 271-94	C	Y	I	*UBV*, Dbl. G
7459	10.18	0.50	11.6	0.102	5.51	10.10	0.52	CPD −61 282	C s O	Y	H	RN, uvby, *UBV*
7687	9.47	0.78	25.8	0.060	6.53	9.37	0.79	HD 10166	C s	Y	I	uvby
7772	8.91	0.38	9.5	0.114	3.80	8.84	0.37	HD 10236	C	Y	D	*UBV*
7935	8.94	0.48	12.6	0.088	4.43	8.90	0.47	HD 10440	C	Y	I	*UBV*
8130	10.40	0.50	11.3	0.127	5.67	10.21	0.50	G 133-35	s O		I	CLLA, uvby
8298	10.14	0.69	15.4	0.123	6.08	10.09	0.69	BD+00 287	C		D	*UBV*
8389	10.89	0.71	14.0	0.128	6.63	10.69	0.92	CD −37 689	C	Y	D	*UBV*
8558	9.05	0.35	9.5	0.081	3.93	9.01	0.37	HD 11569	C s O	Y	H	RN
9634	8.39	0.44	13.7	0.082	4.08	8.34	0.43	HD 12653	C	Y	D	*UBV*
10208	9.11	0.44	12.7	0.099	4.63	9.07	0.42	HD 13441	C	Y	I	*UBV*
10353	9.30	0.46	12.3	0.109	4.76	9.22	0.45	HD 13650	C	Y	I	*UBV*
10360	8.58	0.32	12.6^F	0.095	4.08	8.56	0.32	HD 13721	C s	Y	D	blue straggler
10375	9.18	0.44	9.7	0.126	4.11	9.11	0.43	HD 13670	C	Y	I	*UBV*
10385	11.44	0.58	20.3	0.104	7.97	10.87	1.10	CD −33 758	C	Y	D	K dwarf
10529	9.91	0.46	42.5^F	0.059	8.05	9.91		BD+66 193				Dbl. C D
10637	9.36	0.42	9.9	0.135	4.34	9.28	0.42	HD 14139	C	Y	I	*UBV*
11435	8.69	0.46	13.9	0.113	4.40	8.64	0.45	HD 15276	C	Y	D	*UBV*
12579	9.21	0.50	14.5	0.088	5.02	9.16	0.52	BD+46 610	O		I	AFG, CLLA
13849	10.89	0.60	13.9	0.140	6.60	10.67	0.61		C	Y	D	*UBV*
14192	9.03	0.43	9.5	0.086	3.91	8.94	0.43	HD 19239	C	Y	D	*UBV*
14594	8.10	0.48	25.8	0.044	5.16	8.04	0.49	HD 19445	s O	Y	H	F20, GCC
14946	8.56	0.39	10.9	0.096	3.73	8.48	0.38	HD 19768				
15756	11.01	0.73	12.1	0.127	6.43	10.90	0.95	CD −49 942	C	Y	D	*UBV*
15998	10.41	0.75	16.8	0.107	6.53	10.17	0.85	BD+44 697	s		D	uvby
16089	8.81	0.42	11.2	0.115	4.07	8.77	0.42	HD 21515	C	Y	D	*UBV*
16404	9.97	0.65	17.6	0.087	6.20	9.91	0.67	BD+66 268	s O		H	CLLA, uvby, Dbl. S
16479	8.36	0.43	13.6	0.078	4.03	8.30	0.42	HD 21925	C	Y	D	*UBV*
17085	9.64	0.50	12.6	0.145	5.14	9.58	0.50	HD 22785	C	Y	D	*UBV*, F20
17241	10.27	0.48	8.2	0.127	4.85	10.25	0.44	CPD −59 286	C	Y	H	*UBV*
17481	8.78	0.36	10.1	0.126	3.80	8.70	0.39	HD 23290	C s	Y	D	*UBV*, uvby, Pleiad
17497	9.04	0.37	9.8	0.132	3.99	8.98	0.40	HD 23289	s O		D	Pleiad
17844	9.19	0.49	12.9	0.094	4.74	9.15	0.49	BD+43 817				
18700	9.34	0.55	17.0	0.098	5.49	9.33	0.56	HD 286457	C	Y	I	*UBV*
19007	9.64	0.75	24.2	0.063	6.56	9.53	0.82	HD 25673	C	Y	I	*UBV*, F20
19215	9.02	0.38	9.0	0.140	3.80	8.98	0.36	HD 25821	s O		D	*UBV*, uvby
19637	8.77	0.44	12.4	0.105	4.24	8.71	0.43	HD 26500		Y	D	LCO
19797	9.31	0.37	12.8	0.104	4.85	9.23	0.36	HD 284248	s O	Y	H	GCC, F20
20413	10.38	0.65	13.1	0.148	5.97	10.32	0.67	LP 156-48	O		D	*UBV*
20527	11.43	0.68	22.6	0.123	8.20	10.89	1.29	VR 9	C O		D	Hyad
20895	11.52	0.60	25.0	0.130	8.51	10.92	1.39	LP 358-300	O		D	M0, Hyad, Dbl. C B
21000	9.83	0.60	84.8^{F*}	0.056	9.47	9.83		BD+04 701A	C	Y	D	*UBV*, F20, Dbl. C A
21125	10.27	0.68	14.7	0.113	6.11	10.19	0.68	CPD −30 618	C	Y	I	*UBV*
21261	11.14	0.62	21.1	0.105	7.75	10.74	1.20	Leiden 65	C O		D	Hyades M dwarf
21478	9.60	0.49	10.6	0.146	4.72	9.43	0.57	HD 283749	O	Y	D	LCO
21586	10.73	0.61	15.7	0.130	6.70	10.39	0.62	G 175-43	O		I	F20
21609	9.85	0.64	17.0	0.058	6.00	9.85		HD 29907	C s O	Y	H	uvby, *UBV*, F20
21767	10.49	0.57	14.7	0.140	6.33	10.40	0.70	HD 280067	O		D	F20
22177	11.42	0.65	22.5	0.103	8.17	10.92	1.28	Leiden 119	C O	Y	D	Hyades M dwarf
22246	10.24	0.76	24.1^F	0.129	7.15	10.12	0.80	G 96-1	O		D	*UBV*, F20, CLLA
22632	9.18	0.47	15.6	0.077	5.14	9.13	0.50	HD 31128	C s O	Y	H	*UBV*, F20
23573	10.08	0.68	16.2	0.069	6.12	10.03	0.74	HD 273011	C O	Y	I	*UBV*
24296	9.95	0.54	11.2	0.094	5.21	9.85	0.55	HD 273832	C	Y	I	*UBV*

Table 1 – *continued*

HIP	V_T	$(B-V)_T$	π	σ_π/π	M_V	V_1	$(B-V)_1$	ID	Phot	Spec	sd?	Comments
24316	9.52	0.46	14.6	0.069	5.33	9.43	0.50	HD 34328	C s O	Y	H	GCC, uvby, *UBV*
24421	9.41	0.51	12.1	0.119	4.83	9.34	0.52	HD 34165	C	Y	D	*UBV*
24935	8.84	0.45	13.6	0.060	4.50	8.77	0.45	HD 35138	C	Y	I	*UBV*
25590	9.01	0.35	10.1	0.134	4.03	8.99	0.37	HD 35707				
25717	8.25	0.43	13.6	0.091	3.91	8.19	0.46	HD 36045	C s	Y	D	*UBV*, uvby
26452	9.65	0.51	13.1	0.118	5.25	9.60	0.51	G 248-45	O		I	CLLA, *UBV*
26676	10.34	0.66	14.3	0.139	6.12	10.20	0.65	G 102-20	C s O	Y	H	RN, CLLA, uvby
26688	7.75	0.43	20.6^{F}	0.043	4.32	7.70	0.42	HD 37792	C	Y	I	*UBV*, F20
27361	9.22	0.38	10.5	0.150	4.32	9.19	0.37	BD+35 375				
28122	9.48	0.49	23.6	0.135	6.35	9.48	0.72	HD 40007	C	Y	D	*UBV*, Dbl.
28188	9.07	0.47	16.6	0.089	5.16	9.00	0.47	HD 40057		Y	I	F20
29322	11.59	0.43	33.6	0.126	9.22	11.29	1.42	LHS 1832	C O	Y	D	M dwarf
29510	8.43	0.38	11.4	0.132	3.72	8.39	0.37	HD 42634		Y	D	LCO
30311	9.24	0.45	10.9	0.126	4.43	9.18	0.43	HD 44191				
30481	8.27	0.40	12.7	0.075	3.79	8.23	0.41	HD 44002	s O		I	uvby
31639	9.72	0.65	17.6	0.076	5.94	9.64	0.70	CPD −25 1545	C	Y	I	*UBV*, F20
32009	9.72	0.69	18.4	0.114	6.05	9.63	0.69	G 109-21	C	Y	D	*UBV*
32308	10.79	0.79	18.1	0.125	7.08	10.73	0.80	BD+15 1305	C	Y	D	*UBV*
33282	11.48	0.67	19.3	0.129	7.92	11.30	1.34	LP 205-37	O		D	M dwarf
33283	11.37	0.31	11.4	0.125	6.65	11.10	0.79	L 59-34	C	Y	I	*UBV*
34145	9.76	0.54	14.0	0.112	5.49	9.62	0.55	HD 268542		Y	H?	LCO
34146	8.10	0.45	15.7	0.058	4.09	8.05	0.47	HD 53545	C s	Y	D	*UBV*, F20
34548	9.11	0.47	12.9	0.112	4.67	9.06	0.46	HD 53871			D	F20
35163	10.08	0.75	19.0^{F}	0.142	6.47	9.98	0.73	BD+58 1015	O		D?	Dbl. S
35232	9.74	0.44	8.1	0.109	4.29	9.69	0.46	HD 57489	C	Y	I	*UBV*
35560	8.54	0.44	12.7	0.092	4.06	8.50	0.44	HD 57391	C	Y	I	*UBV*
36491	8.54	0.51	20.0	0.083	5.05	8.48	0.54	HD 59374	C s O	Y	I	*UBV*, F20, CLLA, RN
36818	10.44	0.73	15.3^{F}	0.090	6.37	10.49	0.61	CPD −45 1588	C s O	Y	I/H	RN, uvby
38541	8.37	0.60	35.3	0.030	6.11	8.27	0.62	HD 64090	s O	Y	H	F20, GCC, Dbl.
39911	9.63	0.59	15.0	0.066	5.51	9.60	0.60	HD 68089	C O s	Y	I	*UBV*, uvby
40408	9.31	0.38	8.6	0.147	3.97	9.30	0.37	BD+32 1699				
40778	9.72	0.48	10.4	0.142	4.80	9.73	0.48	HD 233511	O s		H	F20, GCC
41563	8.94	0.33	9.5	0.135	3.82	8.83	0.33	HD 71768	C	Y	D	*UBV*
42278	7.81	0.38	15.1	0.094	3.72	7.79	0.40	HD 73176	C	Y	D	*UBV*, Dbl. G
43445	8.70	0.47	13.5	0.085	4.35	8.63	0.48	HD 75596	C s	Y	I	uvby, *UBV*
43490	9.58	0.53	14.1	0.064	5.33	9.55	0.54	CPD −79 363	C	Y	H	*UBV*
43973	9.60	0.64	18.1	0.080	5.89	9.52	0.66	BD−8 2534	C	Y	I	*UBV*, Dbl.
44116	8.54	0.44	12.7	0.098	4.05	8.48	0.45	HD 76910	C s	Y	I	uvby, F20
44124	9.76	0.41	12.4	0.139	5.22	9.66	0.48	BD−3 2525	O s	Y	H	F20, RN, CLLA
44436	11.23	0.39	14.8	0.073	7.09	11.23		HD 78084B?		Y	D	*UBV*, uvby, Dbl. C D
45162	9.20	0.48	11.7	0.108	4.53	9.18	0.48	BD+38 2007				
46051	9.23	0.57	17.5	0.102	5.44	9.16	0.58	BD+36 1951				
46120	10.14	0.60	16.5	0.060	6.22	10.11	0.56	Gl 345	C O s	Y	H	RN, uvby, *UBV*
46250	8.42	0.46	14.4	0.100	4.21	8.38	0.47	HD 81298	s		D	uvby
46509	4.92	0.41	58.5	0.065	3.76	4.59	0.41	HD 81997	O s		D	uvby, Dbl. X
47161	9.34	0.42	8.6	0.136	4.02	9.29	0.43	HD 83356	C	Y	D	*UBV*
47171	9.40	0.49	11.9	0.112	4.78	9.31	0.58	BD−3 2726	C	Y	I	*UBV*
47640	8.88	0.44	12.3	0.094	4.33	8.84	0.42	HD 83888			D	F20
47948	10.15	0.57	11.9	0.129	5.53	10.08	0.58	BD+0 2554	C	Y	D	F20, *UBV*
48146	9.64	0.50	14.0^{F}	0.112	5.37	9.57	0.50	BD+9 2242	C	Y	D	*UBV*
48152	8.38	0.40	12.4	0.085	3.85	8.33	0.40	HD 84937	C O s	Y	H	F20, GCC, *UBV*
49574	8.82	0.48	12.7	0.134	4.35	8.75	0.48	HD 87908	C	Y	I	*UBV*, Dbl. S X
49785	8.56	0.48	15.9^{F}	0.061	4.57	8.51	0.49	HD 88198	C	Y	D	*UBV*
49868	8.97	0.76	47.1	0.058	7.34	9.48	1.34	BD+75 403	O		D	M dwarf, Dbl. C A
50153	9.71	0.45	7.5	0.128	4.08	9.69	0.44	BD+81 327				
50532	9.97	0.49	10.2	0.147	5.01	9.91	0.55	BD−9 2044	C	Y	D	*UBV*
50965	9.93	0.49	9.7	0.146	4.86	9.80	0.58	G 162-51	C O s	Y	I	RN, CLLA, uvby, *UBV*
51156	9.10	0.43	10.4	0.113	4.18	9.06	0.42	HD 90527	C	Y	D	*UBV*
51298	9.28	0.46	10.4	0.120	4.37	9.24	0.44	HD 90764	C	Y	D	*UBV*
51300	9.29	0.41	8.0	0.123	3.80	9.21	0.41	HD 91043	C W	Y	D	*UBV*, Walraven
51769	10.49	0.72	16.2	0.111	6.53	10.50	0.68	G 162-68	C O s		I	RN, CLLA, uvby, *UBV*
52285	10.13	0.79	18.7	0.130	6.49	9.89	0.91	BD+4 2370	C	Y	I	*UBV*, Dbl. C A
53070	8.26	0.49	19.2	0.059	4.68	8.21	0.50	HD 94028	C O s		H	F20, GCC, *UBV*
53911	11.15	0.70	17.7	0.125	7.39	10.92	0.72	TW Hya	C O	Y	D	M dwarf
54519	11.21	0.75	16.7	0.129	7.32	11.07	1.59	BD+19 2423	C	Y	D	M dwarf
54641	8.22	0.48	17.8	0.043	4.47	8.16	0.48	HD 97320	C O s	Y	H	AFG, *UBV*
54768	9.14	0.52	14.0	0.090	4.88	9.11	0.52	HD 97354	O		I	*UBV*
54834	8.82	0.46	15.2	0.069	4.73	8.88	0.05	CPD −56 4321	C	Y	H	*UBV*
54993	8.89	0.39	9.7	0.118	3.81	8.83	0.38	HD 97874	C	Y	D	*UBV*
55790	9.14	0.47	11.0	0.135	4.34	9.07	0.48	HD 99383	C O s	Y	H	AFG, uvby, *UBV*
55978	9.14	0.39	8.3	0.126	3.73	9.07	0.41	HD 99805	C s W	Y	D	Walraven, uvby, *UBV*

Table 1 – *continued*

HIP	V_T	$(B-V)_T$	π	σ_π/π	M_V	V_1	$(B-V)_1$	ID	Phot	Spec	sd?	Comments
57360	8.80	0.43	12.5	0.096	4.27	8.75	0.43	HD 102200	C O s	Y	H	RN, AFG, uby, *UBV*
57450	9.94	0.56	13.6	0.113	5.61	9.91	0.58	BD+51 1696	O s		H	CLLA
57939	6.51	0.75	109.2	0.007	6.70	6.42	0.75	HD 103095	O s		H	F20, GCC
59258	7.53	0.36	17.3	0.048	3.73	7.51	0.35	HD 105584	s		I	uvby
59750	6.11	0.47	44.3^F	0.023	4.34	6.11		HD 106516	O C1		I	F20, Dbl. O
60251	9.11	0.53	16.5	0.145	5.20	9.00	0.54	HD 107440	C W	Y	D	*UBV*, Walraven, Dbl. X S
60632	9.71	0.42	11.0	0.118	4.91	9.66	0.44	HD 108177	C O s		H	GCC, uvby, *UBV*
60783	12.08	0.70	36.8	0.137	9.91	12.08		G 148-61				Dbl. X S
60852	8.52	0.47	14.4	0.075	4.32	8.48	0.50	HD 108540	C s	Y	I	*UBV*, uvby
61085	9.18	0.45	10.3	0.128	4.24	9.13	0.44	HD 108974				
62261	9.45	0.35	8.9	0.150	4.21	9.42	0.36	HD 110963	s		D	uvby
62858	9.57	0.50	11.0	0.129	4.77	9.51	0.50	BD+16 2432	C		I	*UBV*
63063	9.99	0.73	19.3^F	0.089	6.41	9.93	0.81	BD+8 2658	C O s		D	*UBV*, uvby, CLLA
63553	8.57	0.40	11.1	0.105	3.80	8.51	0.44	HD 113125	C s		D	uvby, *UBV*
63781	9.35	0.40	7.9	0.150	3.83	9.30	0.38	HD 113517	C		D	*UBV*
63912	8.96	0.44	10.3	0.092	4.02	8.93	0.41	HD 113862	O		D	*UBV*
63970	10.14	0.52	12.7	0.130	5.66	10.07	0.52	BD+33 2300			D	F20, Dbl.
64386	9.90	0.61	14.3	0.134	5.67	9.86	1.06	BD+19 2646	O s		I	CLLA, uvby
64765	8.92	0.35	10.9	0.125	4.11	8.86	0.34	HD 115132	C s		D	uvby, *UBV*
65040	9.93	0.64	15.4	0.086	5.87	9.77	0.65	BD+7 2634	O s		I	CLLA, uvby
65201	8.85	0.48	15.5	0.093	4.81	8.80	0.45	HD 116064	C O s		H	GCC, uvby, *UBV*, Dbl. C C
65268	7.71	0.44	19.0	0.050	4.11	7.64	0.49	HD 116316	s		I	uvby, Dbl. S
65322	9.21	0.44	9.5	0.106	4.10	9.18	0.43	HD 116530				
65940	10.51	0.78	16.9	0.093	6.65	10.41	0.92	BD−3 3488	C O		D	*UBV*, K2V - U1
66169	10.07	0.68	15.2	0.121	5.97	10.11	0.70	BD+2 2691	C1		D	*UBV*
66500	9.62	0.48	8.8	0.148	4.34	9.60	0.48	BD+37 2434	s		I	uvby
66815	8.89	0.54	17.6	0.063	5.11	8.83	0.55	HD 119173	C		I	*UBV*, F20
66828	11.23	0.78	26.5	0.080	8.34	10.89	1.33	McC 697	O		D	M dwarf
67189	9.91	0.48	9.6	0.148	4.83	9.85	0.48	HD 119530	C		D	*UBV*
67655	8.03	0.65	40.0	0.025	6.04	7.97	0.66	HD 120559	C1 O s		I	uvby *UBV*
68165	10.04	0.76	21.3	0.090	6.69	9.98	0.88	BD+7 2721	C1 O s	Y	D	uvby *UBV*
68452	8.92	0.47	11.9	0.116	4.30	8.88	0.46	HD 122241	C1	Y	I	LCO
68870	9.52	0.44	9.9	0.140	4.49	9.51	0.43	HD 123192	C1	Y	D	LCO
70152	11.03	0.73	15.1	0.124	6.93	10.60	0.97	BD+9 2879	C1 O s	Y	D	*UBV*, uvby
70622	9.86	0.46	8.4	0.129	4.47	9.83	0.46	HD 126913				
70681	9.34	0.58	19.2	0.075	5.75	9.28	0.61	HD 126681	C O s	Y	H	F20, GCC, uvby, *UBV*
70689	8.58	0.37	11.7	0.090	3.92	8.53	0.37	HD 126488	C		D	*UBV*, Dbl. G
71886	8.96	0.40	11.5	0.127	4.27	8.94	0.38	HD 129392	C	Y	D	*UBV*
71887	8.83	0.47	13.4	0.080	4.47	8.79	0.46	HD 129515				
71939	8.90	0.46	14.3	0.104	4.68	8.81	0.48	HD 129510	C		D	F20, *UBV*
72461	9.82	0.38	10.3	0.138	4.88	9.73	0.44	BD+26 2606	O s		H	uvby, GCC
72765	9.14	0.42	8.7	0.118	3.83	9.10	0.42	HD 131448				
73614	8.39	0.42	12.7	0.094	3.92	8.33	0.44	HD 133614	C s		D	*UBV*
73798	10.06	0.56	15.6	0.111	6.02	9.93	0.63	HD 133338	C		H	*UBV*
74078	8.55	0.45	13.3	0.086	4.18	8.48	0.45	HD 133808	C W	Y	D	Walraven, *UBV*
74590	8.99	0.37	8.8	0.140	3.72	8.93	0.41	HD 135340	s		D	uvby
74994	9.12	0.39	8.3	0.139	3.72	9.07	0.38	HD 135860	s	Y	D	uvby
75432	9.72	0.53	13.2	0.114	5.33	9.64	0.53	HD 137203				
75473	9.71	0.52	12.5	0.139	5.19	9.66	0.52	BD+8 3027				
75475	9.74	0.56	12.9	0.125	5.30	9.63	0.57	HD 137028				
75618	9.80	0.56	13.2	0.122	5.41	9.74	0.56	HD 137593	C s		I	*UBV*, uvby
76670	9.34	0.50	12.4	0.122	4.81	9.30	0.51	HD 139781				
77208	9.35	0.49	11.2	0.135	4.59	9.28	0.49	HD 140849				
77326	10.58	0.67	12.9	0.135	6.13	10.48	0.85	BD−6 4279	O		D	K3V - U1
77432	9.04	0.43	10.1	0.141	4.06	8.96	0.43	HD 141011	C		D	*UBV*
77508	9.88	0.49	9.6	0.109	4.79	9.80	0.49	BD+37 2678				
78143	8.77	0.40	10.1	0.124	3.78	8.74	0.40	HD 142647				
78195	8.36	0.41	11.9	0.087	3.74	8.30	0.43	HD 143108	s		D	uvby
78251	9.06	0.61	20.8	0.077	5.66	8.96	0.64	HD 143007	O		I	*UBV*
78282	8.87	0.41	11.5	0.122	4.17	8.82	0.39	HD 143293				
78296	9.18	0.48	14.1	0.082	4.92	9.07	0.56	HD 143177	s		I	uvby
78952	9.94	0.50	12.1	0.130	5.35	9.85	0.51	HD 144454	C1		I	*UBV*
79139	7.73	0.38	15.8	0.070	3.72	7.67	0.42	HD 145184	s		I	uvby
79856	10.31	0.46	8.9	0.118	5.06	10.23	0.45	BD+77 622				
80295	10.52	0.77	20.7	0.105	7.10	10.40	1.01	LTT 6452	C1 O		D	K3V - U1
80303	9.84	0.54	13.3	0.084	5.46	9.73	0.54	BD+47 2335				
80422	8.57	0.40	10.9	0.126	3.75	8.49	0.44	HD 147685	C1 s W		D	uvby, Walraven
80448	7.33	0.30	22.0	0.128	4.05	7.33	0.64	HD 147633	C1 O		D	Dbl. C A
80781	10.86	0.79	13.9	0.116	6.57	10.74	0.80	BD+62 1487				Dbl. G
80789	10.31	0.57	11.8	0.130	5.67	10.24	0.58	G 169-13	O		I	CLLA
81013	8.95	0.42	10.1	0.124	3.97	8.90	0.44	BD+12 3035			D	VRI

Table 1 – *continued*

HIP	V_T	$(B-V)_T$	π	σ_π/π	M_V	V_1	$(B-V)_1$	ID	Phot	Spec	sd?	Comments
81170	9.72	0.69	20.7	0.072	6.30	9.60	0.74	HD 149414	C1 O s		H	uvby, F20, Dbl.
81251	10.58	0.64	12.8	0.149	6.11	10.58	0.66	BD+23 2961				Dbl. S
81350	8.86	0.41	9.6	0.119	3.77	8.81	0.40	HD 149823				
81617	8.62	0.32	10.8	0.108	3.78	8.58	0.32	HD 150147	C1 s O W		D	uvby, Walraven
82409	9.54	0.52	12.6	0.147	5.05	9.46	0.53	HD 151854	C1		D	*UBV*
82578	10.86	0.73	15.2	0.087	6.78	11.11	1.55	G 257-43			D	M dwarf
83070	8.90	0.41	9.5	0.141	3.79	8.81	0.43	HD 153150	C1			Dbl
83226	10.16	0.66	14.3	0.139	5.93	10.05	0.77	CPD −51 10106	C		D	*UBV*
83332	9.55	0.40	8.8	0.106	4.26	9.43	0.39	BD+82 507				
83443	9.26	0.52	13.5	0.116	4.91	9.25	0.53	HD 153959	C s		D	*UBV*, uvby
84754	10.23	0.78	18.4	0.106	6.55	10.04	0.84	HD 329788	C		D	*UBV*
85999	9.31	0.48	12.4	0.113	4.78	9.15	0.52	HD 159175	C W		D	Walraven, *UBV*
86183	9.37	0.40	7.4	0.109	3.73	9.38	0.33	HD 234462	O		D	*UBV*
86393	9.60	0.50	11.3	0.137	4.87	9.51	0.51	HD 159750	C		D	*UBV*
86536	9.23	0.42	11.0	0.117	4.44	9.15	0.40	HD 159753	C		D	*UBV*
88066	8.87	0.40	9.8	0.141	3.83	8.83	0.39	HD 163398	C		D	*UBV*
88084	9.34	0.56	18.1	0.077	5.62	9.19	0.62	HD 164139	C1		I	*UBV*
88231	10.15	0.52	11.1	0.149	5.38	9.98	0.52	BD−18 4758	C1		D	*UBV*
88648	10.28	0.71	15.4	0.133	6.22	10.21	0.61	HD 321320	C1 O s		H	uvby
88955	9.63	0.58	15.1	0.096	5.52	9.42	0.58	HD 165898	C1		D	Dbl. S, *UBV*
89053	10.49	0.71	16.1	0.116	6.53	10.29	0.84	CPD −50 10562	C		D	*UBV*
89215	10.37	0.75	17.0	0.112	6.52	10.37		BD+5 3640	C1 O s		H	CLLA, uvby
89396	8.05	0.43	21.0	0.054	4.66	7.99	0.43	HD 167038	C1		D	Dbl. S, *UBV*
89554	8.26	0.44	16.1	0.065	4.29	8.22	0.44	HD 166913	C s O		H	GCC, *UBV*, uvby
89734	11.10	0.76	17.0	0.084	7.24	10.98	0.78	LTT 18473				
89877	10.72	0.65	15.3	0.077	6.64	10.56	0.65	G 259-28				
89932	9.19	0.47	11.1	0.119	4.42	9.13	0.47	HD 168375	C W		D	Walraven, *UBV*
90616	10.34	0.60	11.8	0.129	5.70	10.28	0.62	BD+4 3763	C1		I	*UBV*
90724	9.61	0.54	34.3*	0.145	7.28	9.09	0.26	HD 170368	C		D	*UBV*, Sp=A7, Dbl. C C
91489	10.85	0.68	37.5	0.046	8.72	10.85		LP 355-13				Dbl. S
92277	10.59	0.62	14.1	0.137	6.33	10.34	0.70	G 21-25	C O s		D	*UBV*, CLLA
93031	9.31	0.48	12.7	0.136	4.84	9.28	0.49	HD 175479	C W		D	Walraven, *UBV*
93341	10.22	0.61	15.6	0.117	6.19	10.10	0.70	HD 230409	O s		I	uvby
93556	8.96	0.42	11.1	0.064	4.19	8.89	0.40	HD 177672				
93725	9.30	0.42	8.5	0.118	3.93	9.23	0.41	BD+31 3455				
94347	7.31	0.44	22.3	0.087	4.05	7.26	0.44	HD 174930	C s		I	*UBV*, uvby, Dbl. X
94704	11.10	0.74	11.4	0.148	6.38	11.09	0.66	G 207-23	O		H	*UBV*
95031	10.02	0.76	21.7	0.069	6.70	9.90	0.88	BD−3 4564	C O		D	*UBV*. K3V - U1
95190	9.57	0.49	11.6	0.147	4.91	9.45	0.56	HD 181376	C		H	*UBV*
95341	10.19	0.35	6.7	0.142	4.33	10.08	0.34	BD+67 1148				
95429	11.31	0.80	33.1	0.091	8.90	11.19	0.80					Dbl. S
95800	8.81	0.42	11.0	0.105	4.02	8.78	0.41	HD 182163	C O	Y	I	*UBV*
95924	9.46	0.47	10.1	0.136	4.49	9.36	0.46	HD 183705				Dbl. G
95996	10.27	0.47	9.6	0.136	5.17	10.22	0.51	BD+35 3659	O s		H	uvby
96043	9.80	0.57	13.8	0.121	5.49	9.63	0.58	HD 183639	C	Y	D	*UBV*, Dbl. G
97110	8.75	0.45	12.3	0.105	4.20	8.70	0.44	HD 186533				
97127	9.26	0.40	8.5	0.140	3.91	9.22	0.40	HD 186214	C	Y	D	*UBV*
97174	10.40	0.76	18.7	0.087	6.76	10.32	0.77	G 125-48				
97463	9.67	0.54	13.4	0.120	5.30	9.57	0.62	HD 186755	C	Y	I	*UBV*
98020	8.92	0.56	25.3	0.046	5.94	8.83	0.60	HD 188510	O s		H	F20, GCC, CLLA, uvby
98322	10.27	0.69	17.2	0.062	6.45	10.25	0.70	BD+80 642				
99267	10.15	0.51	12.0	0.094	5.55	10.11	0.51	BD+42 3607	O		H	GCC
100207	8.85	0.42	10.7	0.125	3.99	8.77	0.42	HD 192863	C	Y	D	*UBV*
100568	8.72	0.54	22.9	0.054	5.51	8.65	0.55	HD 193901	C O s		H	F20, GCC, *UBV*
101103	9.47	0.44	9.7	0.149	4.41	9.46	0.38	HD 194702	C O	Y	I	*UBV*
101650	9.36	0.44	9.0	0.146	4.14	9.33	0.44	HD 196048	C	Y	D	*UBV*
101814	10.34	0.74	16.2	0.062	6.39	10.25	0.74	BD+76 810				
101892	9.46	0.47	9.3	0.144	4.30	9.43	0.47	HD 196263	C	Y	D	*UBV*
101987	9.22	0.43	9.9	0.138	4.20	9.16	0.43	HD 196682	C	Y	D	*UBV*
101989	10.66	0.73	13.4	0.126	6.30	10.60	0.74	BD+40 4272				
103269	10.37	0.57	14.2	0.102	6.14	10.28	0.59	G 212-7	O		H	AFG, F20, CLLA
103287	9.21	0.73	26.8	0.103	6.35	9.07	0.75	BD+13 4571		Y	D	Dbl. X, LCO
103714	10.19	0.54	12.8	0.137	5.73	10.12	0.55	CPD −34 8839	C	Y	D	*UBV*
104289	10.29	0.65	14.6	0.126	6.11	10.25	0.68	HD 200855	C O s	Y	I	uvby, *UBV*
105773	7.99	0.46	17.5	0.048	4.20	7.95	0.45	HD 204093	s		D	uvby
105849	10.86	0.80	14.9	0.080	6.73	10.60	0.80	LP 75-16				
106204	10.81	0.78	22.9	0.082	7.61	10.67	1.22	CD −24 16689	C1 O	Y	D	K7V - U1
106904	10.29	0.64	13.0	0.146	5.86	10.19	0.64	HD 205682	C	Y	I	*UBV*
106924	10.53	0.55	15.2	0.080	6.44	10.36	0.55	BD+59 2407	O s		H	GCC, CLLA
107873	9.36	0.48	10.1	0.138	4.38	9.31	0.48	HD 207691	C	Y	D	*UBV*
108006	9.18	0.41	9.3^F	0.139	4.01	9.12	0.41	HD 207792	C	Y	D	*UBV*

Table 1 – *continued*

HIP	V_T	$(B-V)_T$	π	σ_π/π	M_V	V_l	$(B-V)_l$	ID	Phot	Spec	sd?	Comments
108095	8.61	0.52	19.7	0.058	5.09	8.52	0.53	HD 208068	C s	Y	I	*UBV*, uvby
108598	9.73	0.71	23.0^F	0.060	6.53	9.57	0.71	HD 208740	C s	Y	I	*UBV*, uvby
108655	8.92	0.40	10.1	0.138	3.93	8.86	0.39	BD+2 4457	C	Y	D	*UBV*
108836	11.25	0.62	24.0	0.119	8.15	10.99	1.14	LTT 8824	C		D	K dwarf
109067	9.61	0.66	21.5^F	0.074	6.27	9.55	0.67	BD+11 4725	C O s	Y	I/H	F20, CLLA, uvby
109869	9.72	0.52	13.8	0.111	5.43	9.57	0.52	HD 211127	C O	Y	D	*UBV*
109945	9.23	0.42	9.4	0.138	4.09	9.18	0.41	BD+17 4720	C	Y	D	*UBV*
110621	9.06	0.42	9.7	0.130	3.99	9.01	0.41	HD 212457		Y	I	LCO
110776	9.80	0.79	21.7^F	0.067	6.48	9.70	0.82	HD 212753	C O s	Y	I	CLLA, uvby
111374	7.90	0.41	15.1	0.067	3.80	7.86	0.42	HD 213763	C s	Y	D	uvby, *UBV*
111426	9.39	0.46	11.0	0.109	4.59	9.35	0.46	HD 213670	C	Y	D	*UBV*
111871	10.53	0.74	15.5	0.117	6.49	10.47	1.31	BD+10 4791	C O s		D	*UBV*, uvby, CLLA
112384	9.06	0.43	9.6	0.142	3.97	9.02	0.43	HD 215437	C	Y	I	*UBV*
112389	11.05	0.80	26.0	0.082	8.12	10.76	1.59	AC+18 1061	C O		D	M dwarf
113430	8.10	0.46	16.8	0.052	4.22	8.05	0.48	HD 216924	C s	Y	D	*UBV*, uvby
113542	8.79	0.40	10.8	0.101	3.97	8.75	0.39	HD 217337	s O	Y	D	uvby
113868	10.18	0.68	14.6	0.123	6.01	10.10	0.68	HD 217740	C	Y	D	*UBV*, Dbl. S
114125	10.00	0.57	13.4	0.119	5.63	9.89	0.57	BD+33 4648				
114271	8.30	0.44	14.3	0.084	4.08	8.25	0.41	HD 219181	C	Y	H	F20, *UBV*
114299	9.20	0.42	9.6	0.131	4.12	9.16	0.41	BD+43 4402				
114487	8.47	0.40	12.0	0.094	3.85	8.40	0.39	HD 218810	C	Y	I	*UBV*
114627	8.91	0.47	14.0	0.105	4.64	8.86	0.47	HD 219101	C		D	*UBV*
114735	8.57	0.40	11.5	0.111	3.88	8.51	0.40	HD 219242	C	Y	I	*UBV*
114837	9.96	0.47	10.1	0.147	4.98	9.89	0.58	HD 219369	C s	Y	I	*UBV*, uvby
115031	8.35	0.47	15.7^F	0.085	4.33	8.28	0.47	HD 219678	C	Y	D	*UBV*, Dbl. O
115194	8.97	0.77	31.5	0.038	6.47	8.87	0.81	HD 219953	s	Y	I	uvby
115361	8.17	0.44	15.3	0.072	4.10	8.13	0.44	HD 220164	C s	Y	D	uvby, *UBV*
116437	9.94	0.40	9.3	0.145	4.79	9.80	0.57	CPD −43 9761	C	Y	D	*UBV*
117121	11.60	0.58	19.9	0.143	8.10	11.60		BD−21 6469	C	Y	D	M dwarf
117242	8.84	0.43	10.8	0.110	4.01	8.80	0.40	HD 236211	O		D	*UBV*
117823	9.42	0.47	11.0	0.119	4.62	9.33	0.50	HD 223923	C	Y	I	*UBV*
117882	9.27	0.48	11.9*	0.122	4.64	9.24	0.45	HD 224040	C s	Y	D	uvby, *UBV*
118165	9.19	0.42	9.2	0.141	4.02	9.14	0.42	HD 224463	C	Y	D	*UBV*

^{F} in column 5 indicates that the goodness-of-fit statistic, $|F|$, listed in the *Hipparcos* catalogue exceeds 2.5, and that the astrometric solution is not reliable.
* in column 5 indicates that the parallax given in the *Hipparcos* catalogue has been revised (see Section 2.2).
Column 10 lists the available photometry: s, Strömgren; W, Walraven; O, *UBV*(*RI*) (literature); C & C1, *UBVRI* (SAAO), C1 indicating single-epoch observations.
Column 12 (sd?) gives our final abundance classification: D ≡ [m/H] ≥ −0.3; I ≡ − 0.3 > [m/H] ≥ −1; H ≡ [m/H] ≤ −1
Column 13 identifies known double stars and gives the basis for the abundance classification: *UBV*–$\delta_{0.6}$/[Fe/H] calibration (Section 4); *uvby* – Strömgren data (Section 3.1); Walraven photometry (Section 3.2); or spectroscopic measurements, referenced as follows: AFG – Axer et al., 1994; CLLA – Carney et al., 1994; F20 – Fulbright 2000; GCC – Gratton et al., 1997; LCO – this paper; RN – Ryan & Norris 1991; U1 – Upgren 1972.
Stars classed as double in the *Hipparcos* catalogue are flagged as Dbl.
Dbl. G indicates the presence of an acceleration term in the *Hipparcos* solution, interpreted as motion in an unresolved binary system;
Dbl. C identifies separately resolved components, solutions with quality A–D;
Dbl. O indicates full orbital solutions;
Dbl. X indicates problems with both single-star and binary *Hipparcos* solutions;
Dbl. S flags suspected double stars. See *Hipparcos* catalogue for full details.

disc main sequence. Fig. 2 plots the Tycho photometry for the 317 stars which match these criteria.[3] Our aim is to sift through this sample, using additional data from the literature, together with our own observations, to eliminate interlopers and identify *bona fide* subdwarfs for future detailed study.

Table 1 lists the *Hipparcos* astrometry and photometry for the candidate subdwarfs plotted in Fig. 2. We list both the *Hipparcos* catalogue number and a more conventional designation. In addition to the Tycho photometry, we include the *BV* literature data cited in the catalogue. A cursory inspection shows that several of the latter measurements are in significant disagreement with the Tycho data. Indeed, as discussed further below, the majority of those stars prove to have entered the present sample due to errors in V_T and B_T.

[3]The *Hipparcos* catalogue includes a number of stars lacking Tycho photometry. Those stars are obviously not included in our present exercise, nor have we eliminated stars with significant formal errors in the Tycho photometry.

The sample outlined in Table 1 forms the starting point for the current investigation. A number of stars have spectroscopic abundance measurements, as described in Section 3. Subsequent sections outline supplementary photometric and spectroscopic observations, drawn both from the literature (based on the extensive cross-referencing in the SIMBAD data base) and from our own observations. Column 10 in Table 1 indicates which stars have accurate ground-based photometry [in addition to the literature-derived V, $(B-V)$ values cited in the *Hipparcos* catalogue, which we denote as V_l and $(B-V)_l$ in Table 1]: s indicates Strömgren photometry (Section 4.1); W, Walraven photometry (Section 4.2); O, Johnson/Cousins *UBVRI* literature data (Section 5.2), and C and C1, Johnson/Cousins *UBVRI* photometry from SAAO observations, where C1 indicates observations at only one epoch (Section 5.3). Column 11 flags stars with spectroscopic observations from Las Campanas (Section 6). Column 12 summarizes our main conclusions by identifying those stars confirmed as likely to have [m/H] < −1

('H', halo subdwarfs); stars of probable intermediate abundance, $-1 > [m/H] > -0.3$ ('I'); and stars likely to have near-solar abundances ('D', disc dwarfs). Finally, column 13 cites the relevant references for the adopted classification.

2.2 A priori exclusions

The stars listed in Table 1 have been selected solely on the basis of parameters given in the published *Hipparcos* catalogue. However, auxiliary criteria can be used to eliminate a number of candidates at the outset. First, five stars are known to be members of nearby stars clusters: HIP 17481 (HD 23290) and HIP 17497 (HD 23289) are both main-sequence members of the Pleiades cluster; HIP 20527 (VR 9), HIP 21261 (Leiden 65) and HIP 22177 (Leiden 119) are known to be M dwarfs in the Hyades cluster. In the case of the Pleiades stars, the *Hipparcos* parallax is overestimated by ~2 mas, while the $(B-V)_T$ colours measured for all three Hyads are all ~0.6 mag too blue.

Second, the formal *Hipparcos* astrometric solutions are known to be unreliable if the target star is a close double. 39 stars in Table 1 are identified as double stars or suspected binaries in the *Hipparcos* catalogue. Of the systems with resolved components (flagged as Dbl. C in Table 1), two are listed as having solutions of quality C (HIP 65201 and 90216), and two as quality D (HIP 10529 and 44436). We have not excluded these systems from consideration, but will interpret the results accordingly.

In some cases, more accurate astrometry can be derived by re-analysing the individual *Hipparcos* measurements. Both Falin & Mignard (1999) and Fabricius & Makarov (2000a) have undertaken such an exercise, and their results show that trigonometric parallaxes of at least two stars listed in Table 1 require revision: re-analysing data for HIP 21000 (BD +4°701A) indicates that π_{Hip} is overestimated by 76 mas, while the catalogued parallax of HIP 90724 (HD 170368) should be reduced by 27 mas. In both cases, the revised parallaxes are ~7 mas, with uncertainties of ~15 per cent. As discussed later, accurate *UBVRI* photometry is consistent with the larger distances and higher luminosities, and both stars are clearly ruled out as possible metal-poor subdwarfs.

Finally, the *Hipparcos* catalogue cites a goodness-of-fit statistic (which we denote $|F|$) for the astrometric solution obtained for most stars (stars flagged as Dbl. X are exceptions). Solutions where $|F|$ is greater than 2.5 can generally be regarded as suspect. 17 stars in Table 1 exceed that limit, and these stars can be eliminated as potential subdwarf calibrators.

3 PREVIOUS SPECTROSCOPIC OBSERVATIONS

A sizeable minority of the sample listed in Table 1 are known metal-poor subdwarfs or subgiants, with previous spectroscopically based abundance determinations. Those stars are useful benchmarks in assessing the accuracy of both photometric abundance estimates and of our own spectrophotometry (Section 6). Table 2 summarizes those data, drawn from seven main sources: low-resolution spectroscopy by Ryan & Norris (1991, hereafter RN), Carney et al.'s (1994, hereafter CLLA) analysis of high-resolution data centred on the Mgb feature; and conventional high-resolution spectroscopic analysis by Axer et al. (1994, hereafter AFG), Gratton et al. (1996, hereafter GCC), Ryan & Deliyannis (1998, hereafter RD), Clementini et al. (1998, hereafter Cl1) and Fulbright (2000, hereafter F20). Several well-known halo stars, such as HD 19445, 64090 and 84937, have numerous abundance determinations; our tabulation is representative, rather than exhaustive. As discussed by Reid (1998) and Clementini et al. (1999), systematic differences exist between the abundance scales used in some of these analyses; in particular, CLLA and RN tend to derive lower abundances for metal-poor ([m/H] < −1) stars. Given our current aims, however, we have not attempted to adjust all measurements on to a single, self-consistent scale.

Table 2. Stars with spectroscopic abundance estimates.

HIP	[m/H]	ref.	HIP	[m/H]	ref.
5004	−1.02	RN	50965	−0.39	RN
7459	−1.17	RN	51769	−0.65	CLLA
8130	−0.64	CLLA	51769	−1.25	RN
8558	−1.10	RN	53070	−1.38	GCC
12579	−0.86	CLLA	53070	−1.55	F20
12579	−0.78	AFG	53070	−1.34	Cl1
14594	−1.87	AFG	54641	−1.04	AFG
14594	−1.89	GCC	54641	−1.01	RN
14594	−2.13	F20	55790	−1.56	AFG
14594	−1.97	Cl1	57360	−1.20	AFG
16404	−1.92	AFG	57360	−1.22	RN
16404	−1.92	GCC	57450	−1.26	GCC
17085	−0.22	F20	57939	−1.22	GCC
19007	−0.62	F20	57939	−1.46	F20
19797	−1.33	AFG	57939	−1.30	Cl1
19797	−1.57	GCC	59750	−0.78	F20
19797	−1.68	F20	60632	−1.38	AFG
21000	−0.16	F20	60632	−1.55	GCC
21586	−0.91	F20	60632	−1.65	F20
21609	−1.76	F20	63063	−0.48	CLLA
21767	−0.44	F20	63970	−0.09	F20
22246	−0.22	CLLA	64386	−0.84	CLLA
22246	−0.38	F20	65040	−0.82	CLLA
22632	−1.59	F20	65201	−1.86	GCC
24316	−1.44	GCC	66815	−0.64	F20
24316	−1.71	F20	70681	−1.25	F20
26452	−0.89	CLLA	71886	−0.40	F20
26676	−1.17	CLLA	71887	−0.49	F20
26676	−1.02	RN	71939	−0.37	F20
26688	−0.60	F20	72461	−2.07	AFG
28188	−0.62	F20	72461	−2.29	GCC
31639	−0.62	F20	80789	−0.96	CLLA
34146	−0.40	F20	81170	−1.26	F20
34548	−0.46	F20	81170	−1.14	Cl1
36491	−0.81	CLLA	89215	−1.36	CLLA
36491	−1.02	AFG	89554	−1.44	AFG
36491	−0.85	RN	89554	−1.44	GCC
36491	−0.93	F20	92277	0.01	CLLA
36491	−0.88	Cl1	98020	−1.62	AFG
36818	−0.75	RN	98020	−1.38	GCC
38541	−1.69	AFG	98020	−1.67	F20
38541	−1.60	GCC	99267	−2.01	AFG
38541	−1.79	F20	100568	−1.00	GCC
38541	−1.54	Cl1	100568	−1.17	F20
40778	−1.70	F20	103269	−1.78	CLLA
44116	−0.58	F20	103269	−1.60	AFG
44124	−1.90	CLLA	103269	−1.81	F20
44124	−2.20	RN	106924	−1.91	CLLA
44124	−1.96	F20	106924	−1.62	Cl1
46120	−2.10	RD	109067	−0.97	F20
47640	−0.08	F20	109067	−0.95	CLLA
48146	−0.05	F20	110776	−0.46	CLLA
48152	−2.07	GCC	111871	−0.50	CLLA
48152	−2.08	F20	114271	−1.80	F20

See text for references.

Table 3. Strömgren photometry of candidate subdwarfs

HIP	V	$b-y$	m_1	c_1	M_V	[m/H]	ref	Comments
435	9.290	0.336	0.100	0.387	4.354	−0.97	O1	
3139	9.269	0.292	0.130	0.412	3.941	−0.49	HM	
4981	9.110	0.380	0.147	0.356	5.313	−0.58	HM	
5004	10.258	0.472	0.248	0.169	6.319	−1.13	S1	
5896	4.856	0.312	0.168	0.444	3.303	0.02	HM	
7459	10.123	0.365	0.092	0.231	5.445	−1.09	S1	
7687	9.364	0.470	0.309	0.250	6.422	−0.34	Ol1	
8130	10.170	0.432	0.203	0.270	5.435	−0.47	S2	
10360	8.530	0.198	0.175	0.648			HM	blue straggler
14594	8.056	0.351	0.058	0.208	5.114	−1.71	HM	
15998	10.165	0.500	0.395	0.307	6.292	−0.08	S2	
16404	9.939	0.451	0.089	0.122	6.167	−1.91	HM	binary
17481	8.702	0.236	0.159	0.627	3.724	−0.05	Ol2	
17497	9.000	0.263	0.158	0.525	3.956	−0.06	HM	
19215	9.000	0.235	0.169	0.639	3.771	0.09	HM	
19797	9.234	0.322	0.071	0.292	4.770	−1.52	HM	
21609	9.940	0.452	0.106	0.132	6.092	−1.81	S1	binary
22632	9.138	0.358	0.068	0.244	5.104	−1.47	Ol2	
24316	10.476	0.371	0.060	0.205	6.298	−1.60	S1	
25717	8.194	0.289	0.150	0.470	3.862	−0.19	HM	
26676	10.195	0.435	0.171	0.155	5.972	−1.29	S1	
30481	8.270	0.262	0.127	0.451	3.789	−0.55	HM	
34146	8.058	0.299	0.140	0.402	4.037	−0.35	HM	
36491	8.480	0.373	0.117	0.282	4.985	−0.84	Ol2	
36818	10.566	0.384	0.143	0.203		−0.92	S1	
38541	8.282	0.430	0.109	0.116	6.021	−1.75	HM	binary
39911	9.584	0.404	0.144	0.236	5.464	−0.92	Ol2	
40778	9.716	0.339	0.071	0.258	4.801	−1.45	HM	
42278	7.790	0.243	0.157	0.519	3.685	−0.08	HM	
43445	8.647	0.320	0.121	0.355	4.299	−0.65	F1	
44116	8.492	0.299	0.120	0.394	4.011	−0.65	F1	
44124	9.653	0.349	0.076	0.250	5.120	−1.34	HM	
44435	7.390	0.237	0.158	0.528	3.241	−0.06	T1	
46120	10.118	0.399	0.086	0.116	6.205	−1.72	S1	
46250	8.382	0.294	0.157	0.448	4.174	−0.10	HM	
46509	4.599	0.296	0.164	0.451	3.435	0.00	HM	
48152	8.342	0.302	0.054	0.369	3.809	−2.24	HM	
50965	9.793	0.377	0.145	0.305	4.727	−0.59	S2	
51769	10.479	0.425	0.202	0.206	6.527	−0.76	S1	
53070	8.229	0.344	0.079	0.258	4.646	−1.29	HM	binary
54641	8.165	0.335	0.084	0.300	4.417	−1.22	Ol2	
55790	9.076	0.343	0.063	0.275	4.283	−1.62	S1	binary?
55978	9.039	0.257	0.167	0.555	3.634	0.07	HM	
57360	8.740	0.333	0.079	0.297	4.225	−1.31	S1	binary?
57450	9.909	0.398	0.099	0.179	5.577	−1.45	HM	
57939	6.427	0.484	0.222	0.155	6.618	−1.41	HM	
59258	7.506	0.245	0.132	0.490	3.696	−0.48	Ol3	
60632	9.671	0.330	0.059	0.287	4.878	−1.79	S1	binary?
60852	8.483	0.314	0.128	0.368	4.275	−0.54	HM	
62261	9.400	0.267	0.149	0.469	4.147	−0.20	HM	
63063	9.920	0.475	0.325	0.264	6.348	−0.25	S2	
63553	8.506	0.274	0.161	0.401	3.733	−0.02	HM	
64386	9.888	0.413	0.170	0.236	5.665	−0.74	S1	
64765	8.843	0.253	0.152	0.566	4.030	−0.15	F2	
65040	9.778	0.418	0.174	0.245	5.716	−0.71	S1	
65201	8.807	0.349	0.050	0.278	4.759	−1.96	S1	binary?
65268	7.656	0.307	0.111	0.384	4.050	−0.79	K1	
66500	9.600	0.303	0.140	0.405	4.322	−0.35	HM	
67655	7.969	0.424	0.173	0.207	5.979	−0.92	S1	
68165	9.970	0.523	0.417	0.275	6.612	−0.23	S1	
70152	10.571	0.567	0.527	0.280	6.466	−0.03	S1	
70681	9.300	0.400	0.130	0.191	5.717	−1.16	S1	
72461	9.730	0.332	0.052	0.289	4.794	−2.00	HM	
72765	9.110	0.265	0.151	0.538	3.808	−0.17	HM	
73614	8.349	0.271			3.868		Ol2	
74590	8.927	0.250	0.163	0.579	3.649	0.01	HM	
74994	9.092	0.248	0.170	0.656	3.687	0.11	HM	
75618	8.877	0.362	0.140	0.501	4.480	−0.56	HM	
78195	8.298	0.274	0.144	0.483	3.676	−0.27	Ol2	
78296	9.075	0.351	0.090	0.209	4.821	−1.11	M1	
79139	7.685	0.263	0.124	0.477	3.678	−0.61	HM	

Table 3 – *continued*

HIP	V	$b-y$	m_1	c_1	M_V	[m/H]	ref	Comments
80422	8.492	0.280	0.141	0.479	3.679	−0.32	HM	
81170	9.611	0.474	0.202	0.159	6.191	−1.39	HM	binary
81617	8.576	0.206	0.164	0.721	3.743	0.17	HM	
83443	9.252	0.333	0.160	0.339	4.904	−0.17	M1	
88648	10.201	0.430	0.078	0.159	6.139	−1.80	S2	binary?
89215	10.348	0.474	0.261	0.141	6.500	−1.34	S1	
89554	8.233	0.327	0.074	0.309	4.267	−1.43	HM	
93341	10.103	0.440	0.202	0.210	6.069	−0.83	HM	
94347	7.259	0.312	0.107	0.366	4.001	−0.85	HM	
95996	10.238	0.355	0.073	0.231	5.149	−1.38	S1	binary?
98020	8.836	0.416	0.100	0.163	5.852	−1.57	S1	binary?
100568	8.660	0.381	0.103	0.217	5.459	−1.27	HM	
104289	10.246	0.434	0.198	0.231	6.068	−0.70	HM	
105773	7.964	0.306	0.144	0.379	4.179	−0.30	HM	
108095	8.523	0.375	0.139	0.297	4.995	−0.64	HM	
108598	9.564	0.486	0.274	0.254		−0.52	Ol1	
109067	9.556	0.423	0.180	0.223		−0.79	S1	
110776	9.670	0.492	0.332	0.256		−0.36	S1	
111374	7.860	0.281	0.151	0.465	3.755	−0.17	Ol2	
111871	10.448	0.468	0.302	0.286	6.400	−0.14	S1	
113430	8.056	0.300	0.149	0.415	4.183	−0.22	T1	
113542	8.760	0.262	0.156	0.506	3.927	−0.09	HM	
114837	9.879	0.362	0.151	0.350	4.901	−0.44	O1	
115194	8.849	0.488	0.319	0.249	6.341	−0.41	S1	
115361	8.115	0.305	0.138	0.405	4.038	−0.39	Ol1	
117882	10.288	0.327	0.195	0.454	5.666	0.37	HM	

Stars lacking M_V estimates have $|F| > 2.5$ (see Section 2.2 and Table 1).
References: F1 – Ferro et al. 1990; F2 – Franco 1994; HM – Hauck & Mermilliod 1998; K1 – Knude 1981; M1 – Manfroid et al. 1987; O1 – Oblak 1990; Ol1 – Olsen 1994a; Ol2 – Olsen 1994b; S1 – Schuster & Nissen 1988; S2 – Schuster et al. 1993; T1 – Twarog 1980.

4 INTERMEDIATE-BAND PHOTOMETRIC OBSERVATIONS

4.1 Strömgren photometry

The *uvby* system devised by Strömgren (1966) provides an effective means of estimating the physical properties of F- and G-type stars. The $(b-y)$ colour is correlated with effective temperature, while the m_1 index, defined as

$$m_1 = (v-b) - (b-y),$$

measures metallicity by determining the relative line−blanketing in blue and ultraviolet passbands. Finally, the c_1 index, defined as

$$c_1 = (u-v) - (v-b),$$

is gravity-sensitive, allowing separation of main-sequence dwarfs and subgiants.

We have located Strömgren photometry of 97 stars from Table 1, notably from Hauck & Mermilliod's (1998) *uvby* catalogue. Table 3 lists the relevant data, together with the source of the photometry. We have used the relations derived by Schuster & Nissen (1989) to derive abundance estimates for those stars with measured m_1 and c_1 indices. As discussed by Reid (1998), there are systematic offsets between high-resolution spectral analyses and this calibration, partially tied to the revision in the value for the solar iron abundance (see Biémont et al. 1991). However, the discrepancies are generally less than 0.2 dex, as illustrated in Fig. 3.

We have combined *Hipparcos* parallax measurements with the *V*-band data listed in Table 3 to derive absolute visual magnitudes M_V. Fig. 4 plots the resulting $[M_V, (b-y)]$ colour–magnitude diagram. Since we are considering each programme star individually, we have not applied Lutz–Kelker corrections. As a reference disc sequence, we plot data for stars with Strömgren abundances $[\mathrm{m/H}] > -0.25$ (from Schuster & Nissen 1988), together with observations of members of the Hyades cluster (Crawford & Perry 1966). Distances for the latter stars are derived from their proper motions and the *Hipparcos* determination of the average convergent point (Perryman et al. 1998).

Several stars deserve special mention. The bluest star listed in Table 3 is HIP 10360, which is classified as a field blue straggler by Bond & MacConnell (1971); the goodness-of-fit statistic, $|F|$, is 3.51, indicating unreliable *Hipparcos* astrometry. Two other stars listed in Table 4, HIP 36818 and 109067, are moderately metal-poor, but lack accurate parallax data. The bluest star plotted in Fig. 4 is HIP 81617, which lies close to the Galactic plane and has near-solar abundance. As discussed further in Section 4.2, this is probably a reddened, early-type main-sequence star. Finally, the *Hipparcos* catalogue lists identical parallax measurements for HIP 44436 and 44435. We include Strömgren photometry of HIP 44435 (HD 78084) in Table 3; however, as discussed further in Section 6, spectroscopy shows that the two stars are unrelated.

Considering the other stars in Table 3, 19 have photometric abundances $[\mathrm{Fe/H}]_S < -1.4$. These are plotted as solid points in Fig. 4, and many lie closer to the disc main sequence than might be expected. Several are known binaries, notably HIP 16404 (BD +66°268), HIP 21609 (HD 29907) and HIP 38541 (HD 64090). The four stars which fall significantly below the main group of subdwarfs are HIP 24316, 46120, 109067 and 117882. Only HIP 24316 (HD 34328) and HIP 46120 (Gl 345) have photometric abundances $[\mathrm{Fe/H}]_S < -1.4$. Both Strömgren photometry and our spectroscopic observations (Section 6.2) of the last star, HIP 117882 [HD 224040; $(b-y) = 0.327$], indicate near-solar

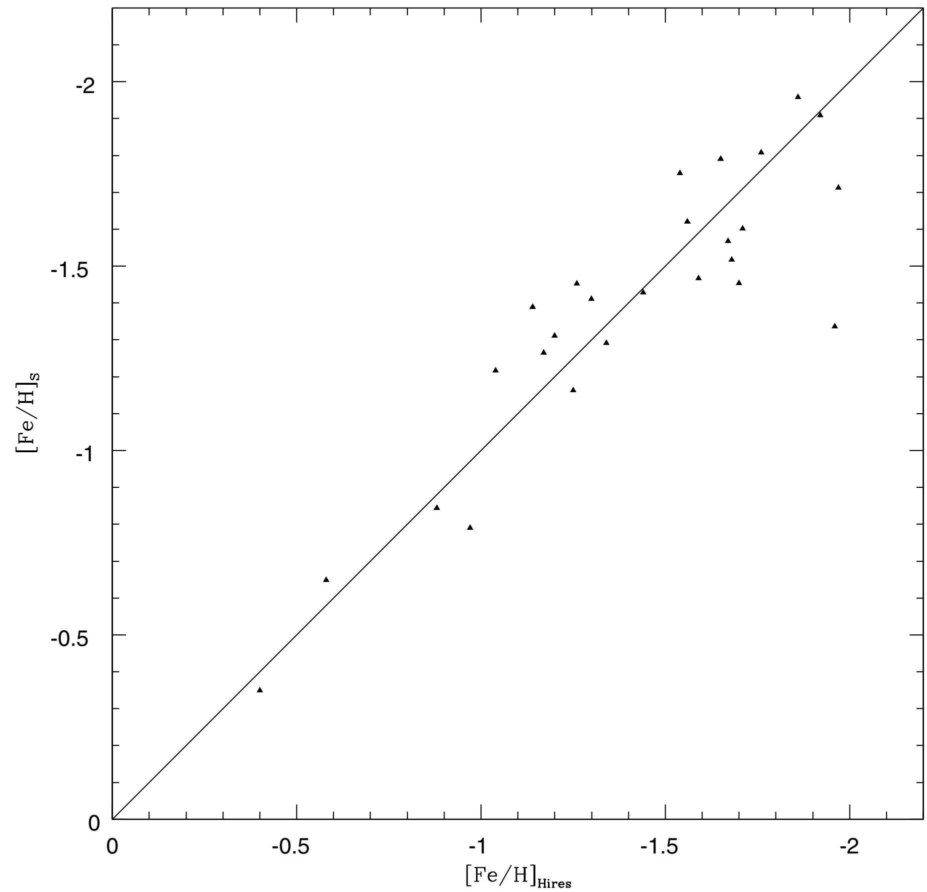

Figure 3. A comparison of abundances derived using Schuster & Nissen's (1989) calibration of Strömgren photometry against results from conventional, high-resolution spectroscopic analysis.

Table 4. Walraven photometry of candidate subdwarfs.

HIP	Name	V	$V-B$	$B-U$	$U-W$	$B-L$
51300	HD 91043	−0.9313	0.1771	0.3142	0.1669	0.1939
55978	HD 99805	−0.8785	0.1631	0.3482	0.1845	0.2063
60251	HD 107440	−0.8755	0.2303	0.3064	0.1899	0.2274
74078	HD 133808	−0.6397	0.1958	0.3083	0.1814	0.2069
80422	HD 147685	−0.6591	0.1749	0.3131	0.1728	0.1928
81617	HD 150147	−0.6795	0.1365	0.3838	0.1678	0.1970
85999	HD 159175	−0.9128	0.2325	0.2714	0.1935	0.2021
89932	HD 168375	−0.9010	0.2275	0.2980	0.1890	0.2246
93031	HD 175479	−0.9679	0.2271	0.2977	0.1939	0.2230

abundance. The star is double (CCDM 23546−2302), and the *Hipparcos* double-star annex lists a parallax of 8.6 mas for each component (as opposed to 11.9 mas in the main catalogue), but it seems likely that even this value is an overestimate.

4.2 Walraven photometry

The Walraven photometric system covers the wavelength range from 5700 Å to the ultraviolet atmospheric cut-off with a series of five intermediate- and narrow-band filters (Lub & Pel 1977). The $[(B-L), (V-B)]$ two-colour diagram is particularly sensitive to abundance variations (and insensitive to changes in gravity). Nine stars from Table 1, lying near the Galactic plane, have Walraven photometry by de Geus et al. (1990). All are expected to be early-type disc dwarfs at distances exceeding 100 pc.

Fig. 5 plots data for the five stars, superimposed on the full catalogue of AFG dwarfs observed in the de Geus et al. (1991) survey. As the figure shows, subdwarfs with $[m/H] < -1$ lie over 0.05 mag blueward of the disc main sequence in $(V-B)$. None of the stars listed in Table 4 falls above the $[m/H] = -1.0$ sequence, and only HIP 60251 (HD 107440) appears likely to have an abundance significantly below the solar value. Our *UBV* observations of the last-mentioned star, discussed in the following section, reveal only a modest ultraviolet excess, while spectroscopy (Section 6.2) shows line strengths consistent with an abundance within a factor of 2 of the solar value. We conclude that none of the stars listed in Table 4 is a halo subdwarf.

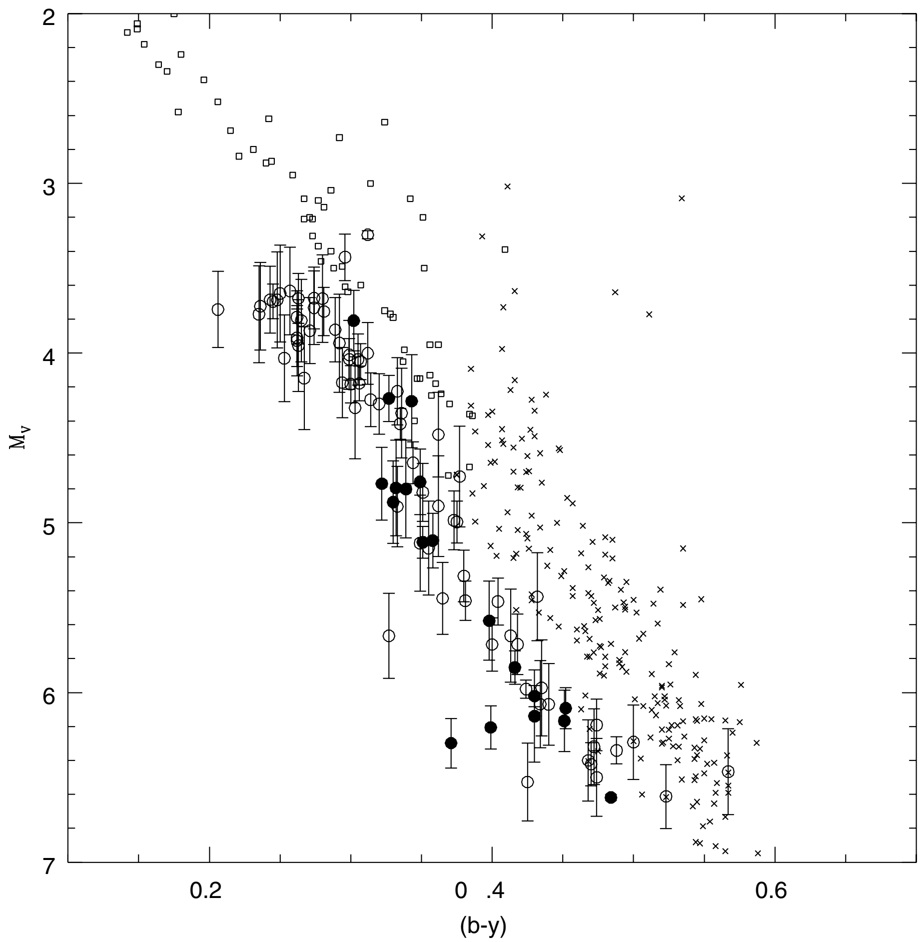

Figure 4. The $[M_V, (b-y)]$ diagram: crosses mark stars with $[m/H] < -0.25$ from Schuster & Nissen (1988) and Schuster et al. (1993); points with error bars plot data for stars from Table 3, where solid points identify stars with $[m/H] < -1.3$. Open squares mark stars in the Hyades cluster (Crawford & Perry, 1969).

5 BROAD-BAND PHOTOMETRIC OBSERVATIONS

5.1 Ultraviolet excess and stellar abundances

The Johnson–Cousins *UBVRI* system is by far the most widely used broad-band photometric system. The main characteristics are described by Bessell (1979, 1983). The *U*-band covers the wavelength range from the atmospheric cut-off (~3200 Å) to ~3950 Å. As a result, the total flux in *U* depends strongly on the extent of line blanketing, and hence the abundance of heavy elements. Shortly after the inception of the *UBV* system, Wallerstein & Carlson (1960) showed that ultraviolet excess, defined as

$$\delta(U-B) = (U-B)_{\mathrm{Hyades}} - (U-B)_{\mathrm{obs}},$$

could be calibrated against stellar metallicity, [Fe/H] (where Fe is taken as representative of all metals).

The degree of excess ultraviolet flux at a given chemical abundance depends on the effective temperature, with the maximum variation occurring at $(B-V) = 0.6$ mag. Sandage (1969) took this variation into account by using differential blanketing calculations by Wildey et al. (1962) to compute the correction factors required to scale an observed $\delta(U-B)$ to the appropriate value for a star at $(B-V) = 0.6$, $\delta_{0.6}$. Carney (1979) compiled data for stars with high-resolution spectroscopic abundance analyses, and derived a relation between $\delta_{0.6}$ and [Fe/H]. As noted above, there have been changes in both the zero-point and the scale of abundance determinations since Carney's analysis, so we have recomputed the calibration. Using *UBV* photometry from Carney (1979) and CLLA, we have calculated $\delta_{0.6}$ for 42 stars with [Fe/H] measurements by either GCC or AFG. The relevant data are listed in Table 5. The best-fitting second-order polynomial is

$$[\mathrm{Fe/H}] = 0.203 - 5.517\delta_{0.6} - 5.512\delta_{0.6}^2.$$

Fig. 6 compares our revised calibration against Carney's original relation. The main discrepancies lie at abundances below $[\mathrm{Fe/H}] = -1.0$.

The dispersion about the mean relation is significant: $\sigma_{[\mathrm{Fe/H}]} = 0.26$ dex, with the uncertainties increasing with decreasing abundance. Moreover, Fig. 7 shows that the majority of the calibrating stars fall within a relatively restricted range in $(B-V)$ colour. However, our main purpose is identifying candidate subdwarfs, rather than deriving accurate abundances. Fig. 6 shows that stars with halo-like abundances ($[\mathrm{Fe/H}] < -1$) can be expected to have ultraviolet excess values of $\delta_{0.6} > 0.18$ ($[\mathrm{Fe/H}] = -0.97$ dex from our calibration). We adopt this as our primary selection criterion in identifying new subdwarf candidates from *UBV* data.

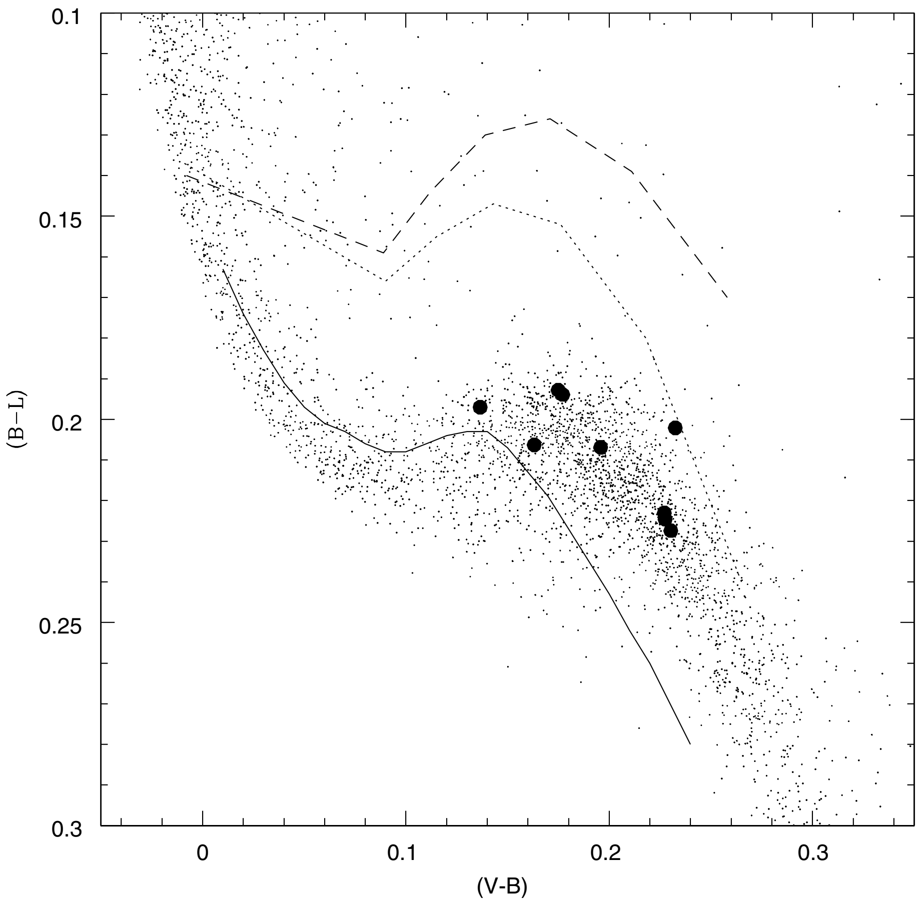

Figure 5. The Walraven [$B - L$), ($V - B$)] two-colour diagram from de Geus et al. (1990). The solid line plots the Hyades sequence, the dotted line marks the predicted location of [m/H] = −1.0 subdwarfs, and the dashed line plots the expected [m/H] = −2.0 sequence (from Lub & Pel 1977). The nine stars listed in Table 4 are plotted as filled circles, and none lie above the [m/H] = −1.0 sequence outlined by the stellar models.

5.2 Published *UBVRI* observations of candidate subdwarfs

Using the SIMBAD data base, we have located 76 *UBVRI* photometric observations of 69 stars from Table 1. These data are listed in Table 6, where we list *R* and *I* magnitudes on the Cousins system, using the relations given by Bessell (1979, 1983) and Bessell & Weis (1987) to transform data where necessary. We note that several subdwarfs (e.g., HD 19445) have Johnson *RI* photometry from the 1960s: we have not included those data in the current compilation.

Fig. 8 plots the $(U-B)/(B-V)$ two-colour diagram, and Fig. 9 shows the location of these stars on the [M_V, $(V - I)$] and [M_V, $(B - V)$] colour–magnitude planes. As with the Strömgren and Walraven data sets, the majority have photometric properties consistent with abundances [Fe/H] > -1. Indeed, several stars are identified as late-type K or early-type M dwarfs with highly discrepant Tycho photometric colours. Of the relatively small number of stars in Table 6 identified as having halo-like abundances, most are well-known subdwarfs. Only HIP 94704 (G207-23) stands out as a possible addition to current samples, and that star has a $\delta_{0.6}$ abundance of [Fe/H] = −1.0, close to the upper boundary of the halo distribution.

5.3 SAAO *UBVRI* observations

In addition to compiling literature photometry, we have undertaken a programme of new observations using the facilities at the Sutherland station of the South African Astronomical Observatory (SAAO). Between two and four photometric measurements have been obtained of 175 stars from Table 1. In addition, *UBVRI* data have been obtained for 13 known metal-poor subdwarfs. Combined with the literature data discussed above, these measurements provide the first extensive, reliable Cousins *R*- and *I*-band data for metal-poor dwarfs with accurate trigonometric parallax measurements.

The observations were made between 1998 July and 1999 December using the modular photometer on the 0.5-m telescope. The photometer employs a Hamamatsu R943-02 (GaAs) photomultiplier and a Johnson–Cousins *UBVRI* filter set (Kilkenny et al. 1998). The data were reduced using standard techniques, and calibrated through observations of E-region standard stars (Cousins 1973; Menzies et al. 1989). Full details on the techniques employed are given by Kilkenny et al. (1998). Table 7 lists the derived colours and magnitudes for the *Hipparcos* candidate subdwarfs; 23 stars were observed at only one epoch, and these data are listed separately at the end of the table. Table 8 presents SAAO data for additional subdwarfs, where we also list *Hipparcos* astrometry (G113-26 was not observed by *Hipparcos*) and, if appropriate, inferred absolute magnitudes.

All of the programme stars are bright and, as a result, the photometric uncertainties are typically less than 0.01 mag in *V* and in each colour. Six stars have *V*-band photometric uncertainties exceeding 0.015 mag. These include the known variable TW

Table 5. Abundance standards for $\delta_{0.6}$ calibration.

Name	$\delta_{0.6}$	$(U-B)$	$(B-V)$	[Fe/H]
HD 3567	0.195	−0.160	0.460	−1.17
HD 16031	0.257	−0.210	0.440	−1.66
HD 19445	0.284	−0.240	0.460	−1.88
HD 22879	0.163	−0.080	0.540	−0.76
HD 25329	0.211	0.380	0.860	−1.69
HD 30649	0.103	0.020	0.590	−0.46
HD 59374	0.175	−0.110	0.520	−1.02
HD 63077	0.173	−0.070	0.570	−0.78
HD 64090	0.262	−0.120	0.610	−1.60
HD 64606	0.140	0.170	0.730	−0.93
HD 69611	0.135	−0.020	0.580	−0.55
HD 74000	0.281	−0.230	0.430	−1.52
HD 84937	0.275	−0.200	0.370	−2.04
HD 91324	0.055	−0.020	0.500	−0.23
HD 94028	0.213	−0.170	0.470	−1.38
HD 103095	0.194	0.160	0.750	−1.22
HD 108177	0.270	−0.220	0.430	−1.55
HD 114762	0.141	−0.080	0.520	−0.67
HD 118659	0.136	0.090	0.680	−0.59
HD 134169	0.154	−0.070	0.550	−0.68
HD 134439	0.203	0.170	0.760	−1.57
HD 134440	0.310	0.360	0.870	−1.57
HD 136352	0.118	0.060	0.640	−0.21
HD 140283	0.282	−0.220	0.490	−2.38
HD 148816	0.141	−0.070	0.530	−0.68
HD 157089	0.103	−0.010	0.560	−0.51
HD 158226A	0.182	−0.040	0.610	−0.63
HD 158226B	0.144	0.130	0.710	−0.63
HD 184499	0.125	−0.010	0.580	−0.53
HD 188510	0.292	−0.150	0.610	−1.37
HD 193901	0.243	−0.150	0.560	−1.00
HD 194598	0.249	−0.190	0.490	−1.03
HD 201891	0.220	−0.160	0.510	−0.94
BD+17 4708	0.222	−0.190	0.450	−1.65
G74-5	0.191	−0.090	0.570	−0.99
G78-1	0.152	−0.090	0.520	−0.78
G246-38	0.275	−0.080	0.650	−1.92
G194-22	0.242	−0.190	0.480	−1.49
G165-53	0.232	−0.150	0.550	−1.26
G166-45	0.281	−0.230	0.430	−2.29
G207-5	0.130	−0.050	0.540	−0.46
G125-64	0.288	−0.220	0.510	−2.01

Hydrae, HIP 53911, a 10-Myr-old K7 T Tauri star, and the early-type M dwarf, AC +18°1061 (HIP 112389).

Comparing the SAAO photometry against the literature data included in the *Hipparcos* catalogue (i.e., V_l, not V_T), we find

$$\Delta V = (V_{SAAO} - V_l) = -0.007 \pm 0.042.$$

The largest discrepancy is for HIP 117121, where $V_{SAAO} = 11.12$, 0.48 mag brighter than the value listed in the *Hipparcos* catalogue. Since no $(B-V)_l$ measurement is given, the SAAO data are clearly more reliable. Eliminating that point gives

$$\Delta V = -0.005 \pm 0.021.$$

Fig. 10 plots the *UBV* two-colour diagram outlined by the stars with SAAO data; 90 per cent of the sample fall between the Hyades sequence and the $\delta_{0.6}$ calibration. The star lying well above the main sequence, at $(B-V) = 0.88$, $(U-B) = -0.45$, is TW Hydrae, while HIP 90724 (HD 170368) has an unusually red $(U-B)$ colour and falls below the Hyades sequence. Neither star has unusual colours in $(V-R)$ or $(V-I)$. SIMBAD lists a spectral type of A7V for HIP 90724 and, as noted above, the true parallax is less than 10 mas. The location on the *UBV* plane is consistent with its being a distant A dwarf, reddened by $E(B-V) \sim 0.3$ mag. The star lies towards the Galactic bulge, albeit at a modest distance from the plane ($l = 358°$, $b = -12°$), and patchy foreground reddening at the observed level is not unreasonable.

We have used the $\delta_{0.6}$ calibration outlined above to estimate abundances for stars with $(B-V)$ colours between 0.35 and 1.10 mag, and these estimates are listed in Tables 7 and 8. 29 stars have $[Fe/H]_{0.6} \le -1.0$.

Of these, 22 were previously known to be halo stars; seven (HIP 4750, 17241, 43490, 54834, 73798, 95190 and 114271[4]) are additions to the list of metal-poor calibrators.

The VR_CI_C observations listed in Table 6 are drawn from a variety of literature sources. The $(B-V)/(V-I)$ and $(V-R)/(V-I)$ two-colour diagrams plotted in Figs 11 and 12 allow us to assess how well those observations match the well-defined SAAO Cousins system. Fig. 11 shows that the *BVI* data are in excellent agreement. Discrepancies are more evident in the *VRI* plane, both individual (HIP 20527 and 92277) and systemic: the literature data for M dwarfs $[(V-I) > 1]$ lie blueward of the SAAO sequence in $(V-R)$. This is not unexpected, since the extended red tail of the Cousins R band is difficult to reproduce exactly, and different filter/detector combinations lead to significant colour terms.

Finally, Fig. 13 plots the distribution of the candidate subdwarfs listed in Table 7 in the $[M_V, (B-V)]$ and $[M_V, (V-I)]$ planes. In most cases, the locations of individual stars are consistent with abundances inferred from the $\delta_{0.6}$ ultraviolet excess, and the overwhelming majority are mildly metal-poor disc dwarfs.

One star stands out from the main body of data: HIP 28122, at $[M_V = 6.37,\ (B-V) = 0.42]$. While the *Hipparcos* catalogue notes no duplicity problems, inspection of the Palomar plates in the Digital Sky Survey shows that this star (HD 40007, or BD +10°936) lies ~20 arcsec from another star of similar brightness. That star is BD +10°936B [$V = 10.02 \pm 0.03$, $(B-V) = 0.45 \pm 0.02$; Kilkenny, private communication], star 28121 in the *Hipparcos* input catalogue, but unobserved in the survey itself. The goodness-of-fit statistic for the astrometry of HIP 28122 is $|F| = 2.48$, barely within our adopted limits. As discussed further below, spectroscopy indicates that both stars are of near-solar abundance, with no evidence for peculiarities. It seems likely that the proximity of the bright companion has affected the *Hipparcos* analysis, and the parallax has been overestimated.

5.4 Summary

We have catalogued the available photometric observations of the 317 stars listed in Table 1: 97 stars have Strömgren photometry; 220 stars have Johnson/Cousins $UBV(RI)$ measurements, including 201 from our SAAO observing programme; and nine stars have Walraven photometry. Combined, these observations provide accurate colours and magnitudes for 251 stars, or 75 per cent of the sample. 44 stars have photometric abundances $[Fe/H] \le -1.0$, although 12 are identified as confirmed or probable binary stars. 31 metal-poor stars (including six binaries) have accurate *UBVRI* Johnson/Cousins photometry, the most extensive such data set compiled to date for subdwarfs with well-determined trigonometric parallaxes. We shall discuss these stars in more detail in Section 7.

[4]The inclusion of HIP 114271 in Fulbright's (2000) sample was prompted by its location in Fig. 2.

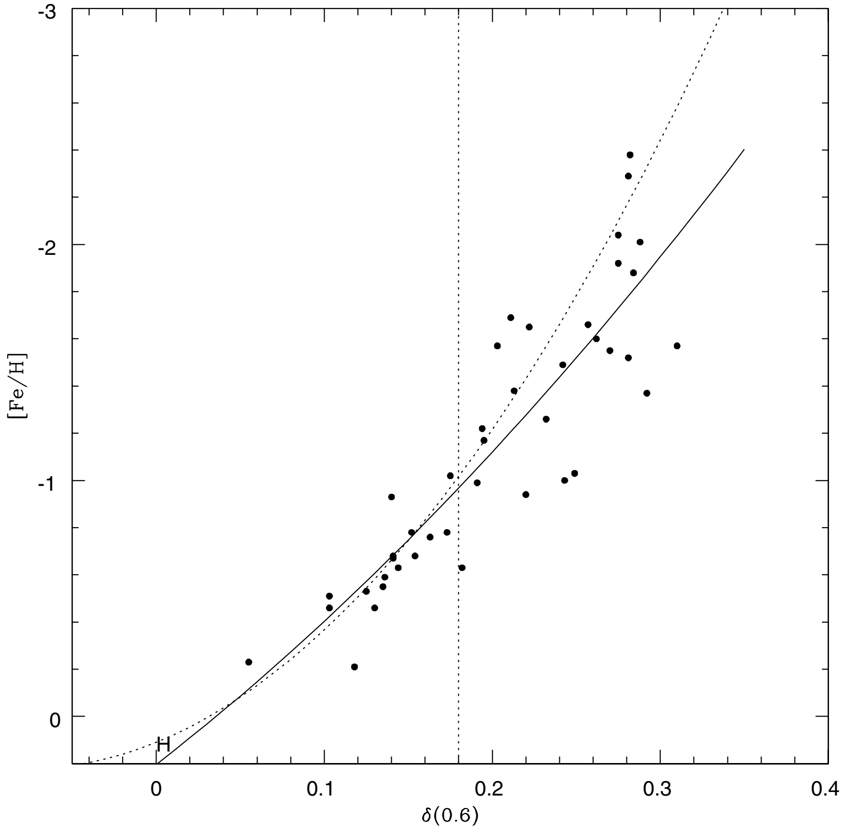

Figure 6. The calibration of ultraviolet excess, $\delta_{0.6}$, as a function of metal abundance. The solid line shows the present calibration; the dotted relation plots Carney's (1979) relation; H marks the location of Hyades stars, the reference point of the calibration, and the dotted vertical line shows $\delta_{0.6} = 0.18$, the criterion we adopt to segregate candidate halo subdwarfs.

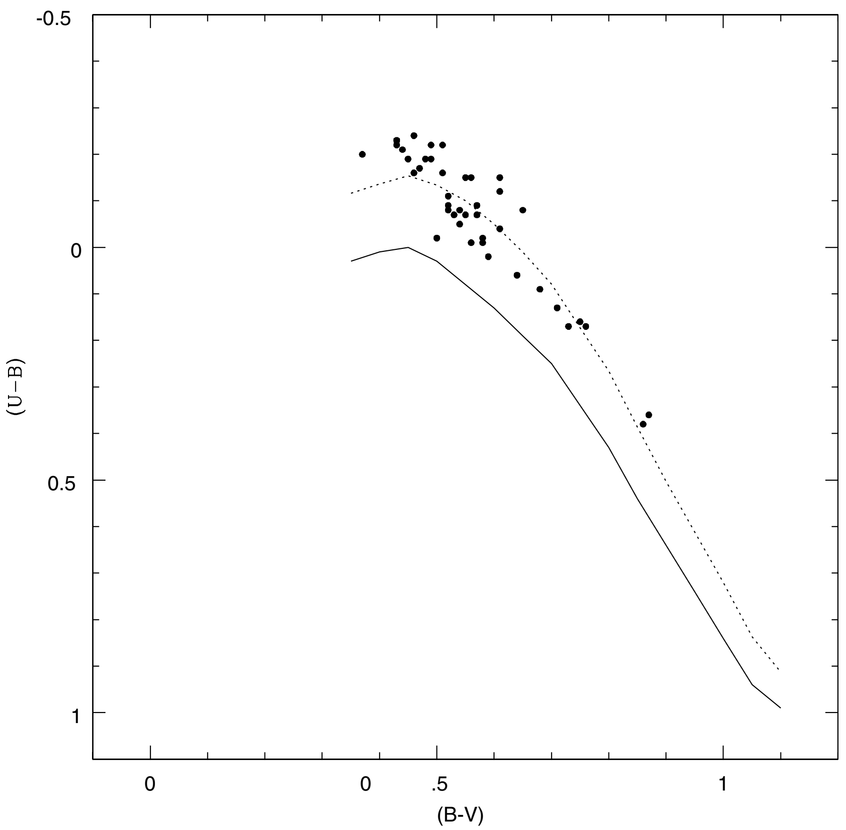

Figure 7. The $(U-B)/(B-V)$ distribution of the stars which calibrate the $\delta_{0.6}$/[Fe/H] relation. The solid line plots the Hyades $(U-B)/(B-V)$ relation (from Sandage 1969), while the dotted line plots the two-colour relation for $\delta_{0.6} = 0.18$ mag.

Table 6. Published *UBVRI* photometry of candidate subdwarfs.

HIP	$U-B$	$B-V$	V	$V-R$	$V-I$	δ_{U-B}	$\delta_{0.6}$	$[Fe/H]_{0.6}$	M_V	ref
3855			10.56	0.61	1.14				7.01	W1
5004	0.17	0.75	10.24	0.44	0.86	0.17	0.18	−1.0	6.30	RN1
7459	−0.16	0.52	10.12	0.33	0.68	0.21	0.23	−1.4	5.44	RN1
8130	0.14	0.68	10.52			0.09	0.09	−0.3	5.79	CLLA
8558		0.40	9.02	0.18	0.40				3.91	E1
12579	−0.09	0.52	9.16			0.14	0.15	−0.8	4.97	CLLA
14594	−0.24	0.46	8.06			0.25	0.28	−1.8	5.12	C1
16404	−0.08	0.65	9.91			0.27	0.28	−1.8	6.14	CLLA
19215	0.06	0.34	8.97			0.14	0.00	0.2	3.74	O1
20413	0.20	0.67	10.32	0.40	0.76	0.01	0.01	0.1	5.91	F1
20527		1.29	10.90	0.73	1.46				7.67	R1
20895	1.26	1.37	10.99	0.83	1.63				7.98	W2
21261		1.20	10.75	0.71	1.33				7.37	R1
21478		0.61	9.43						4.56	K1
21586	0.39	0.77	10.36	0.49	0.94	−0.01	−0.01	0.3	6.34	R2
21609	−0.13	0.64	9.84			0.31	0.31	−2.0	5.99	RN1
22177		1.28	10.91	0.76	1.44				7.67	R1
22246	0.46	0.80	10.24			−0.03	−0.03	0.4		CLLA
22632		0.51	9.18	0.26	0.56				5.15	E1
24316		0.55	9.45	0.30	0.61				5.27	E1
26452	−0.08	0.55	9.57			0.16	0.16	−0.8	5.16	CLLA
26676	−0.02	0.65	10.22			0.21	0.21	−1.2	6.00	CLLA
26676	0.01	0.67	10.20	0.41	0.82	0.20	0.20	−1.2	5.98	RN1
30481	−0.07	0.35	8.30			0.10	0.12	−0.5	3.82	O3
33282	1.32	1.34	11.27	0.80	1.51				7.70	F1
35163	0.30	0.73	10.02	0.38	0.74	0.00	0.00	0.2		F1
36491	−0.11	0.52	8.49			0.16	0.17	−0.9	5.00	CLLA
36491	−0.13	0.53	8.44	0.31	0.64	0.19	0.21	−1.2	4.95	RN1
36818	−0.02	0.61	10.50			0.16	0.16	−0.8		RN1
38541	−0.12	0.61	8.26			0.26	0.26	−1.6	6.00	C1
40778	−0.19	0.48	9.76			0.21	0.24	−1.5	4.85	CLLA
44124	−0.19	0.48	9.66			0.21	0.24	−1.5	5.13	CLLA
44124	−0.19	0.48	9.67			0.21	0.24	−1.5	5.14	RN1
46120	−0.16	0.59	10.10			0.28	0.29	−1.8	6.19	RN1
46509	0.04	0.46	4.59			−0.03	−0.04	0.4	3.43	C2
50965	0.00	0.57	9.80			0.10	0.10	−0.4	4.73	CLLA
50965	0.00	0.57	9.80			0.10	0.10	−0.4	4.73	RN1
51769	0.05	0.68	10.52			0.18	0.18	−0.9	6.57	CLLA
51769	0.08	0.69	10.47	0.40	0.78	0.16	0.16	−0.8	6.52	RN1
54768	−0.04	0.52	9.14			0.09	0.10	−0.4	4.87	O1
57450	−0.15	0.55	9.92			0.23	0.23	−1.4	5.59	CLLA
57939	0.17	0.75	6.43			0.17	0.18	−0.9	6.62	CLLA
63063	0.40	0.80	9.93			0.03	0.03	0.0		CLLA
63912	−0.04	0.41	8.93			0.05	0.05	−0.1	3.99	O2
64386	0.04	0.64	9.89			0.14	0.14	−0.7	5.67	CLLA
65040	0.02	0.64	9.78			0.16	0.16	−0.8	5.72	CLLA
66828		1.33	10.89	0.78	1.52				8.01	W2
70152	1.29	1.35	10.58	0.82	1.57				6.47	RN1
72461	−0.24	0.42	9.74			0.25	0.29	−1.8	4.80	C4
78251		0.64	8.96						5.46	CS
80448	0.16	0.64	7.33	0.38	0.73	0.02	0.02	0.0	4.10*	C3
80789	0.03	0.61	10.24			0.11	0.11	−0.5	5.60	CLLA
81013			8.77	0.25	0.52				3.79	M1
81170	0.10	0.75	9.63			0.24	0.28	−1.8	6.21	SK
86183	0.02	0.33	9.38			0.18	0.00	0.2	3.73	O2
88648	−0.11	0.62	10.24	0.39	0.79	0.26	0.26	−1.6	6.18	RN1
89215	0.21	0.73	10.43			0.09	0.10	−0.4	6.58	CLLA
92277	0.14	0.73	10.35			0.16	0.17	−0.9	6.10	CLLA
92277	0.14	0.69	10.33	0.38	0.68	0.10	0.10	−0.4	6.08	RN1
93341	0.10	0.69	10.07	0.40	0.79	0.14	0.14	−0.7	6.04	RN1
94704	0.02	0.66	11.29	0.40	0.84	0.18	0.18	−1.0	6.57	R2
95800	−0.07	0.43	8.79	0.26	0.51	0.07	0.08	−0.3	4.00	D1
95996	−0.12	0.48	10.25	0.33	0.65	0.14	0.16	−0.7	5.16	R3, W3
98020	−0.15	0.61	8.82			0.29	0.29	−1.8	5.84	C1
99267	−0.22	0.51	10.11			0.26	0.29	−1.8	5.51	CLLA
101103	−0.10	0.39	9.46	0.24	0.49	0.11	0.13	−0.6	4.39	D1
103269	−0.11	0.62	10.27			0.26	0.26	−1.6	6.03	CLLA
104289	0.08	0.68	10.23	0.39	0.78	0.15	0.15	−0.7	6.05	RN1
106924	−0.07	0.63	10.34			0.24	0.24	−1.4	6.25	CLLA
109067	0.04	0.65	9.55			0.15	0.15	−0.7		CLLA
110776	0.39	0.82	9.71			0.08	0.09	−0.3		CLLA

Table 6 – *continued*

HIP	$U-B$	$B-V$	V	$V-R$	$V-I$	δ_{U-B}	$\delta_{0.6}$	$[Fe/H]_{0.6}$	M_V	ref
111871	0.37	0.82	10.44			0.10	0.11	−0.5	6.39	CLLA
112389		1.24	10.67	0.74	1.40				7.74	W2
113542	−0.07	0.38	8.75			0.09	0.10	−0.4	3.92	G1
117242	−0.03	0.40	8.80			0.04	0.04	−0.1	3.97	O2

*: HIP 80448 is an unresolved X-ray binary. Fabricius & Makarov (2000b) derive individual magnitudes of $V_T = 8.13$ and 8.32.
Stars lacking M_V values have unreliable *Hipparcos* parallax measurements.
References: C1 – Carney 1979; C2 – Celis 1975; C3 – Cutispoto et al. 1991; C4 – Carney 1983; CS – Cousins & Stoy 1962; CLLA – Carney et al. 1994; D1 – Dean 1981; E1 – Eggen 1990; F1 – Figueras et al. 1990; G1 – Guetter 1980; K1 – Kenyon et al. 1994; O1 – Oja 1986; O2 – Oja 1985; O3 – Oja 1991; R1 – Reid 1993; R2 – Rossello et al. 1988; R3 – Roman 1955 (*UBV* only); SK – Sandage & Kowal 1986; W1 – Weis 1986; W2 – Weis 1993; W3 – Weis 1996.

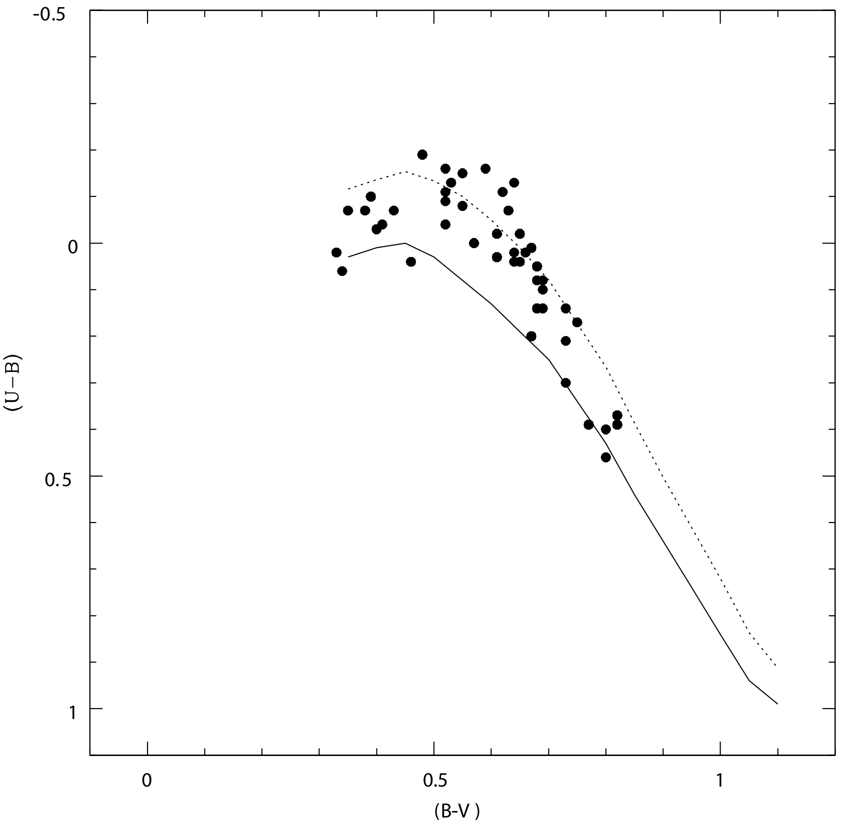

Figure 8. The $(U-B)/(B-V)$ distribution for the stars listed in Table 6. As in Fig. 7, the solid and dotted lines are the Hyades and $\delta_{0.6} = 0.18$ sequences.

6 SPECTROSCOPIC OBSERVATIONS

In addition to photometric observations, we have obtained spectroscopy of over 170 stars from Table 1. These spectra cover a number of prominent metal lines and molecular bands, and therefore provide additional abundance information.

6.1 Las Campanas observations

Our observations were obtained in 1998 January and November, using the modular spectrograph at Las Campanas Observatory (LCO). The initial observations were made from January 1 to 6 (UT), with the spectrograph mounted on the 100-inch Du Pont telescope; the later observations were made on November 28, 29 and 30 (UT), with the same spectrograph mounted on the Swope 40-inch telescope. In both cases, we employed a 600 line mm^{-1} grating, blazed at 5000 Å with the spectrum centred at 4700 Å on the detector, a SITE CCD chip. The 100-inch observations provide wavelength coverage from 3780 to 6000 Å at a dispersion of 1.3 Å pixel^{-1}; the 40-inch data span 3790 to 5900 Å at a dispersion of 1.1 Å pixel^{-1}. The former observations have a resolution of 2.6 Å, the latter a resolution of 2.9 Å.

The data were reduced using standard techniques incorporated in the IRAF software analysis package. The spectra were flat-field-corrected using observations of tungsten lamps, and the individual spectra extracted using the *apextract* task. The wavelength calibration for both data sets was set using observations of hollow-cathode arc lamps obtained at the start of each night. Given the relatively low resolution of these spectra, we have not attempted to determine radial velocities for the target stars.

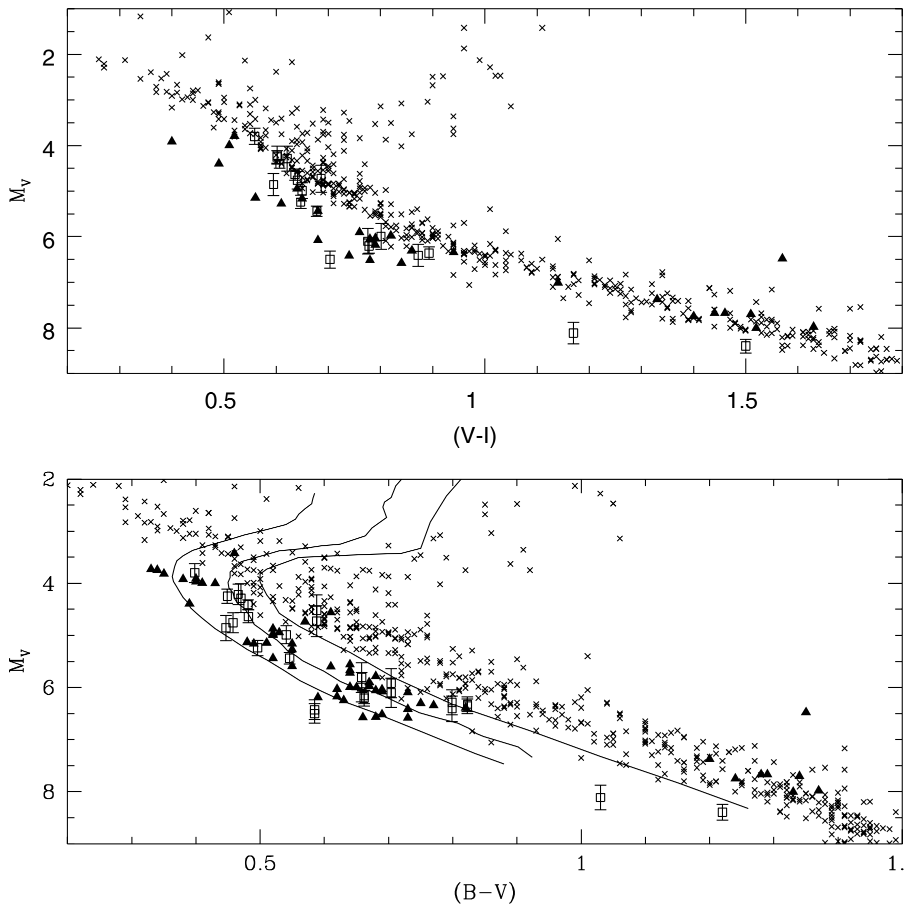

Figure 9. The [M_V, $(V-I)$] and [M_V, $(B-V)$] colour–magnitude diagrams outlined by the candidate subdwarfs listed in Table 6. The disc main sequence (crosses) is delineated by stars from the Gliese/Jahreiss Nearby Star Catalogue with both accurate photometry (Bessell 1990; Leggett 1992) and accurate trigonometric parallaxes (ESA 1997); known subdwarfs are plotted as open squares with error bars; the mean colour–magnitude relations for 47 Tuc, M5 and NGC 6397 are superimposed on the [M_V, $(B-V)$] diagram, and the candidate subdwarfs are plotted as filled triangles.

Once wavelength calibration was established, the spectra were set on a flux scale using observations of the standard stars LTT 1020, LTT 2415 and Hiltner 600 (Baldwin & Stone 1984). Inter comparison of standards shows that the calibration is generally accurate to better than 5 per cent on large scales (>150 Å). Since our main priority is measuring equivalent widths of individual atomic features, these data are adequate for our present purposes.

6.2 Metallicities of programme stars

The wavelength régime spanned by our observations includes a number of strong atomic lines and molecular bands in common use as abundance indicators for F-, G- and K-type stars. These include the Ca II H and K lines, Ca I 4227 Å, the G-band at 4300 Å, the Mgb triplet and numerous Fe I lines (notably at 5270 and 5331 Å), besides the hydrogen Balmer lines Hβ to H9. The Balmer lines, particularly Hβ, are important in offering temperature calibration, since many of the *Hipparcos* stars lack reliable photometric colours.

Tables 9 and 10 list our equivalent width measurements of several key features: the Ca II K line, the G-band, the strongest Mgb feature (5170 Å), Hβ, and the Fe I 5270 and 5331 Å lines (Fe1 and Fe2, respectively). The 100-inch spectra were measured by SM, and the 40-inch spectra by INR. Although both sets of measurements are internally consistent, there are systematic differences in approach. There are only a few of stars in common between the two sets of observations, but each encompasses a substantial number of stars of known abundance. Since our goals are qualitative, rather than quantitative, we analyse the two data sets separately.

All of the measured features are strong lines, since our primary aim remains identifying metal-poor stars likely to have [Fe/H] ≤ -1. The chosen indicators are insensitive to metallicity variation at near-solar abundance, but provide good discrimination at halo abundances. Repeat observations of a number of stars show that the random uncertainties associated with the measured equivalent widths are typically ± 0.15 Å. These uncertainties are likely to be characteristic of the errors in our observations of metal-poor stars. However, systematic errors, notably regarding continuum placement, are undoubtedly present at a comparable level in line-rich, disc-abundance dwarfs.

We have calibrated our chosen abundance indicators using observations of stars with spectroscopically determined abundances, either from Table 2 or from the extensive CLLA catalogue. In both cases, we supplement these calibrators with programme stars whose metallicity has been determined using Strömgren photometry (Table 3). Fig. 14 illustrates the methods employed. Since our chosen indices lack sensitivity at near-solar abundances, we have not attempted to separate metal-rich and intermediate-abundance stars, and identify only the candidate halo-abundance

Table 7. SAAO *UBVRI* photometry.

HIP	$U-B$	$B-V$	V	$V-R$	$V-I$	σ_{U-B}	σ_{B-V}	σ_V	σ_{V-R}	σ_{V-I}	N_{obs}	δ_{U-B}	$\delta_{0.6}$	[Fe/H]	M_V
435	−0.081	0.469	9.309	0.282	0.574	5	2	1	1	2	4	0.092	0.107	−0.4	4.37
1051	−0.089	0.434	8.750	0.261	0.540	0	0	12	2	0	2	0.092	0.106	−0.4	3.98
1719	0.460	0.840	9.653	0.478	0.923	2	6	6	4	3	4	0.058	0.058	−0.1	6.48
3139	−0.078	0.438	9.309	0.263	0.527	6	7	20	6	11	4	0.080	0.091	−0.3	3.98
3531	1.208	1.220	10.895	0.734	1.390	5	22	12	4	5	4				7.27
3855	0.923	1.061	10.566	0.635	1.178	14	30	11	8	13	4	0.028	0.031	0.0	7.02
4450	0.008	0.506	9.642	0.290	0.576	2	4	5	3	6	4	0.028	0.031	0.0	4.62
4576	−0.038	0.436	9.511	0.259	0.516	1	5	5	1	0	4	0.041	0.045	−0.1	4.33
4750	−0.107	0.566	10.087	0.315	0.641	3	2	5	3	3	5	0.203	0.203	−1.1	5.27
4981	0.031	0.597	9.110	0.342	0.676	3	2	6	3	4	3	0.096	0.098	−0.4	5.31
5004	0.182	0.758	10.266	0.442	0.877	2	7	5	2	3	4	0.172	0.186	−1.0	6.33
5097	−0.053	0.456	9.300	0.274	0.556	2	5	4	0	3	4	0.057	0.062	−0.2	4.30
6251	−0.040	0.522	8.417	0.297	0.605	2	10	13	3	0	3	0.092	0.100	−0.4	
6758	0.067	0.615	9.701	0.347	0.688	9	6	17	4	8	5	0.081	0.081	−0.3	5.45
7303	−0.012	0.607	9.845	0.354	0.709	0	2	4	4	6	3	0.150	0.150	−0.8	5.41
7459	−0.147	0.514	10.107	0.329	0.679	2	7	3	0	1	4	0.191	0.210	−1.2	5.43
7687[1]	0.373	0.807	9.397	0.452	0.869	9	8	28	8	12	4	0.072	0.074	−0.2	6.46
7772	−0.044	0.405	8.817	0.237	0.470	1	2	4	3	2	3	0.053	0.058	−0.1	3.71
7935	−0.079	0.486	8.886	0.286	0.590	6	8	8	2	4	3	0.101	0.117	−0.5	4.39
8298	0.304	0.775	10.079	0.435	0.842	3	11	3	2	3	3	0.081	0.084	−0.3	6.02
8389	0.637	0.914	10.688	0.549	1.030	9	13	9	2	2	3	0.031	0.031	0.0	6.42
8558	−0.147	0.369	9.002	0.234	0.486	4	9	5	4	5	3	0.169	0.208	−1.2	3.89
9634	−0.075	0.435	8.335	0.267	0.537	1	2	6	6	6	4	0.078	0.088	−0.3	4.02
10208	−0.092	0.439	9.065	0.261	0.528	1	4	5	1	0	3	0.094	0.109	−0.5	4.58
10353	−0.104	0.469	9.211	0.284	0.580	3	3	5	0	4	3	0.115	0.136	−0.6	4.66
10360	0.009	0.294	8.546	0.170	0.345	2	3	6	2	2	4				
10375	−0.098	0.447	9.098	0.266	0.550	4	4	7	3	5	4	0.099	0.115	−0.5	4.03
10385	0.993	1.098	10.872	0.673	1.278	6	24	3	6	6	3	−0.005	−0.005	0.2	7.41
10637	−0.083	0.451	9.274	0.274	0.555	1	12	5	3	1	3	0.084	0.095	−0.4	4.25
11435	−0.033	0.453	8.635	0.262	0.528	3	4	3	1	4	4	0.035	0.038	0.0	4.35
13849	0.784	0.966	10.650	0.549	1.022	6	4	7	3	6	3	−0.012	−0.012	0.3	6.37
14192	−0.029	0.462	8.931	0.268	0.528	4	1	3	5	2	3	0.036	0.040	0.0	3.82
15756	0.716	0.961	10.887	0.544	1.010	12	9	3	6	2	4	0.046	0.046	−0.1	6.30
16089	−0.019	0.396	8.774	0.231	0.461	3	6	2	1	3	5	0.031	0.034	0.0	4.02
16479	−0.032	0.429	8.296	0.250	0.498	0	1	2	1	2	3	0.036	0.040	0.0	3.96
17085	−0.047	0.431	9.585	0.255	0.506	2	3	4	5	6	3	0.051	0.056	−0.1	5.09
17241	−0.184	0.447	10.247	0.290	0.612	2	4	1	4	5	4	0.185	0.226	−1.3	4.82
17481	0.027	0.367	8.700	0.206	0.433	3	5	7	13	1	3	−0.004	−0.004	0.2	3.72
18700	−0.008	0.573	9.335	0.327	0.661	2	10	7	6	4	3	0.111	0.115	−0.5	5.49
19007	0.404	0.823	9.532	0.467	0.910	8	9	10	8	13	3	0.077	0.079	−0.3	6.45
20527	1.352	1.311	10.892	0.788	1.465	4	35	7	1	7	2				7.66
21000	0.097	0.613	9.841	0.361	0.728	2	4	8	3	4	3	0.049	0.049	−0.1	
21125	0.104	0.674	10.217	0.382	0.754	1	8	9	4	8	3	0.115	0.115	−0.5	6.05
21261	1.165	1.219	10.709	0.723	1.321	12	22	1	4	4	2				7.33
21609	−0.076	0.640	9.855	0.387	0.798	5	7	4	3	1	4	0.254	0.254	−1.6	6.01
22177	1.259	1.292	10.901	0.777	1.433	3	39	2	0	13	2				7.66
22632	−0.197	0.489	9.135	0.309	0.634	1	3	6	1	3	3	0.220	0.256	−1.6	5.10
23573	0.214	0.752	10.046	0.423	0.834	7	7	5	3	6	3	0.130	0.140	−0.7	6.09
24296	0.019	0.592	9.854	0.337	0.675	8	6	14	1	5	3	0.103	0.106	−0.4	5.10
24316	−0.199	0.496	9.427	0.312	0.647	3	4	8	1	2	3	0.227	0.263	−1.6	5.25
24421	−0.009	0.523	9.340	0.301	0.599	2	4	8	3	8	3	0.062	0.068	−0.2	4.75
24935	−0.097	0.470	8.767	0.280	0.570	2	3	8	1	1	3	0.109	0.128	−0.6	4.43
25717	−0.014	0.429	8.192	0.254	0.512	19	13	16	6	6	3	0.018	0.020	0.1	3.86
26676	0.024	0.658	10.217	0.414	0.801	48	11	54	38	32	5	0.176	0.176	−0.9	5.99
26688	−0.091	0.419	7.697	0.249	0.517	4	6	7	4	4	3	0.097	0.113	−0.5	
28122	−0.051	0.424	9.507	0.250	0.512	6	5	8	5	5	4	0.056	0.062	−0.2	
29322	1.209	1.433	11.282	0.930	1.938	5	22	2	5	2	2				8.91
31639	0.170	0.705	9.645	0.397	0.784	3	10	4	1	5	3	0.089	0.091	−0.3	5.87
32009	0.233	0.734	9.628	0.407	0.792	7	16	5	1	5	3	0.078	0.079	−0.3	5.95
32308	0.829	0.974	10.718	0.545	1.001	9	54	5	4	2	3	−0.041	−0.041	0.4	7.01
33283	0.346	0.816	11.104	0.469	0.908	10	15	1	3	3	3	0.119	0.129	−0.6	6.39
34146	−0.069	0.456	8.047	0.268	0.539	5	6	9	3	4	3	0.073	0.082	−0.3	4.03
35232	−0.080	0.461	9.696	0.272	0.561	4	6	1	5	5	3	0.087	0.099	−0.4	4.24
35560	−0.097	0.414	8.511	0.247	0.499	9	2	3	1	6	3	0.104	0.122	−0.6	4.03
36491	−0.086	0.541	8.485	0.324	0.650	7	3	6	8	6	3	0.157	0.171	−0.9	4.99
36818	−0.077	0.585	10.573	0.350	0.703	2	2	5	3	2	3	0.192	0.193	−1.1	
39911	−0.018	0.616	9.591	0.356	0.714	4	2	4	1	4	3	0.167	0.167	−0.9	5.47
41563	−0.034	0.382	8.813	0.228	0.454	2	6	2	2	12	3	0.051	0.056	−0.1	3.70
42278	−0.050	0.363	7.783	0.219	0.435	2	2	6	6	1	3	0.075	0.084	−0.3	3.68
43445	−0.083	0.481	8.634	0.286	0.578	5	2	6	3	9	3	0.102	0.119	−0.5	4.29
43490	−0.113	0.550	9.554	0.321	0.664	15	7	19	17	23	3	0.193	0.194	−1.1	5.30

Table 7 – *continued*

HIP	$U-B$	$B-V$	V	$V-R$	$V-I$	σ_{U-B}	σ_{B-V}	σ_V	σ_{V-R}	σ_{V-I}	$N_{\rm obs}$	δ_{U-B}	$\delta_{0.6}$	[Fe/H]	M_V
43973	0.048	0.666	9.520	0.380	0.756	6	4	5	2	6	3	0.161	0.161	−0.8	5.81
44124	−0.185	0.486	9.648	0.317	0.647	3	2	0	2	4	3	0.207	0.241	−1.4	5.12
44436	−0.038	0.367	7.382	0.210	0.435	4	4	4	3	4	3	0.061	0.068	−0.2	3.23
46120	−0.182	0.577	10.108	0.352	0.728	5	12	9	6	7	4	0.289	0.297	−1.9	6.20
47161	−0.039	0.436	9.271	0.251	0.505	2	5	1	1	3	3	0.042	0.046	−0.1	3.94
47171	−0.004	0.582	9.303	0.332	0.658	5	4	5	4	3	3	0.116	0.120	−0.5	4.68
47948	0.140	0.682	10.061	0.378	0.741	4	5	6	5	1	3	0.088	0.088	−0.3	5.44
48146[2]	0.009	0.558	9.595	0.310	0.627	26	10	34	14	2	3	0.079	0.080	−0.3	
48152	−0.203	0.398	8.329	0.263	0.559	1	2	2	5	5	3	0.214	0.264	−1.6	3.80
49574[3]	−0.122	0.477	8.777	0.291	0.578	2	29	25	30	23	4	0.138	0.163	−0.8	4.30
49785	−0.054	0.489	8.512	0.287	0.580	4	5	4	3	6	4	0.077	0.088	−0.3	
50532	−0.005	0.544	9.906	0.310	0.613	2	7	2	4	7	3	0.079	0.086	−0.3	4.95
50965	−0.008	0.588	9.794	0.343	0.686	3	3	2	3	5	3	0.126	0.131	−0.6	4.73
51156	−0.052	0.436	9.059	0.260	0.523	4	3	1	2	4	3	0.055	0.060	−0.1	4.14
51298	−0.039	0.438	9.243	0.256	0.511	5	3	1	3	2	3	0.041	0.046	−0.1	4.33
51300	−0.042	0.408	9.196	0.244	0.479	4	1	3	0	1	3	0.050	0.055	−0.1	3.71
51769	0.079	0.691	10.479	0.393	0.777	6	8	3	2	4	3	0.160	0.160	−0.8	6.53
52285	0.569	0.925	9.869	0.537	1.027	8	2	5	2	3	3	0.121	0.136	−0.6	6.23
53070	−0.190	0.482	8.218	0.306	0.636	5	3	2	1	4	3	0.209	0.243	−1.5	4.63
53911[4]	−0.446	0.884	10.825	0.849	1.520	147	184	227	96	127	2	1.054	1.486		7.06
54519	0.821	0.980	10.957	0.599	1.087	14	10	6	21	29	2	−0.021	−0.021	0.3	7.07
54641	−0.153	0.481	8.161	0.295	0.607	4	4	7	1	1	3	0.172	0.201	−1.1	4.41
54834	−0.177	0.464	8.782	0.296	0.609	2	4	1	2	1	3	0.185	0.217	−1.3	4.69
54993	−0.053	0.418	8.818	0.236	0.475	10	2	0	7	3	2	0.059	0.066	−0.2	3.75
55790	−0.192	0.470	9.080	0.300	0.621	3	6	5	4	2	3	0.204	0.238	−1.4	4.29
55978	0.008	0.387	9.065	0.226	0.450	3	2	1	4	1	3	0.007	0.008	0.2	3.66
57360	−0.164	0.466	8.736	0.293	0.602	4	4	1	4	2	3	0.174	0.203	−1.1	4.22
60251[5]	0.015	0.558	9.007	0.325	0.650	15	13	34	10	24	3	0.073	0.074	−0.2	5.09
60632	−0.206	0.447	9.661	0.286	0.595	4	10	3	5	3	3	0.207	0.251	−1.5	4.87
60852	−0.075	0.472	8.477	0.276	0.563	1	2	5	5	4	3	0.088	0.101	−0.4	4.27
62858	−0.050	0.549	9.510	0.322	0.641	7	0	0	7	7	3	0.129	0.140	−0.7	4.72
63063	0.392	0.812	9.934	0.457	0.896	1	2	2	2	2	3	0.064	0.065	−0.2	
63553	−0.074	0.408	8.504	0.243	0.491	2	1	0	1	3	3	0.082	0.094	−0.4	3.73
63781	−0.043	0.390	9.290	0.234	0.467	2	13	0	4	4	2	0.057	0.063	−0.2	3.78
64765	−0.007	0.379	8.846	0.229	0.473	2	1	5	5	6	3	0.025	0.028	0.0	4.03
65201	−0.204	0.458	8.803	0.312	0.641	5	7	4	0	4	2	0.209	0.243	−1.5	4.75
65940	0.670	0.935	10.367	0.529	0.987	5	13	1	1	9	3	0.040	0.040	0.0	6.51
66815	−0.072	0.552	8.828	0.325	0.652	4	4	0	1	5	3	0.154	0.158	−0.8	5.06
67189	0.003	0.502	9.862	0.296	0.598	2	12	1	0	1	2	0.029	0.032	0.0	4.77
70681	−0.082	0.601	9.296	0.359	0.727	6	4	0	1	2	2	0.213	0.213	−1.2	5.71
70689	−0.044	0.373	8.540	0.225	0.455	7	5	2	4	1	2	0.065	0.072	−0.2	3.88
71886	−0.064	0.438	8.934	0.265	0.529	9	7	2	0	4	2	0.066	0.074	−0.2	4.24
71939	−0.068	0.483	8.809	0.288	0.575	3	4	2	3	2	2	0.088	0.101	−0.4	4.59
73614	−0.028	0.414	8.323	0.250	0.500	1	10	9	0	0	2	0.035	0.039	0.0	3.84
73798	−0.036	0.642	9.933	0.375	0.755	1	9	0	3	2	2	0.216	0.216	−1.2	5.90
74078	−0.034	0.458	8.466	0.264	0.528	3	1	1	2	4	3	0.039	0.043	0.0	4.09
75618	0.040	0.609	9.739	0.342	0.682	8	3	16	1	5	3	0.101	0.101	−0.4	5.34
77432	−0.038	0.452	8.954	0.268	0.518	8	2	10	2	3	2	0.039	0.043	0.0	3.98
83226	0.347	0.779	10.035	0.429	0.829	9	18	11	3	6	4	0.045	0.045	−0.1	5.81
83443	−0.024	0.510	9.248	0.294	0.594	3	1	4	0	0	2	0.064	0.070	−0.2	4.90
84754	0.524	0.844	10.057	0.466	0.884	6	4	5	7	15	3	0.003	0.003	0.2	6.38
85999	−0.066	0.533	9.141	0.320	0.647	2	8	6	2	5	3	0.129	0.140	−0.7	4.61
86393	−0.011	0.515	9.497	0.304	0.620	3	10	8	4	2	3	0.056	0.062	−0.2	4.76
86536	−0.026	0.446	9.132	0.266	0.545	2	2	2	1	7	2	0.027	0.029	0.0	4.34
88066	−0.035	0.377	8.832	0.224	0.454	6	5	3	3	3	3	0.054	0.060	−0.1	3.79
89053	0.516	0.848	10.300	0.478	0.913	2	2	3	5	7	3	0.020	0.020	0.1	6.33
89554	−0.181	0.449	8.216	0.290	0.602	6	4	6	3	6	3	0.181	0.222	−1.3	4.25
89932	−0.014	0.518	9.124	0.296	0.582	1	5	3	4	6	3	0.062	0.068	−0.2	4.35
90724[6]	0.277	0.616	9.032	0.362	0.720	2	5	8	2	3	4	−0.128	−0.128	0.8	
92277	0.141	0.704	10.355	0.398	0.776	3	0	1	4	26	2	0.116	0.121	−0.5	6.10
93031	−0.015	0.526	9.285	0.299	0.597	5	5	12	13	18	5	0.071	0.078	−0.3	4.80
94347	−0.105	0.444	7.259	0.268	0.563	1	9	0	9	3	2	0.106	0.125	−0.6	4.00
95031	0.576	0.884	9.868	0.518	0.990	4	5	2	4	8	2	0.032	0.032	0.0	6.55
95190	−0.081	0.570	9.466	0.341	0.696	4	10	13	9	8	5	0.181	0.183	−1.0	4.79
95800	−0.075	0.413	8.771	0.247	0.510	3	0	3	7	4	2	0.082	0.094	−0.4	3.98
96043	0.097	0.637	9.625	0.358	0.707	1	6	4	2	9	3	0.077	0.077	−0.3	5.32
97127	−0.036	0.438	9.200	0.262	0.525	1	4	5	2	1	3	0.038	0.042	0.0	3.85
97463	0.025	0.613	9.573	0.352	0.700	3	4	3	6	2	3	0.121	0.121	−0.5	5.21
100207	−0.049	0.438	8.758	0.262	0.525	1	1	4	4	1	3	0.051	0.057	−0.1	3.90
100568	−0.126	0.546	8.642	0.332	0.678	0	2	6	1	3	3	0.202	0.222	−1.3	5.44
101103	−0.116	0.385	9.456	0.234	0.482	3	2	7	3	2	3	0.132	0.158	−0.8	4.39

Table 7 – *continued*

HIP	$U-B$	$B-V$	V	$V-R$	$V-I$	σ_{U-B}	σ_{B-V}	σ_V	σ_{V-R}	σ_{V-I}	$N_{\rm obs}$	δ_{U-B}	$\delta_{0.6}$	[Fe/H]	M_V
101650	−0.005	0.455	9.311	0.264	0.523	2	0	9	1	3	4	0.008	0.009	0.2	4.08
101892	−0.024	0.456	9.410	0.258	0.517	2	1	5	2	2	4	0.028	0.030	0.0	4.25
101987	−0.040	0.457	9.140	0.268	0.542	3	9	4	0	2	3	0.044	0.049	−0.1	4.12
103714	0.039	0.568	10.128	0.328	0.655	13	11	18	5	14	3	0.059	0.059	−0.1	5.66
104289	0.098	0.687	10.243	0.395	0.783	3	7	2	1	5	3	0.136	0.136	−0.7	6.06
106904	0.040	0.640	10.186	0.365	0.734	2	4	4	2	2	3	0.138	0.138	−0.7	5.76
107873	0.000	0.511	9.293	0.299	0.593	4	3	2	2	2	3	0.041	0.045	−0.1	4.31
108006	−0.051	0.409	9.108	0.246	0.498	5	2	1	1	3	3	0.059	0.065	−0.2	
108095	−0.030	0.558	8.527	0.333	0.659	3	2	8	5	6	3	0.118	0.123	−0.6	5.00
108598	0.339	0.800	9.574	0.466	0.903	4	9	0	3	6	3	0.091	0.095	−0.4	
108655	−0.034	0.392	8.848	0.236	0.477	9	1	2	3	8	3	0.047	0.052	−0.1	3.87
108836	1.062	1.166	10.966	0.708	1.297	11	12	4	4	4	2				7.87
109067	0.054	0.662	9.543	0.386	0.778	6	9	4	4	3	3	0.150	0.150	−0.8	
109869	0.058	0.593	9.554	0.331	0.656	2	15	0	1	6	3	0.065	0.065	−0.2	5.25
109945	−0.042	0.421	9.154	0.246	0.502	11	7	7	3	8	3	0.048	0.053	−0.1	4.02
110776	0.424	0.823	9.680	0.463	0.893	9	13	4	6	10	3	0.057	0.057	−0.1	
111374	−0.030	0.416	7.847	0.241	0.478	6	4	8	5	6	3	0.037	0.040	0.0	3.74
111426	−0.060	0.444	9.348	0.262	0.530	3	2	4	4	7	4	0.061	0.068	−0.2	4.55
111871	0.365	0.799	10.453	0.452	0.872	7	7	19	3	13	3	0.063	0.064	−0.2	6.40
112384	−0.103	0.401	9.020	0.253	0.518	1	2	4	2	1	4	0.113	0.133	−0.6	3.93
112389[7]	1.210	1.219	10.663	0.771	1.388	34	9	60	17	21	2				7.74
113430	−0.046	0.437	8.054	0.263	0.524	4	2	6	6	4	3	0.049	0.053	−0.1	4.18
113868	0.309	0.756	10.088	0.421	0.806	4	3	2	3	2	4	0.042	0.042	0.0	5.91
114271	−0.188	0.420	8.256	0.280	0.580	4	3	4	1	3	4	0.194	0.237	−1.4	4.03
114487	−0.101	0.395	8.408	0.252	0.521	6	3	4	1	1	3	0.113	0.134	−0.6	3.80
114627	−0.032	0.503	8.851	0.294	0.599	4	6	7	6	5	4	0.065	0.071	−0.2	4.58
114735	−0.080	0.404	8.493	0.248	0.500	3	9	6	3	8	3	0.089	0.103	−0.4	3.80
114837	0.003	0.545	9.882	0.310	0.615	1	3	1	3	0	2	0.072	0.079	−0.3	4.90
115031	−0.048	0.473	8.275	0.288	0.574	1	7	3	2	6	3	0.062	0.069	−0.2	
115361	−0.053	0.446	8.106	0.263	0.523	2	3	8	3	7	2	0.054	0.059	−0.1	4.03
116437	−0.063	0.515	9.813	0.304	0.623	1	2	2	3	0	2	0.108	0.117	−0.5	4.66
117121	1.021	1.103	11.123	0.668	1.239	6	19	11	4	7	4				7.62
117823	−0.083	0.493	9.334	0.299	0.598	5	2	8	7	16	5	0.109	0.128	−0.6	4.54
117882	−0.023	0.467	9.242	0.270	0.536	2	3	10	4	4	4	0.033	0.037	0.0	4.62
118165	−0.014	0.416	9.129	0.241	0.481	3	6	2	2	3	4	0.021	0.023	0.1	3.95
59750	−0.121	0.466	6.104	0.286	0.571						1	0.131	0.154	−0.8	4.34
66169	0.341	0.778	10.108	0.437	0.837						1	0.049	0.049	−0.1	6.02
67655	0.040	0.659	7.971	0.376	0.755						1	0.161	0.161	−0.8	5.98
68165	0.601	0.902	9.981	0.523	0.995						1	0.043	0.043	0.0	6.62
68452	−0.073	0.452	8.877	0.266	0.554						1	0.074	0.084	−0.3	4.25
68870	−0.018	0.433	9.506	0.255	0.508						1	0.021	0.024	0.1	4.48
70152	0.858	0.988	10.600	0.566	1.037						1	−0.042	−0.042	0.4	6.49
78952	0.027	0.632	9.830	0.362	0.713						1	0.141	0.141	−0.7	5.24
80295	0.883	1.023	10.383	0.585	1.067						1	0.003	0.003	0.2	6.96
80422	−0.034	0.409	8.500	0.248	0.499						1	0.042	0.046	−0.1	3.69
80448	0.100	0.634	7.344	0.370	0.729						1	0.071	0.071	−0.2	4.06
81170	0.120	0.746	9.607	0.447	0.900						1	0.213	0.225	−1.3	6.19
81617	0.052	0.324	8.565	0.189	0.388						1				3.73
82409	0.047	0.577	9.456	0.328	0.655						1	0.060	0.060	−0.1	4.96
83070	−0.070	0.430	8.799	0.260	0.520						1	0.074	0.083	−0.3	3.69
88084	0.040	0.622	9.192	0.349	0.713						1	0.116	0.116	−0.5	5.48
88231	0.031	0.591	9.960	0.357	0.710						1	0.090	0.092	−0.3	5.19
88648	−0.144	0.611	10.184	0.387	0.782						1	0.287	0.287	−1.8	6.12
88955	0.098	0.627	9.456	0.344	0.658						1	0.064	0.064	−0.2	5.35
89215	0.188	0.773	10.351	0.435	0.860						1	0.193	0.209	−1.2	6.50
89396	−0.049	0.472	7.992	0.279	0.553						1	0.062	0.069	−0.2	4.60
90616	0.014	0.617	10.294	0.370	0.738						1	0.136	0.136	−0.7	5.65
106204	1.246	1.250	10.620	0.751	1.369						1				7.42

Notes:
1. HIP 7687 = HD 10166, $\sigma_V = 0.028$ mag.
2. HIP 48146 = BD + 9°2242, $\sigma_V = 0.034$ mag.
3. HIP 49574 = HD 87908, $\sigma_V = 0.025$ mag.
4. HIP 53911 = TW Hydrae, $\sigma + V = 0.227$ mag, known variable.
5. HIP 60251 = HD 107490, $\sigma_V = 0.034$ mag.
6. HIP 90724 = HD 170368, reddened A star.
7. HIP 112389 = AC + 18°1061, $\sigma_V = 0.060$ mag, M dwarf.
Stars with no listed M_V have unreliable parallax measurements (see Section 2.2).

Table 8. SAAO *UBVRI* photometry of known subdwarfs.

Name HIP	$U-B$ π (mas)	$B-V$ σ_π	V M_V	$V-R$	$V-I$	N_{obs}	δ_{U-B}	$\delta_{0.6}$	$[Fe/H]_{0.6}$	$[Fe/H]_{ref}$
−12 2669	−0.155 ± 0.003	0.308 ± 0.003	10.232 ± 0.008	0.205 ± 0.001	0.430 ± 0.001	3				−1.49[1]
43099	5.76	1.50	4.03 ± 0.50							
G48-29	−0.206 ± 0.005	0.389 ± 0.010	10.467 ± 0.001	0.259 ± 0.001	0.550 ± 0.007	3	0.220	0.272	−1.7	−2.66[1]
47480	1.20	4.79								
G80-15	−0.083 ± 0.003	0.550 ± 0.010	6.679 ± 0.005	0.325 ± 0.001	0.662 ± 0.006	3	0.163	0.166	−0.9	−0.85[1]
17147	41.07	0.86	4.75 ± 0.05							
G112-36	0.293 ± 0.004	0.826 ± 0.007	9.239 ± 0.007	0.462 ± 0.001	0.932 ± 0.005	3	0.194	0.217	−1.3	−0.82[2]
37335	3.53	1.46								
G112-43	−0.153 ± 0.004	0.484 ± 0.007	9.853 ± 0.002	0.306 ± 0.003	0.634 ± 0.003	3	0.173	0.203	−1.1	−1.51[1]
37671	3.08	5.4								
G112-54	0.146 ± 0.006	0.728 ± 0.001	7.437 ± 0.005	0.430 ± 0.001	0.864 ± 0.004	3	0.154	0.161	−0.8	−0.95[1]
38625	52.01	1.85	6.02 ± 0.08							
G113-22	−0.053 ± 0.018	0.603 ± 0.010	9.704 ± 0.013	0.360 ± 0.003	0.736 ± 0.010	3	0.187	0.187	−1.0	−1.30[1]
G157-93	0.102 ± 0.005	0.672 ± 0.002	10.116 ± 0.001	0.380 ± 0.001	0.763 ± 0.002	2	0.114	0.114	−0.5	−0.99[1]
117041	8.46	1.76	4.75 ± 0.40							
G159-50	−0.063 ± 0.001	0.583 ± 0.002	9.084 ± 0.003	0.341 ± 0.001	0.696 ± 0.002	2	0.176	0.178	−1.0	−0.77[3]
10449	16.17	1.34	5.12 ± 0.17							
G270-23	−0.131 ± 0.000	0.469 ± 0.002	9.247 ± 0.000	0.291 ± 0.004	0.609 ± 0.004	2	0.142	0.167	−0.9	−1.30[3]
3026	9.57	1.38	4.15 ± 0.30							
G271-62	−0.177 ± 0.002	0.426 ± 0.004	10.361 ± 0.005	0.285 ± 0.001	0.607 ± 0.003	2	0.182	0.223	−1.3	−2.62[1]
8572	3.22	1.75								
HD 16031	−0.189 ± 0.007	0.438 ± 0.000	9.777 ± 0.003	0.285 ± 0.001	0.600 ± 0.004	2	0.191	0.234	−1.4	−1.66[4]
11952	8.67	1.81	4.47 ± 0.41							
HD 74000	−0.218 ± 0.001	0.423 ± 0.002	9.665 ± 0.003	0.279 ± 0.007	0.580 ± 0.004	3	0.223	0.269	−1.7	−1.52[4]
42592	7.26	1.32	3.97 ± 0.36							

References: 1. Carney et al. 1994; 2. Clementini et al. 1999; 3. Axer et al. 1994; 4. Gratton et al. 1997.

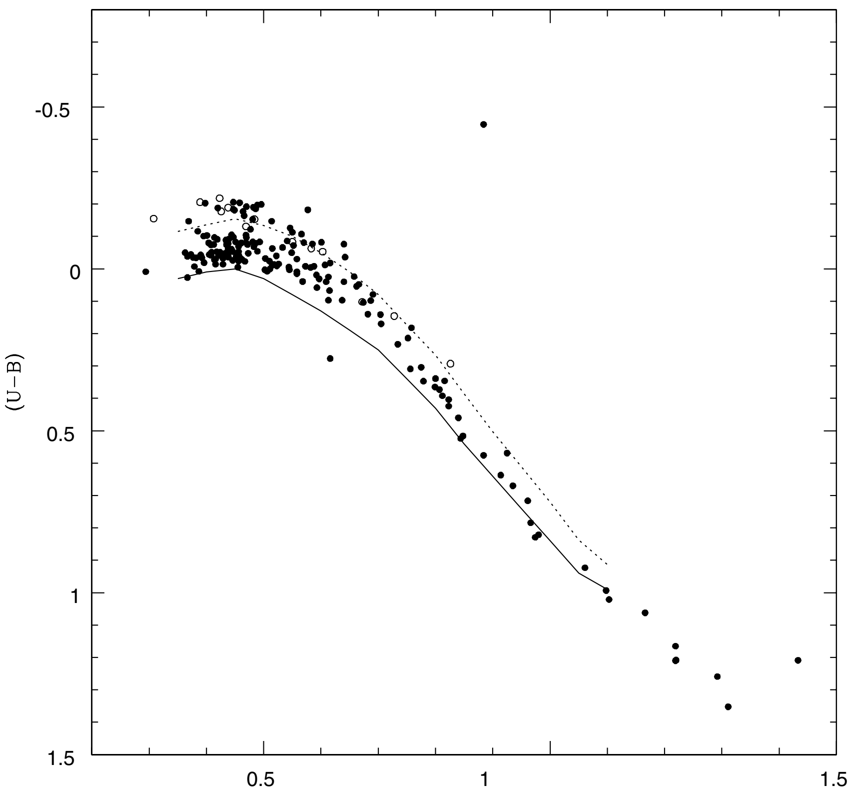

Figure 10. The $(U-B)/(B-V)$ distribution for *Hipparcos* stars with SAAO photometry (Table 7). Additional observations of known subdwarfs (from Table 8) are plotted as open circles. As in Fig. 6, the solid and dotted lines are the Hyades and $\delta_{0.6}$ sequences.

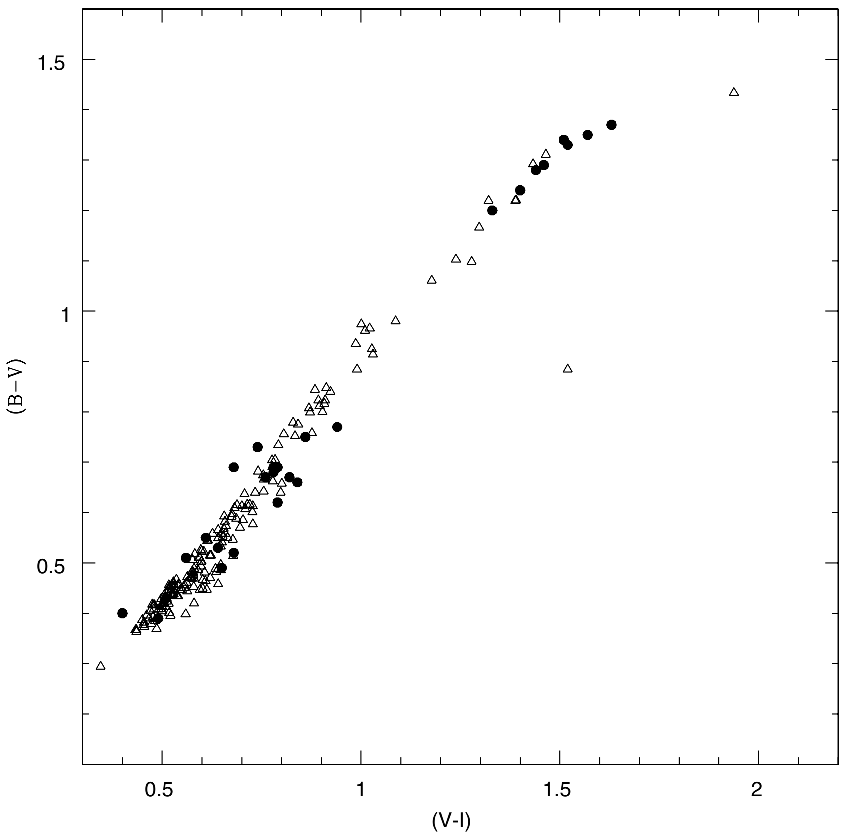

Figure 11. The $(B - V)/(V - I)$ distribution for *Hipparcos* stars from Tables 6 and 7. Literature data are plotted as filled circles, and SAAO photometry as open triangles. The two data sets produce sequences in good agreement.

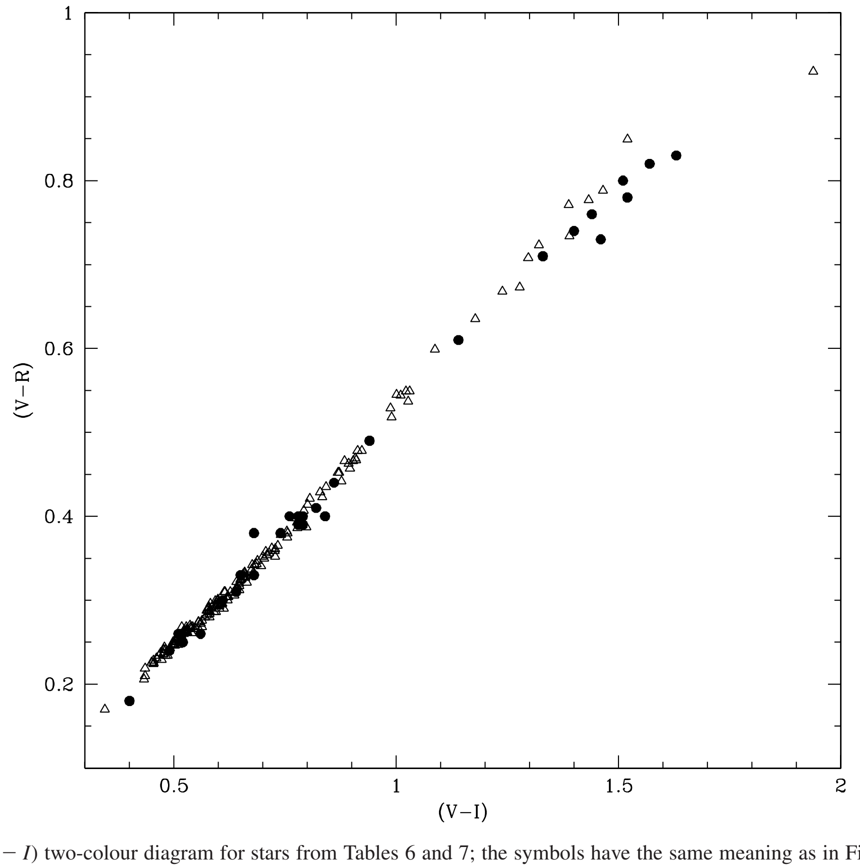

Figure 12. The $(V - R)/(V - I)$ two-colour diagram for stars from Tables 6 and 7; the symbols have the same meaning as in Fig. 11. There is a systematic offset between the two data sets for K and M dwarfs. Given the good agreement evident in Fig. 11, this offset probably arises from differences in the *R* bandpass employed in different observations.

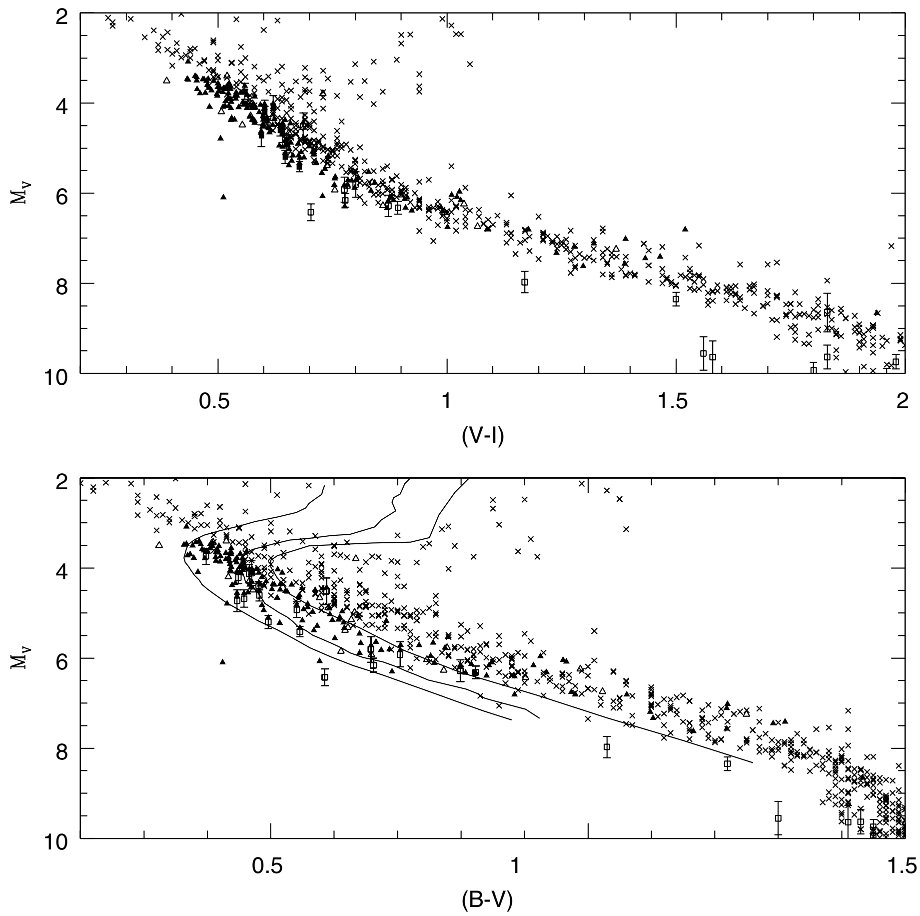

Figure 13. The $[M_V, (V-I)]$ and $[M_V, (B-V)]$ colour–magnitude diagrams for stars listed in Table 7. As in Fig. 9, known subdwarfs are plotted as open squares with error-bars; solid triangles are stars with multiple-epoch observations; open triangles mark stars with single-epoch photometry,

subdwarfs. Where necessary, we have also used our our spectroscopic data to estimate spectral types, and determine whether those values are compatible with the $(B-V)_T$ colours.

We have spectroscopy of 175 stars from Table 1. 46 have prior metallicity determinations, either from spectroscopic observations or Strömgren photometry. The majority of the remainder have line strengths consistent with disc-like abundances. Only 13 are candidate subdwarfs, showing potential for abundances $[Fe/H] < -1.0$. These stars are identified in Tables 8 and 9 ('H' in column 8). 12 of the 13 have *UBV* data and $\delta_{0.6}$ measurements: seven have $[Fe/H]_{0.6} \leq -0.7$; HIP 10353, 24935 and 97463 have $[Fe/H]_{0.6} \sim -0.6$, and HIP 5097 and 35232 have near-solar metallicity estimates. HIP 17241 and 54834, in contrast, have line strengths comparable with those of extreme halo subdwarfs, such as HD 19445 and 64090. More detailed spectroscopic observations of these stars will provide more accurate abundance estimates.

As Fig. 14 shows, our C40 observations include a higher proportion of earlier type dwarfs, with Hβ equivalent widths exceeding 6 Å. G271-11 is the only calibrator with Balmer lines of comparable strength; both Ca II K and Mgb are significantly stronger in that star than the *Hipparcos* stars. CLLA measure a spectroscopic abundance of $[Fe/H] = -0.57$; however, the *UBV* colours $[(U-B) = 0.06, (B-V) = 0.59]$ imply $\delta_{0.6} = 0.06$, and $[Fe/H] \approx -0.2$. Fortunately, the C40 *Hipparcos* sample includes both Pleiades members, HIP 17481 and 17494, and their location in the Hβ/Mg and Hβ/Ca K diagrams confirms that none of the earlier type stars is a candidate halo subdwarf.

There are only nine stars where our abundance estimates are based solely on the LCO spectroscopic data: HIP 895, 19637, 21478, 29510, 34145, 68452, 68870, 103287 and 110621. As already noted, the line indices measured for HIP 34145 suggest a halo metallicity. HIP 895, 68452 and 110621 have Ca II, Mgb and Fe equivalent widths of intermediate strength, and are classed as mildly metal-poor ('I' in Table 1); the remaining stars have near-solar abundances.

Several stars require individual mention.

HIP 3531AB: Also known as BD $-8°133$, our observations indicate that this is a close double star, separation ~ 5 arcsec. The primary is a late-type K dwarf; the secondary, an M2/M3 dwarf, is ~ 2.5 mag fainter. Both are near-solar-abundance disc dwarfs.

HIP 4750: Ca, Mg and Fe equivalent widths are consistent with $[Fe/H] < -1$; the G-band is significantly stronger than average. We identify this as a likely CH-strong subdwarf.

HIP 10360: Our spectroscopy confirms that this star is of spectral type A. The strong Ca II K line suggests a relatively high metallicity.

HIP 28121/28122: As noted above, these stars form the binary BD +10 936A/B. The fainter star, HIC 28121, was not observed by *Hipparcos*. Our measured line strengths indicate that both stars are at most mildly metal poor, $[Fe/H] > -0.5$.

HIP 43490: Also known as CD -79 347A, this subdwarf has a

Table 9. Spectroscopic indices: LCO 100-inch data.

Name	Ca K	CH	Mg	Fe1	Fe2	Hβ	[Fe/H]
HIP 435	7.0	4.4	2.3	1.6	1.7	4.3	−0.97
1719	14.4	10.9	8.2	3.9	3.0	1.4	
3139	7.4	3.5	2.1	1.6	1.5	4.4	−0.49
3531[1]	13.2	10.8	11.4	6.3	7.1	0.8	
3531B[1,2]2	11.3	4.4	11.3	3.4	4.9	0.1	
4450	9.8	6.0	3.0	2.2	2.2	2.5	
4576	8.5	4.1	2.5	2.0	2.0	3.8	
4750	7.1	8.5	2.0	1.1	1.1	2.3	H
4981	10.9	7.9	4.0	2.2	2.3	2.1	−0.58
5004	13.8	9.4	6.4	2.2	2.4	1.4	−1.02
5097	8.1	4.3	2.2	1.7	1.8	2.8	H
6758	11.1	8.3	4.1	2.6	2.3	2.1	
6758	9.8	6.5	3.3	2.3	2.3	2.3	
7303	10.8	7.7	3.9	1.9	1.7	2.7	
7459	8.1	4.3	2.5	1.2	1.4	2.0	−1.17
7687	13.7	9.8	7.2	3.7	3.5	1.3	
7772	7.2	3.0	2.0	1.9	1.8	5.0	
8389	15.5	10.8	10.1	4.2	4.0	1.0	
8558	4.5	1.3	1.4	1.0	1.1	3.8	−1.10
9634	7.7	3.4	2.1	1.5	1.6	4.5	
10208	7.5	3.5	2.1	1.6	1.6	4.3	
10360[3]	4.7	1.2	1.6	1.5	1.4	9.5	
10385	14.3	10.8	10.5	5.4	5.5	1.1	
10637	7.8	3.8	2.1	1.6	1.4	4.4	
11435	8.7	4.1	2.5	2.0	2.0	4.4	
13849	15.2	11.1	10.2	5.1	5.2	1.0	
14192	9.2	4.6	2.6	2.1	2.0	2.7	
15756	14.0	11.4	9.4	5.1	5.0	1.3	
16479	8.2	3.7	2.2	1.9	2.0	4.6	
16089	7.5	3.0	2.2	2.1	1.7	5.7	
17085	8.1	3.4	2.2	1.8	1.8	4.7	−0.22
17241	5.5	2.0	1.3	0.7	0.8	3.0	H
19007	14.2	10.0	7.6	3.5	3.4	1.2	−0.62
21000A	9.2	4.6	2.6	2.1	2.0	4.2	−0.16
21000B[2]	9.0	5.0	2.6	2.1	2.0	4.3	−0.16
21125	12.1	9.3	5.2	2.5	2.2	1.7	
21609	10.4	6.5	3.4	1.4	1.3	1.6	−1.76
22177[1]	11.4	8.4	10.2	5.8	6.6	0.8	
22632	6.7	2.9	1.8	0.8	0.7	3.3	−1.59
23573	13.1	10.2	6.5	2.7	2.6	1.5	
24296	10.5	7.1	4.0	2.2	2.3	2.1	
24316	6.3	3.1	1.7	0.7	0.6	2.0	−1.52
24935	8.3	4.4	2.4	1.5	1.5	2.5	H
24421	10.1	5.8	3.0	2.1	2.1	3.8	
26688	5.9	3.4	1.5	1.0	1.0	4.7	
29322[1]	10.6	5.7	8.8	4.0	4.4	0.2	
31639	12.7	9.3	5.9	2.7	2.5	1.4	
33283	13.6	10.1	8.2	3.2	2.8	1.4	
34146	8.3	4.0	2.1	1.1	1.3	4.1	−0.40
35232	7.8	4.2	2.2	1.5	1.5	2.5	H
36818	10.6	6.1	3.3	1.6	1.9	1.9	−0.75
39911	11.0	7.5	4.2	1.8	2.0	1.8	−0.92
41563	6.8	2.6	1.7	1.8	1.8	5.3	
43445	8.4	4.5	2.3	1.6	1.5	3.8	
43490	10.6	5.8	3.0	1.5	1.1	2.0	H
43973	11.8	8.3	4.8	2.2	2.0	2.4	
44116	7.2	3.5	1.9	1.4	1.5	4.2	−0.58
44124	5.4	2.2	1.6	0.7	0.8	3.3	−2.00
44435	6.3	2.5	2.1	1.9	1.3	5.6	−0.06
44436	1.2	0.0	0.6	0.4	0.4	15.6	
46120	6.4	3.7	1.7	0.6	0.6	1.9	−2.10
47171	10.7	7.2	3.5	2.1	2.2	3.3	
47948	12.1	8.9	5.1	2.7	2.7	2.8	
49574	6.8	4.9	2.0	1.3	1.3	3.5	H
49785	9.2	4.9	2.9	1.8	1.7	3.8	
50532	10.3	6.2	3.1	2.2	2.1	3.6	
50965	10.8	7.2	3.7	1.8	1.9	2.8	−0.39
51156	7.7	3.6	2.1	1.6	1.7	4.5	
51298	8.1	3.6	2.2	1.9	2.0	4.6	
51300	7.2	3.2	2.2	1.8	1.8	5.2	
51769	11.9	9.1	5.1	2.2	1.8	1.4	−0.65
54641	6.8	3.9	2.0	1.0	0.9	3.5	−1.04
54834	5.9	2.4	1.5	0.8	0.8	3.4	H
55790	5.7	2.4	1.5	0.7	0.7	3.1	−1.56
55978	6.4	2.5	1.8	1.8	1.2	5.7	0.07
57360	6.8	3.0	1.7	0.9	1.0	3.0	−1.22
59750	7.9	4.0	2.0	0.4	0.4	3.8	−0.78
60251	9.9	6.1	3.0	2.1	2.2	3.6	
60632	5.4	2.0	1.2	0.6	0.6	3.4	−1.45
60852	8.2	4.6	2.3	1.7	1.8	4.2	−0.54
63781	6.3	2.2	1.9	1.8	1.5	5.4	
64765	5.7	2.3	1.9	1.8	1.6	6.4	−0.15
65040	12.0	8.4	4.8	2.2	1.9	2.2	−0.71
65201	3.9	1.2	1.4	0.6	0.6	3.4	−1.96
65940[3]	14.8	11.2	9.7	4.9	4.7	1.2	
66169	14.0	10.5	7.3	3.6	3.4	1.4	
66815	9.4	6.4	3.0	1.7	1.7	2.7	
67189	7.7	4.1	2.6	2.1	2.0	4.7	
67655	11.4	8.5	4.8	2.1	1.8	1.6	−0.92
66815	9.5	6.3	2.8	1.7	1.5	3.0	−0.64
68165	15.7	9.8	9.9	4.1	3.9	0.9	−0.23
68452	7.4	3.7	2.1	1.6	1.6	4.0	
68870	7.8	3.3	2.3	1.9	2.0	4.9	
70152	15.0	11.4	10.1	5.4	5.4	1.0	−0.03
70681	10.6	6.3	3.4	1.5	1.5	2.2	−1.25
70689	6.0	2.5	1.9	1.7	1.3	5.5	
71886	7.6	3.5	2.0	1.6	1.5	4.4	
73798	10.9	8.1	4.2	1.7	1.7	1.6	H
74078	8.7	4.5	2.6	2.0	1.9	4.6	
74994	5.5	2.6	2.0	2.0	1.9	7.0	−0.06
107873	9.2	5.4	2.8	2.1	2.0	3.9	
108095	10.0	6.3	3.4	2.1	1.9	3.2	
109869	11.5	7.5	3.8	2.8	2.6	3.0	
111426	8.1	4.0	2.2	1.8	1.5	4.4	
112384	5.8	2.6	1.6	1.2	0.9	4.8	
113430	8.1	4.0	2.5	1.8	1.8	4.5	−0.22
113868	13.4	9.9	6.4	3.5	3.3	1.6	
114271	3.7	1.3	0.9	0.4	0.6	3.6	−1.80
114487	5.5	2.4	1.6	1.2	1.0	5.1	
114735	6.6	2.7	1.8	1.5	1.5	4.6	
114837	9.9	6.1	3.4	2.3	2.3	3.8	−0.44
115031	7.7	4.2	2.5	2.0	1.1	4.1	
115361	7.7	3.8	2.3	1.8	1.9	4.3	−0.39
116437	9.5	5.5	2.9	1.8	1.8	3.4	
117121[1]	13.8	10.0	10.9	5.7	5.7	0.9	
117823	8.7	5.3	2.7	1.6	1.6	3.6	
117882	9.1	4.2	2.5	2.1	2.0	4.5	0.20
118165	7.9	3.4	2.3	2.0	2.0	5.7	
vB 100	9.4	2.5	2.5	2.3	2.1	6.3	0.15
vB 101	8.8	4.2	1.6	2.2	2.5	4.8	0.15
vB 105	9.9	7.5	4.1	3.0	2.9	3.8	0.15
vB 142	11.6	8.2	5.1	3.5	3.2	1.8	0.15
HD 3567	6.9	2.6	1.5	0.9	1.1	3.3	−1.50
HD 19445	4.0	2.0	1.2	0.5	0.6	3.1	−1.81
HD 84937	2.6	0.6	0.7	0.3	0.5	4.2	−2.04
G1-9	11.7	8.5	4.2	2.6	2.6	3.0	−0.51
G1-28	14.9	10.3	8.2	3.5	3.2	1.2	−0.37
G8-15	30.0	5.5	9.9	4.5	3.7	1.2	−0.85
G30-52	10.2	8.9	4.6	3.9	3.9	1.1	−2.10
G32-26	20.7	6.9	4.3	3.0	3.5	1.6	−1.53
G64-12	0.9	0.0	0.3	0.2	0.5	4.2	−3.52
G158-100	8.7	4.7	2.4	0.9	1.4	1.3	−2.64
G270-71	9.4	5.7	2.6	1.9	2.2	3.9	−0.49
G271-11	11.3	8.1	3.9	2.0	2.0	2.5	−0.57
G271-34	10.7	7.8	3.9	1.9	1.8	2.5	−0.03

Notes: 1. M dwarf; 2. Possible companion; 3. K dwarf. vB 100, 101, 105 and 142 are all members of the Hyades cluster.

Table 10. Spectroscopic indices: LCO 40-inch data.

Name	Ca K	CH	Mg	Fe1	Fe2	Hβ	[Fe/H]
HIP 895	7.0	2.9	1.5	1.6	0.6	5.9	
1051	7.1	3.2	1.1	1.2	0.4	5.5	
3855[1]	16.6	18.2	11.0	4.6	2.4	0.9	
6251	9.7	7.4	2.0	1.5	0.5	5.2	
7935	8.6	5.4	1.5	1.5	0.5	5.7	
8298	14.6	10.8	3.7	2.9	1.4	1.7	
10353	7.8	3.5	1.4	1.3	0.5	4.5	H
10375	6.8	3.5	1.2	1.2	0.5	5.9	
14594	4.3	1.7	0.7	0.3	0.2	3.2	−1.81
17481[2]	5.3	1.9	1.0	1.5	0.4	10.0	−0.1
17497[2]	6.7	3.1	1.3	1.6	0.5	9.1	−0.1
19637	8.2	3.7	1.2	1.2	0.5	6.0	
18700	10.2	9.3	2.2	1.6	0.7	5.2	
19797	5.0	1.7	0.8	0.4	0.3	4.4	−1.57
21478	11.4	7.9	2.8	2.0	0.8	4.6	
25717	6.2	3.7	1.3	2.1	0.6	8.7	
26676	12.7	10.9	2.3	1.6	0.9	2.4	
28122A[3]	7.2	3.5	1.2	1.5	0.6	7.9	
28122B	8.9	4.3	1.6	1.6	0.6	5.0	
28188	8.2	4.8	1.5	1.2	0.6	5.2	
29510	6.8	2.4	1.1	1.9	0.4	10.5	
32009	13.9	15.7	3.0	2.7	1.4	2.8	
32308[1]	15.9	12.3	5.4	4.7	2.4	1.2	
34145	11.1	8.5	2.0	1.8	0.6	2.7	H
36491	9.6	5.7	1.7	1.1	0.5	3.7	−0.90
36818	11.1	6.8	1.7	1.4	0.6	2.7	−0.75
38541	8.4	7.9	1.5	0.9	0.5	2.0	−1.70
42278	5.9	1.8	1.0	1.1	0.4	9.7	
47161	8.4	4.4	1.4	1.8	0.5	6.8	
48146	10.7	9.4	1.8	1.8	0.6	5.6	−0.05
52285A[1,3]	16.4	12.2	3.6	3.5	1.7	1.5	
52285B[1,3]	13.1	15.4	7.6	5.0	2.5	0.6	
54519[1]	12.6	12.9	4.9	4.2	2.2	1.5	
54993	7.6	3.0	1.4	1.8	0.5	7.6	
95800	6.7	2.5	1.2	1.3	0.4	7.3	
97127	6.8	2.7	1.4	1.8	0.5	6.7	
97463	11.6	8.6	2.2	1.7	0.6	3.2	H
100207	6.9	3.3	1.3	1.4	0.5	6.4	
101103	5.9	2.4	1.1	1.1	0.4	6.8	
101650	8.4	4.2	1.4	1.8	0.6	7.0	
101892	8.4	4.3	1.6	1.7	0.6	7.4	
101987	8.4	5.1	1.5	1.7	0.7	6.9	
103287	16.1	15.7	3.2	3.4	1.5	1.6	
103714	10.4	8.6	2.2	2.7	0.9	5.2	
104289	12.7	14.4	3.3	1.9	1.1	2.9	
106204[1]	13.2	18.8	11.9	5.4	2.9	1.2	
106904	11.6	11.0	2.9	1.7	0.9	2.9	H
108006	6.7	3.3	1.4	1.4	0.5	8.4	
108598	13.8	11.9	4.4	2.9	1.3	1.2	
108655	7.0	2.1	1.2	1.5	0.4	7.4	
109067	14.5	12.3	2.6	1.8	1.0	2.4	−0.97
110621	8.0	3.5	1.4	1.4	0.4	5.1	
110776	14.2	17.5	5.5	4.1	1.7	2.0	
111374	7.8	3.8	1.4	1.5	0.4	7.2	
113542	6.1	1.0	1.2	1.4	0.4	9.2	
114627	8.6	5.2	1.6	1.5	0.5	6.2	
114837	9.3	6.2	2.0	1.9	0.7	4.5	
115194	16.2	11.4	4.1	3.1	1.4	1.5	
−33 3337	5.9	3.3	0.9	0.5	0.2	3.7	−1.33
−3 740	3.0		0.8	1.0	0.3	18.4	−2.73
HD 16031	5.4	1.9	0.7	0.4	0.2	4.6	−1.82
HD 59984	7.9	6.7	1.3	1.2	0.3	3.3	−0.64
Gl 105A	16.5	15.9	4.6	4.2	2.3	1.1	
Gl 135	12.5	13.1	2.7	2.1	0.9	3.4	
Gl 764.1A	15.8	12.3	5.2	4.3	2.0	1.1	
Gl 764.1B	16.8		7.3	4.7	2.5	0.6	
Gl 775	15.0	15.9	6.4	5.2	2.7	0.8	
G2-47	13.6	14.8	3.4	2.5	1.2	2.4	−1.00
G5-42	12.3	8.8	2.9	2.6	1.2	3.6	0.04
G5-46	10.2	8.1	1.9	1.6	0.6	3.4	−0.34
G41-34	13.7	21.8	3.6	3.3	1.5	3.2	−0.20
G41-41	2.0	0.5	0.3	0.1	0.1	5.7	−2.80
G43-7	15.1	15.8	3.8	3.3	1.2	2.3	−0.68
G71-27	9.5	7.8	1.8	1.7	0.5	4.6	−0.63
G73-67	13.0	11.9	3.5	2.8	1.3	2.8	−0.43
G82-5	13.3	11.0	2.4	2.0	1.1	3.5	−0.70
G82-18	14.5	21.0	3.6	4.0	2.2	1.9	−1.41
G82-44	7.2	4.8	1.3	0.6	0.4	3.2	−2.10
G82-47	9.7	6.4	1.6	2.0	0.6	6.8	−0.55
G83-42	16.0	12.4	3.8	2.3	1.2	1.5	−1.47
G83-45	12.1	6.7	1.8	2.0	0.9	7.4	−2.49
G83-51	10.5	15.3	2.1	1.5	1.2	5.2	−1.51
G84-9	10.0	6.2	1.7	1.4	0.5	3.7	−0.94
G84-16	12.0	9.9	2.0	1.3	0.8	1.3	−1.95
G84-37	9.1	5.4	1.4	1.0	0.3	4.1	−0.92
G89-14	5.4	1.9	0.7	0.5	0.2	4.4	−1.90
G89-21	11.7	9.8	2.1	1.4	0.7	3.1	−1.15
G94-3	12.4	8.2	1.9	0.9	0.7	1.8	
G98-42	15.9	14.6	3.8	4.0	1.9	1.6	−0.18
G99-48	10.6	8.5	1.6	0.9	0.5	2.1	−2.14
G110-34	5.6	2.2	0.8	0.6	0.3	2.8	−1.73
G112-43	6.5	2.7	0.8	0.7	0.2	4.3	−1.51
G112-44	7.3	4.4	1.2	0.9	0.3	4.1	−1.27
G112-56	14.0	11.5	2.8	2.2	0.9	3.3	
G113-22	10.7	7.6	1.5	1.2	0.5	3.0	−1.30
G113-24	10.5	10.6	1.9	1.4	0.6	4.2	−0.51
G160-1	12.4	8.9	2.1	2.1	0.8	5.0	0.07
G160-3	12.5	14.6	3.0	2.5	1.0	4.2	−0.23
G160-13	15.8	16.5	3.7	2.8	1.3	2.5	−0.45
G271-11	8.8	5.2	1.7	1.9	0.7	8.3	−0.57
G271-34	11.0	7.9	2.2	1.7	0.7	3.2	−0.78
G271-57	15.9	16.9	3.7	2.8	1.4	1.8	−0.62
G271-62	2.8	0.8	0.6	0.2	0.2	4.3	
G271-69	12.1	11.4	2.8	2.3	1.1	3.4	−0.56
G271-75	14.6	15.2	3.9	3.7	1.6	1.5	−0.29

Notes: 1. late-type K/early-type M dwarf; 2. Pleiades member; 3. known binary.

common proper motion companion, ~1 arcmin south and ~2 mag fainter. Photometry and spectroscopy of CD −79°347B will therefore provide additional calibration of the [Fe/H] ~ −1 main sequence.

HIP 44436: As noted above, our spectroscopy shows that this is an early-type star. In addition to strong Balmer lines, we detect Mg II 4481 Å with an equivalent width of 0.5 Å.

HIP 49574: Another candidate CH-strong subdwarf

HIP 52285: Also known as BD +4°2370, spectral type K2. The companion, BD +4°2370B, is ~1 mag fainter.

HIP 65940: Upgren (1972) classifies this star as spectral type K2V.

HIP 106204: Upgren (1972) classifies this star as spectral type K7V.

HIP 106904: Another subdwarf with CH bandstrengths apparently stronger than normal for metal-poor stars.

HIP 117882: As noted in Section 4.1, the line strength measured for this star indicates a near-solar abundance, inconsistent with the absolute magnitude implied by the *Hipparcos* parallax.

7 DISCUSSION

7.1 The subdwarf sample

Combining all of the photometric and spectroscopic observations discussed in the previous sections, we have ancillary data for 270 of the 317 stars identified originally as candidate subdwarfs with

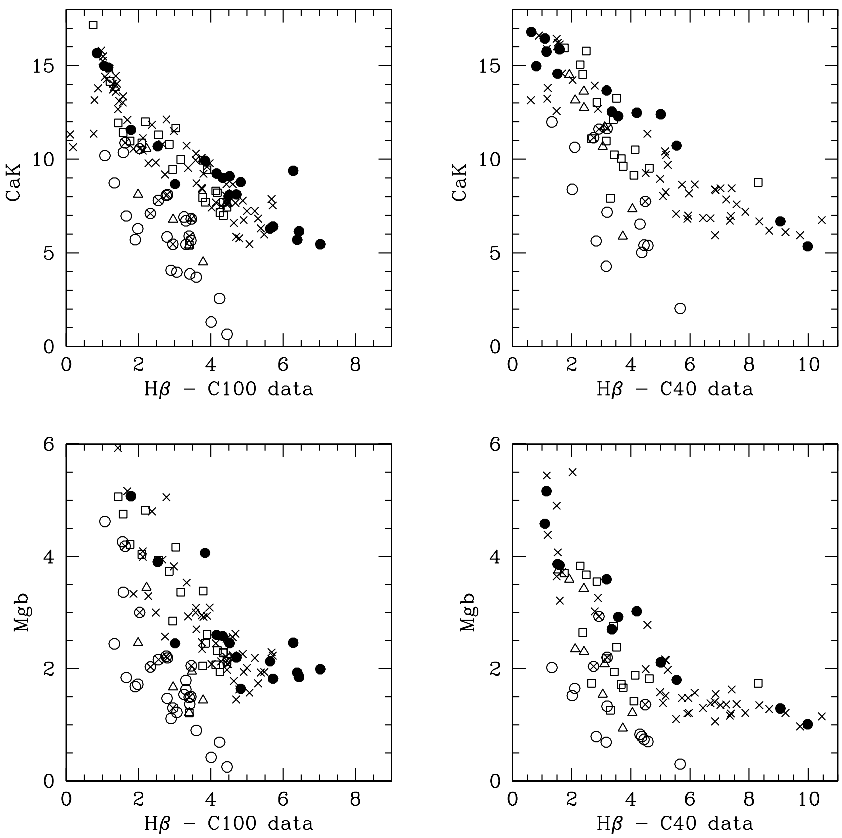

Figure 14. Ca II K-line and Mgb equivalent width measurements from our Las Campanas observations plotted against Hβ equivalent widths. Stars with spectroscopic or Strömgren metallicities [Fe/H] > -0.3 are plotted as filled circles; open squares mark stars with $-0.3 \le$ [Fe/H] < -1.0; open triangles are halo subdwarfs with $-1.0 \le$ [Fe/H] < -1.5; and open circles identify extreme subdwarfs. *Hipparcos* stars lacking such abundance measurements are plotted as crosses; candidate subdwarfs are marked as encircled crosses.

parallaxes measured to an accuracy of 15 per cent. SIMBAD lists *BV* photometry and spectral types for most of the remaining stars, although with no attributed source for either parameter. Several stars have discrepant colours and spectral types.

(1) HIP 88231 and 95924 are classified as A0 and B9 respectively. Both lie close to the Galactic plane, and are likely to be distant, reddened early-type stars, like HIP 81617 and 90724.

(2) HIP 70622, 76670 and 78952 are all classed as G5, but have $(B-V)_1 = 0.46$.

(3) HIP 83070 has a fainter companion at a separation of 10 arcsec, which may affect the *Hipparcos* astrometry.

(4) HIP 80781 is also noted as double in the *Hipparcos* catalogue.

More accurate photometry and spectroscopy of all 47 stars currently lacking population classification is clearly desirable.

Table 11 summarizes the available photometric data and metallicity estimates for 45 stars we consider confirmed as halo subdwarfs. We have omitted stars with abundance determinations [Fe/H] > -1, including those with ambiguous results (e.g., HIP 35232: $[\mathrm{Fe/H}]_{0.6} = -0.2$, spectral class 'H'). We add HIP 3026 from Table 8, which has a formal parallax uncertainty of $\sigma_\pi/\pi = 0.144$, *UBVRI* photometry and an abundance [Fe/H] ~ -1. The extensive observations described in this paper succeed in making only nine additions (including HIP 114721) to the canon of fiducial subdwarfs. However, the data presented in Table 11 mark the most reliable and homogeneous compilation of broad-band photometry currently available. These values should be used in preference to those derived by averaging results from inhomogeneous sources (e.g., as in Carretta et al. 2000b).

Amongst the stars listed in Table 11, at least 12 were previously known or suspected to be binary stars. We add HIP 95190 to that list, based on its location in the HR diagram. 31 stars (19 currently classed as single) have Strömgren data; 34 stars (25 single) have *UBV* measurements, and 32 stars (22 single) have *VRI* (Cousins) photometry. Carretta et al. (2000b) have recently compiled their own sample of high-weight metal-poor stars, with reliable abundance estimates and *Hipparcos* parallaxes accurate to $\sigma_\pi/\pi < 0.12$. Their data set spans a wider range in both colour and abundance than our sample, and includes 11 stars with [Fe/H] < -1 which are not in Table 11. For completeness, we have searched the literature for $UBVR_\mathrm{C}I_\mathrm{C}$ and Strömgren observations of those stars, and these data are presented in Table 12. Six of the 12 stars (HIP 7869, 33221, 49616, 73385 and 76976, and HD 211998) are subgiants.

Fig. 15 plots the resultant colour–magnitude diagrams, combining data from both Tables 11 and 12. The disc main sequence is defined in the Johnson/Cousins system by nearby stars with $\sigma_\pi/\pi < 0.15$ and *BVRI* photometry from Bessell (1990); the Strömgren sequence is defined by the same stars plotted in Fig. 3. We have included the $[M_R, (R-I)]$ diagram to illustrate the insensitivity to abundance of the location of the main sequence in that plane. With few strong absorption features in either band,

Table 11. Confirmed subdwarfs: photometry and abundances.

HIP	M_V	σ_V	$U-B$	$B-V$	$V-R$	$V-I$	$(b-y)$	$[Fe/H]_{sp}$	$[Fe/H]_S$	$[Fe/H]_{0.6}$	
4750	5.27	0.35	−0.107	0.566	0.315	0.641				−1.1	n
5004	6.33	0.25	0.182	0.758	0.442	0.877	0.472	−1.02	−1.13	−1.0	*
7459	5.43	0.23	−0.147	0.514	0.329	0.679	0.365	−1.17	−1.09	−1.2	*
8558	3.89	0.18	−0.147	0.369	0.234	0.486		−1.10		−1.2	*
14594	5.11	0.10		0.49			0.351	−1.95	−1.71		*
16404	6.17	0.20		0.65			0.451	−1.92	−1.91		*, bin
17241	4.81	0.29	−0.184	0.447	0.290	0.612				−1.3	n
19797	4.77	0.24		0.36			0.322	−1.55	−1.52		*
21609	6.01	0.13	−0.076	0.640	0.387	0.798	0.452	−1.76	−1.81	−1.6	*, bin
22632	5.10	0.17	−0.197	0.489	0.309	0.634	0.358	−1.59	−1.47	−1.6	*
24316	5.25	0.16	−0.199	0.496	0.312	0.647	0.371	−1.55	−1.60	−1.6	*
26676	5.99	0.32	0.024	0.658	0.414	0.801	0.435	−1.10	−1.29	−1.0	*
34145	5.35	0.26		0.55				H			n
38541	6.02	0.07		0.62			0.430	−1.7	−1.75		*, bin
40778	4.80	0.33		0.48			0.339	−1.7	−1.45		*
43490	5.30	0.14	−0.113	0.550	0.321	0.664		H		−1.1	n
44124	5.12	0.32	−0.185	0.486	0.317	0.647	0.349	−1.96	−1.34	−1.4	*
46120	6.20	0.13	−0.182	0.577	0.352	0.728	0.399	−2.09	−2.1	−1.9	*
48152	3.80	0.19	−0.203	0.398	0.263	0.559	0.302	−2.07	−2.24	−1.6	*
53070	4.63	0.13	−0.190	0.482	0.306	0.636	0.344	−1.4	−1.29	−1.5	*, bin
54641	4.41	0.10	−0.153	0.481	0.295	0.607	0.335	−1.04	−1.22	−1.1	*
54834	4.69	0.16	−0.177	0.464	0.296	0.609				−1.3	n
55790	4.29	0.31	−0.192	0.470	0.300	0.621	0.343	−1.56	−1.62	−1.4	*, bin
57360	4.22	0.22	−0.164	0.466	0.293	0.602	0.33	−1.21	−1.31	−1.1	*, bin
57450	5.59	0.6	−0.15	0.55			0.398	−1.26	−1.45	−1.4	*
57939	6.61	0.02		0.75			0.484	−1.32	−1.41		*
60632	4.88	0.27	−0.206	0.447	0.286	0.595	0.330	−1.55	−1.79	−1.5	*, bin
65201	4.75	0.21	−0.204	0.458	0.312	0.641	0.349	−1.86	−1.96	−1.5	*, bin
70681	5.71	0.17	−0.082	0.601	0.359	0.727	0.400	−1.25	−1.16	−1.2	*
72461	4.79	0.32		0.44			0.332	−2.15	−2.0		*
73798	5.90	0.26	−0.036	0.642	0.375	0.755				−1.2	n
81170	6.19	0.16	0120	0.746	0.447	0.900	0.474	−1.20	−1.39	−1.30	*, bin
88648	6.14	0.31	−0.144	0.611	0.387	0.782	0.430		−1.8	−1.8	*, bin
89215	6.50	0.26	0.188	0.773	0.435	0.860	0.474	−1.36	−1.34	−1.2	*
89554	4.25	0.15	−0.181	0.449	0.290	0.602	0.327	−1.44	−1.43	−1.3	*
94704	6.75	0.35	0.02	0.66	0.40	0.84				−1.0	n
95190	4.79	0.35	−0.081	0.570	0.341	0.696				−1.0	n, bin
95996	5.15	0.36		0.49	0.33	0.65	0.355		−1.38		*, bin
98020	5.85	0.10		0.60			0.416	−1.6	−1.57		*, bin
99267	5.51	0.21		0.51				−2.01			*
100568	5.46	0.12	−0.126	0.546	0.332	0.678	0.381	−1.10	−1.27	−1.3	*
103269	6.03	0.23	−0.11	0.62				−1.70		−1.6	*
106924	6.25	0.18	−0.07	0.63				−1.62		−1.4	*
114271	4.03	0.19	−0.188	0.420	0.280	0.580		−1.80		−1.4	n
3026	4.15	0.34	−0.131	0.469	0.291	0.609		−1.30		−0.9	*

Notes: No Lutz–Kelker corrections have been applied to the absolute magnitude listed in column 2; column 9 lists spectroscopic abundance estimates (see Table 2 – high-resolution analyses are given preference for stars with multiple estimates); column 10 lists Strömgren-based metallicities; column 11 gives $\delta(0.6)$ values; column 12 indicates whether the subdwarf was known previously (*) or is an addition (n), and identifies known or suspected binaries (bin).

decreasing abundance produces a relatively small change in the differential blanketing. Such is not the case at lower luminosities, where variations in TiO bandstrength lead to more substantial offsets between disc and halo (Gizis 1997).

7.2 Metal-poor subdwarfs and globular cluster distances

Our main aim in undertaking this programme was the identification of previously unrecognized unevolved extreme subdwarfs. We have, not unexpectedly, had little success. Table 11 includes nine single stars with metallicities below $[Fe/H] = -1.6$, of which only four (HIP 46120, 99267, 103269 and 106924) are redder than $(B-V) = 0.50$. However, all of those stars save HIP 40778 have abundances derived from high-resolution observations, and, crucially, HIP 46120 has $[Fe/H] < -2$. The last-mentioned star is the only lower main-sequence star with both an accurate parallax and a reliable abundance measurement.[5]

It is not our intention to re-examine globular cluster distances in this paper. None the less, Fig. 16 offers a single comparison, matching the nine extreme subdwarfs discussed above against NGC 6397 in the $[M_V, (B-V)]$ plane. Table 12 includes three subdwarfs from Carretta et al. (2000b) with $[Fe/H] < -1.6$: HIP 18915, 31332 and 79537. However, Fig. 15 shows that HIP 31332

[5]Carretta et al. (2000b) include HIP 46120 = CD − 80°328 in their recent re-analysis of globular cluster distances, but they adopt $[Fe/H] = -1.75$, rather than −2.07, as derived by RD. They comment that, at the adopted metallicity, the star occupies an anomalous position in the colour–magnitude diagram. Those anomalies are not present at the lower abundance adopted in our analysis.

Table 12. Subdwarfs from Carretta et al.: photometry and abundances.

HIP	M_V	σ_V	$U-B$	$B-V$	$V-R$	$V-I$	$(b-y)$	$[Fe/H]_{sp}$	$[Fe/H]_S$	$[Fe/H]_{0.6}$	
7869	4.07	0.11	−0.07	0.56	0.34	0.69	0.372	−1.13	−0.82	−0.8	R1, HD 10607
	8.18	0.11	1.01	1.21	0.75	1.45					R1, LHS 1279
18915	7.17	0.04	0.37	0.87			0.533	−1.69	−1.64	−1.8	R1, HD 25329
31332	6.24	0.23	0.52	0.94	0.57	1.08		−2.11		−2.0	R2, HD 46663
33221	3.87	0.26	−0.15	0.48			0.334	−1.33		−1.1	C1, CD −33 3337
49616	3.42	0.19	−0.02	0.72	0.42	0.87	0.502	−1.91	−2.00	−2.2	R2, HD 89499
73385	3.75	0.24	−0.15	0.56			0.401	−1.73	−1.98	−1.5	R1, HD 132475
74234	7.07	0.11	0.34	0.84	0.52	1.01	0.524	−1.28	−1.24	−1.1	R1, HD 134440
74235	6.71	0.09	0.16	0.78	0.45	0.91	0.484	−1.30	−1.33	−1.6	R1, HD 134439
76976	3.43	0.09	−0.19	0.49			0.380	−2.40	−0.6	−1.5	CL, HD 140283
79537	6.84	0.03	0.28	0.82	0.48	0.94	0.509	−1.64	−1.22	−1.2	B, C2, Gl 615
	2.98	0.14	−0.06	0.65			0.450	−1.43	−1.51	−1.5	S, HD 211998

Notes: LHS 1279 is a cpm companion of HD 10607; HD 89499 is a spectroscopic binary;
CD −33°3337 is identified as an astrometric binary by Carretta et al. 2000b;
$[FeH]_{sp}$ from Carretta et al., 2000b;
All of the Strömgren data are from Schuster & Nissen 1988;
References for *UBVRI*: B – Bessell 1990 (*BVRI*); C1 – Cousins 1972; C2 – Carney 1978 (*UBV*); CL – Carney & Latham 1987; R1 – Ryan 1992; R2 – Ryan 1989; S – SIMBAD data base.

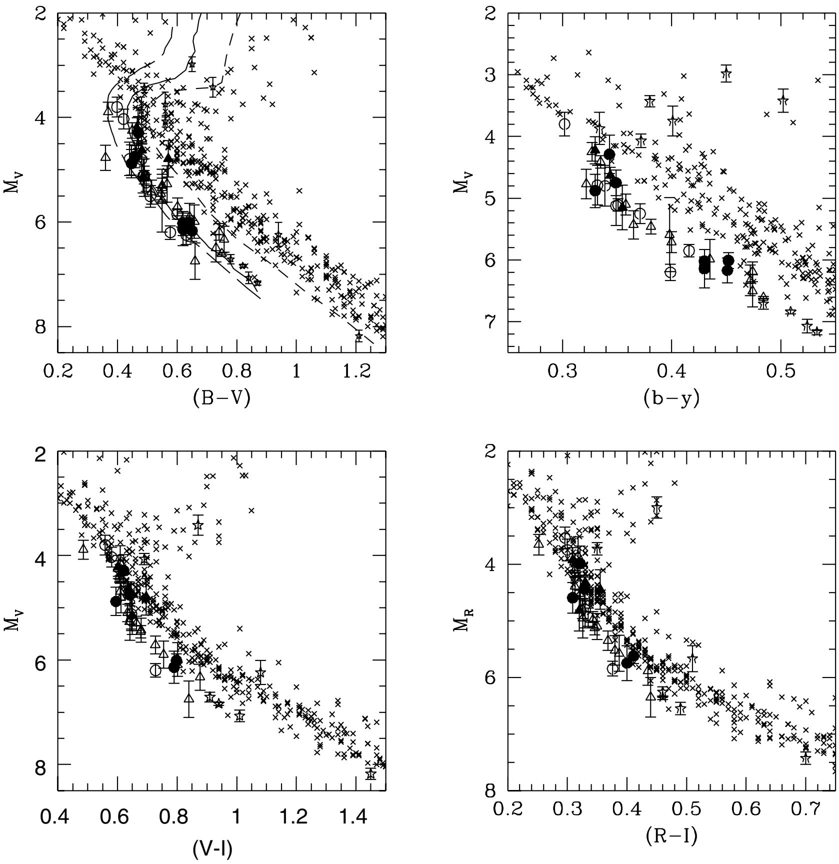

Figure 15. Colour-magnitude diagrams for the stars listed in Tables 11 and 12. In each case, disc main-sequence stars are plotted as crosses. Subdwarfs from Table 11 with $[Fe/H] \leq -1.6$ are plotted as circles; triangles mark higher abundance subdwarfs; known or suspected binaries are plotted as filled symbols, and data for stars from Table 12 are plotted as five-point stars. The cluster $[M_V, (B-V)]$ sequences are identical to those plotted in Fig. 2.

lies above the disc main sequence, suggesting either that the star is a binary, or that there is an error in either the abundance measurement or the photometry; moreover, HIP 79537 has discordant metallicity estimates, with RD measuring $[Fe/H] = -1.38$, rather than -1.64. We therefore include only HIP 18915 in Fig. 16.

Fig. 15 plots the subdwarf absolute magnitudes derived directly from the *Hipparcos* trigonometric parallax measurements; in Fig. 16 the absolute magnitudes have been corrected for Lutz–Kelker bias using the $n = 3$ approximation from Hanson (1979). The corrections are small: $\Delta_{LK} < 0.2$ mag. for all stars, and $\Delta_{LK} < 0.1$ for $(B-V) > 0.5$. We have also used theoretical models from

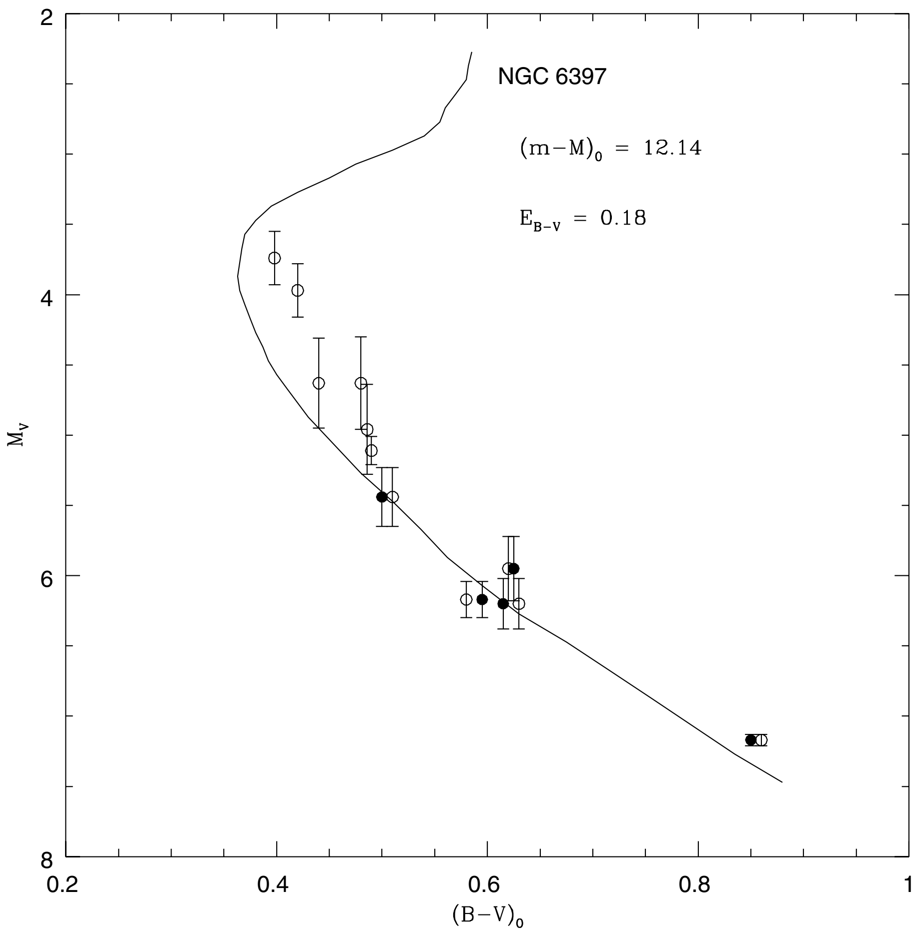

Figure 16. The [M_V, $(B-V)$] diagram for extreme subdwarfs, [Fe/H] < -1.6. The absolute magnitudes have been adjusted for Lutz–Kelker bias using Hanson's $n=3$ relation. Open circles plot the stars at their measured colours, and filled circles mark the location of the redder stars after correction to [Fe/H] $= -1.82$. The NGC 6397 sequence, at the specified distance modulus and reddening, is superimposed directly on the diagram.

Straniero & Chieffi (1991) to determine the appropriate colour corrections to adjust the lower main-sequence stars to match [Fe/H] $= -1.82$, the abundance derived by Gratton et al. (1996) for NGC 6397. The NGC 6397 fiducial sequence, adjusted to a true distance modulus of 12.14 mag and a reddening of $E(B-V) = 0.18$ mag, is simply superimposed on the diagram. The subdwarf data are not inconsistent with the adopted cluster distance modulus. Following the arguments outlined by Reid (1998), the corresponding distance modulus inferred for the Large Magellanic Cloud is $(m-M)_0 = 18.62$.

8 CONCLUSIONS

We have searched the *Hipparcos* catalogue for previously unrecognized halo subdwarfs which might be added to the current meagre sample of stars suitable for globular cluster main-sequence fitting. Our survey, covering 263 of 317 candidates with $(B-V)_T < 0.8$ and $\sigma_\pi/\pi \leq 0.15$, shows that few such stars remain hidden in the current data base. However, in the course of this exercise we have compiled the first catalogue of reliable $UBVR_CI_C$ photometry of spectroscopically confirmed halo subdwarfs with accurate trigonometric parallax measurements. Our sample includes only a few extreme subdwarfs, notably HIP 46120, suitable for matching against metal-poor clusters such as M15, M68 and M92.

Globular cluster main-sequence fitting distance determinations have been undertaken almost exclusively in the [M_V, $(B-V)$] plane. This concentration reflects necessity rather than choice: the [M_R, $(R-I)$] plane, for example, may offer significant advantages in greater tolerance to abundance uncertainties, but even with the observations contributed in this paper, many key subdwarfs still lack reliable photometry. Filling the gaps in Tables 11 and 12 should be a high priority.

As has been pointed out elsewhere, the dominant uncertainty in cluster distance analysis lies with the available photometry, rather than parallax measurements. Indeed, at a more general level, it remains the case that many stars in the *Hipparcos* catalogue, which have astrometric measurements at sub milliarcsecond precision, have received no attention from ground-based observatories since the completion of the Henry Draper or Bonner Durchmusterung catalogues. We are in the paradoxical situation of knowing their distances with higher accuracy than their apparent magnitudes or spectral types. This is a matter which should be borne in mind when considering future large-scale astrometric projects.

ACKNOWLEDGMENTS

INR thanks the director and the Time Assignment Committee of the Carnegie Observatories for the allocation of telescope time on both the 100-inch DuPont and the 40-inch Swope telescopes at Las Campanas Observatory. Partial support for SM was provided by a grant from the Space Telescope Science Institute, GO-08146.01-97A. Both the SIMBAD data base and the ADS bibliographic service were invaluable in this research project.

REFERENCES

Anthony-Twarog B. J., Twarog B. A., 2000, AJ, 120, 1311
Axer M., Fuhrmann K., Gehren T., 1994, A&A, 291, 895 (AFG)
Baldwin J. A., Stone R. P. S., 1984, MNRAS, 206, 241
Bessell M. S., 1979, PASP, 91, 589
Bessell M. S., 1983, PASP, 95, 480
Bessell M. S., 1990, A&AS, 83, 357
Bessell M. S., 2000, PASP, 112, 961
Bessell M. S., Weis E. W., 1987, PASP, 99, 642
Biémont E., Baudoux M., Kurucz R. L., Ansbacher W., Pinnington E. H., 1991, A&A, 249, 538
Bond H. E., MacConnell D. J., 1971, ApJ, 165, 51
Carney B. W., 1978, AJ, 83, 1087
Carney B. W., 1979, ApJ, 233, 211
Carney B. W., 1983, AJ, 88, 610
Carney B. W., Latham D. W., 1987, AJ, 93, 116
Carney B. W., Latham D. W., Laird J. B., Aguilar L. A., 1994, AJ, 107, 2240 (CLLA)
Carretta E., Gratton R. G., 1997, A&AS, 121, 95
Carretta E., Gratton R. G., Clementini G., Fusi Pecci F., 2000a, ApJ, 533, 215
Carretta E., Gratton R. G., Sneden C., 2000b, A&A, 356, 238
Celis L., 1975, A&AS, 22, 9
Clementini G., Gratton R. G., Carretta E., Sneden C., 1999, MNRAS, 302, 22
Cousins A. W. J., 1972, MNASSA, 31, 7
Cousins A. W. J., 1973, Mem. RAS, 77, 223
Cousins A. W. J., Stoy R. H., 1962, Royal Obs. Bull., 64, 103
Crawford D. L., Perry C. L., 1966, AJ, 71, 206
Cutispoto G., Tagliaferri G., Giommi P., Gouiffes C., Pallavicini R., Pasquini L., Rodono M., 1991, A&AS, 87, 233
Dean J., 1981, MNASSA, 40, 14
de Geus E. J., Lub J., van der Grifte E., 1990, A&AS, 85, 915
Eggen O. J., 1990, AJ, 100, 1159
ESA, 1997, The *Hipparcos* Catalogue
Fabricius C., Makarov V. V., 2000a, A&AS, 144, 45
Fabricius C., Makarov V. V., 2000b, A&A, 356, 141
Falin J. L., Mignard F., 1999, A&AS, 135, 231
Ferro A. A., Parrao L., Schuster W., González-Bedolla S., Peniche R., Pena J. H., 1990, A&AS, 83, 225
Figueras F., Jordi C., Rossello G., Torra J., 1990, A&AS, 82, 57
Franco G. A. P., 1994, A&AS, 104, 9
Fulbright J. P., 2000, AJ, 120, 1841
Giclas H. L., Burnham R., Thomas N. G., 1963, Lowell Obs. Bull., 6, 1
Gizis J. E., 1997, AJ, 113, 806
Gratton R. G., Carretta E., Castelli F., 1996, A&A, 314, 191 (GCC)
Gratton R. G., Fusi-Pecci F., Carretta E., Clementini G., Corsi C. E., Lattanzi M., 1997, ApJ, 491, 749
Guetter H. H., 1980, PASP, 92, 215
Hanson R. B., 1979, MNRAS, 186, 875
Hauck B., Mermilliod M., 1998, A&AS, 129, 431
Kenyon S. J., Dobrzycka D., Hartmann L., 1994, AJ, 108, 1872
Kilkenny D., van Wyk F., Roberts G., Marang F., Cooper D., 1998, MNRAS, 294, 93
Knude J., 1981, A&AS, 44, 225
Leggett S. K., 1992, ApJS, 82, 351
Lub J., Pel J. W., 1977, A&A, 54, 137
Manfroid J., Oblak E., Pernier B., 1987, A&AS, 69, 505
Menzies J. W., Cousins A. W. J., Banfield R. M., Laing J. D., 1989, SAAO Circ., 13, 1
Oblak E., 1990, A&AS, 83, 467
Oja T., 1985, A&AS, 59, 461
Oja T., 1986, A&AS, 65, 405
Oja T., 1991, A&AS, 89, 415
Olsen E. H., 1994a, A&AS, 104, 429
Olsen E. H., 1994b, A&AS, 106, 257
Perlmutter S. et al., 1998, Nat, 391, 51
Perryman M. A. C. et al., 1998, A&A, 331, 81
Pont F., Mayor M., Toron C., Vandenberg D. A., 1998, A&A, 329, 87
Reid I. N., 1993, MNRAS, 265, 785
Reid I. N., 1998, AJ, 115, 204
Reid I. N., 1999, ARA&A, 37, 191
Riess A. G. et al., 2000, ApJ, 536, 62
Roman N. G., 1955, ApJS, 2, 195
Rossello G., Figueras F., Jordi C., Nunez J., Paredes J. M., Sala F., Torra J., 1988, A&AS, 75, 21
Ryan S. G., 1989, AJ, 98, 1693
Ryan S. G., 1992, AJ, 104, 1144
Ryan S. G., Deliyannis C. P., 1998, ApJ, 500, 398 (RD)
Ryan S. G., Norris J. E., 1991, AJ, 101, 1835 (RN)
Sandage A., 1969, ApJ, 158, 1115
Sandage A., Kowal C., 1986, AJ, 91, 1140
Schmidt B. P. et al., 1998, ApJ, 507, 46
Schuster W. J., Nissen P. F., 1988, A&AS, 73, 225
Schuster W. J., Nissen P. F., 1989, A&A, 221, 65
Schuster W. J., Parrao L., Contreras Martínez M. E., 1993, A&AS, 97, 951
Straneiro O., Chieffi A., 1991, ApJS, 76, 525
Strömgren B., 1966, ARA&A, 4, 433
Twarog B., 1980, ApJS, 44, 1
Upgren A. R., 1972, AJ, 77, 486
Wallerstein G., Carlson M., 1960, ApJ, 132, 276
Weis E., 1986, AJ, 91, 626
Weis E., 1993, AJ, 105, 1962
Weis E., 1996, AJ, 112, 2300
Wildey R. L., Burbidge E. M., Sandage A. R., Burbidge G. R., 1962, ApJ, 135, 94

This paper has been typeset from a TEX/LATEX file prepared by the author.